Neutrino Astronomy

M. Taiuti

XXXII INTERNATIONAL SEMINAR of NUCLEAR and SUBNUCLEAR PHYSICS "Francesco Romano"

Otranto School

OUTLINE

Part I – The Neutrino and its role in Astronomy

- A non-exhaustive chronology of primary discoveries in astronomy
- A short history of neutrino studies
- The neutrino sources
- Detecting a neutrino

Part II – The Sun

- Production mechanisms
- The solar neutrino puzzle and its solution
- Borexino and the CNO cycle

Part III – In Search of Cosmic Rays Sources

- The high energy cosmic neutrinos
- Building a HE neutrino telescope (ANTARES, GVD, ICECube, KM3NeT)
- Where we are

Optic - astronomy

G. Galilei
tried by the Inquisition, found "vehemently suspect of heresy", and forced to recant

1604

First observation: Medicean Planets

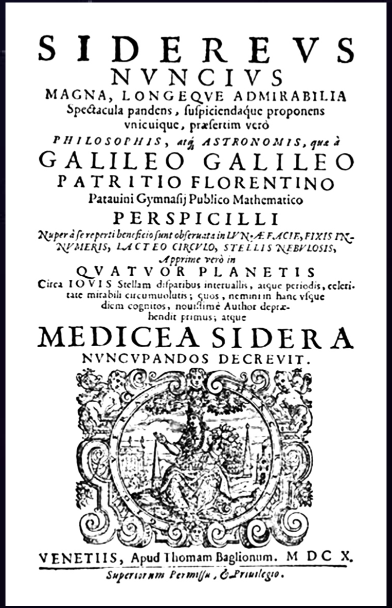

SIDEREVS
NVNCIVS
MAGNA, LONGEQVE ADMIRABILIA
Spectacula pandens, suspiciendaque proponens
vnicuique, præsertim verò
PHILOSOPHIS, atq; ASTRONOMIS, quæ à
GALILEO GALILEO
PATRITIO FLORENTINO
Patauini Gymnasij Publico Mathematico
PERSPICILLI
Nuper à se reperti beneficio sunt obseruata in LVNÆ FACIE, FIXIS INNVMERIS, LACTEO CIRCVLO, STELLIS NEBVLOSIS,
Apprime verò in
QVATVOR PLANETIS
Circa IOVIS Stellam disparibus interuallis, atque periodis, celeritate mirabili circumuolutis; quos, nemini in hanc vsque diem cognitos, nouissimè Author depræhendit primus; atque
MEDICEA SIDERA
NVNCVPANDOS DECREVIT.

VENETIIS, Apud Thomam Baglionum. M DC X.
Superiorum Permissu, & Priuilegio.

G.Galilei
Sidereus Nuncius,
1610

Cosmic Rays

V.F. Hess - Nobel Prize 1936

1604

1912

“The investigations so far have shown that the penetrating radiation observed in closed vessels is of very complex origin. Part of the radiation comes from the radioactive substances on the Earth’s surface and in the uppermost soil layers and fluctuates relatively little. A second component, which is influenced by meteorological factors, arises from the radioactive substances of the atmosphere, essentially from RaC. My balloon observations seem to indicate that there is still a third component of the total radiation, which increases in height and also shows remarkable intensity fluctuations on the ground.”

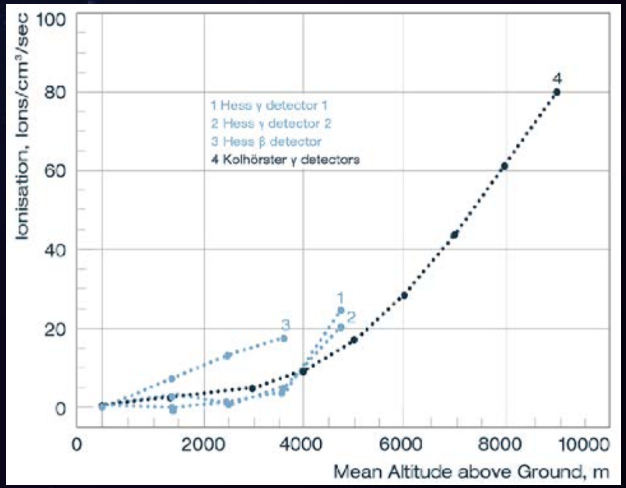

Physikalische Zeitschrift, vol. 13, 1912, pp. 1084–1091
arXiv:1808.02927v2

X-ray - astronomy

R. Giacconi - Nobel Prize 2002

R. Giacconi, The dawn of x-ray astronomy Rev. Mod. Phys., Vol. 75, No. 3, July 2003

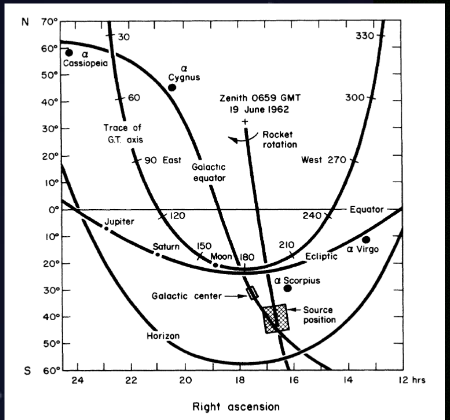

FIG. 2. Chart showing the portion of sky explored by the counters.

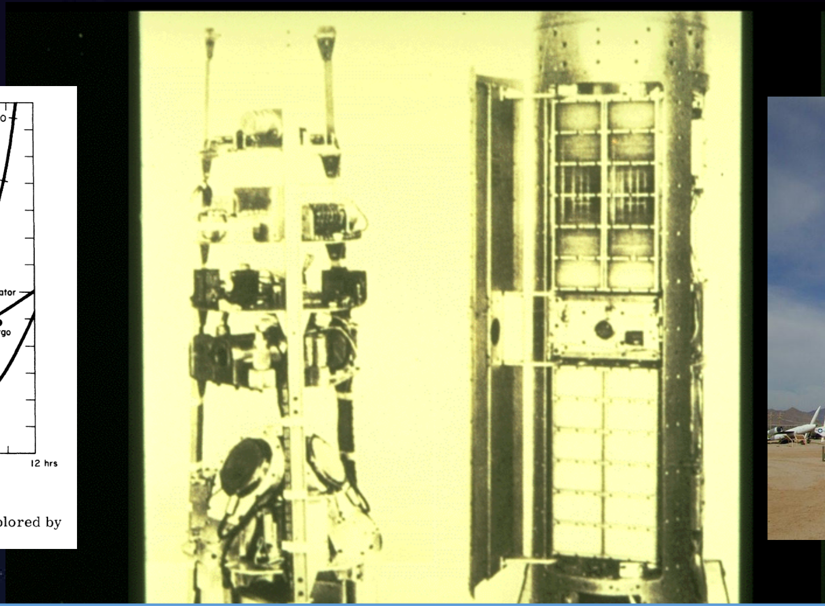

1962

1604

1912

First observation: diffuse X-ray “background” and the first discrete X-ray sources

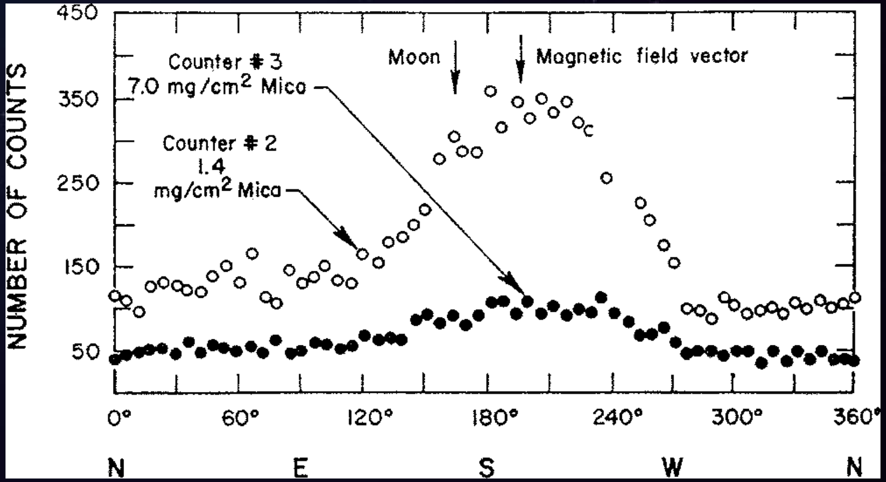

R. Giacconi, H. Gursky, F. Paolini, and B. B. Rossi, Evidence for x Rays From Sources Outside the Solar System, Phys. Rev. Lett. 9 (1962) 439

Radio - astronomy

A. Hewish - Nobel Prize 1974

1604

1962

1912

1964

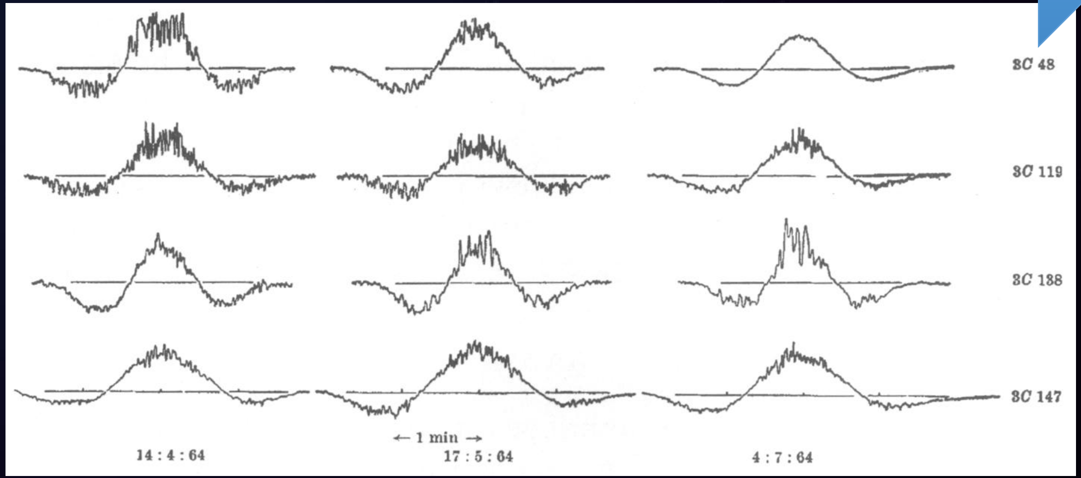

First observation: signals from a pulsar

A. Hewish, P.F. Scott, D. Wills Interplanetary Scintillation of Small Diameter Radio Sources. Nature 203, 1214–1217 (1964). https://doi.org/10.1038/2031214a0

Microwave - astronomy

A.A. Penzias and R.W. Wilson - Nobel Prize 1978

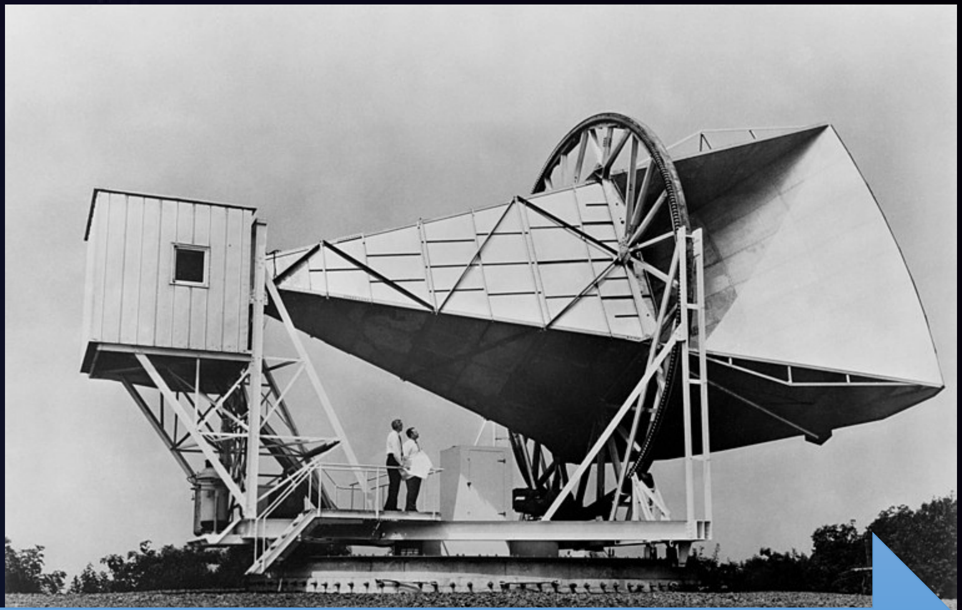

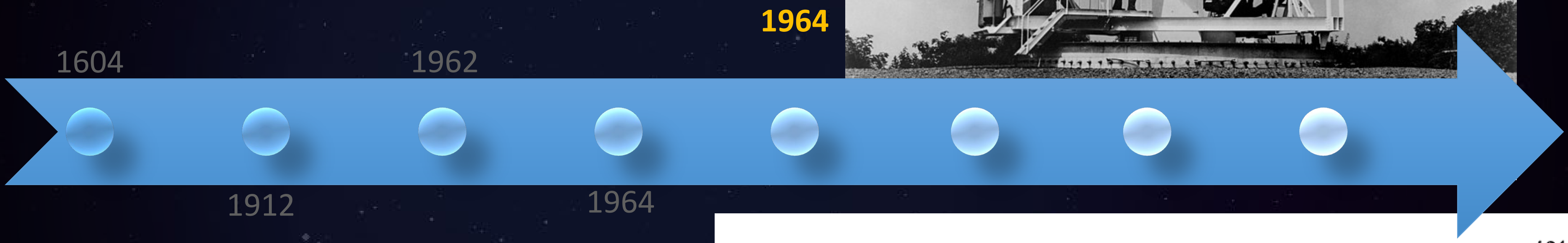

First observation of the MWCB

No. 1, 1965 LETTERS TO THE EDITOR 421

Note added in proof.—The highest frequency at which the background temperature of the sky had been measured previously was 404 Mc/s (Pauliny-Toth and Shakeshaft 1962), where a minimum temperature of 16° K was observed. Combining this value with our result, we find that the average spectrum of the background radiation over this frequency range can be no steeper than $\lambda^{0.7}$. This clearly eliminates the possibility that the radiation we observe is due to radio sources of types known to exist, since in this event, the spectrum would have to be very much steeper.

A. A. Penzias
R. W. Wilson

May 13, 1965
Bell Telephone Laboratories, Inc
Crawford Hill, Holmdel, New Jersey

A.A. Penzias and R.W. Wilson A Measurement of Excess Antenna Temperature at 4080 Mc/s. The Astrophysical Journal, (1965) 142, 419-421

(Solar) Neutrino - astronomy

R. Davis Jr. - Nobel Prize 2002

1604 1912 1962 1964 1964 **1970s**

First observation of the solar neutrinos

B.T. Cleveland et al. Measurement of the Solar Electron Neutrino Flux with the Homestake Chlorine Detector, 1998 ApJ 496 505

INTRODUCTION

The Homestake solar neutrino experiment was built in the period 1965–1967 to observe the total solar neutrino flux above 0.814 MeV by a radiochemical method based upon the inverse beta process, $^{37}Cl + \nu \rightarrow e^- + {}^{37}Ar$ of Pontecorvo, 1948. The construction of the Homestake experiment was stimulated by the fact that measurements of the $^3He(^4He, \gamma)^7Be$ reaction by Holmgren and Johnston (1959) showed that the cross section for this capture reaction was higher than anticipated by theoretical arguments and therefore must play a significant role in the Bethe–Critchfield proton–proton fusion chain. It followed that two new branches in the termination of this chain were necessary, the now familiar P–PII and P–PIII branches (Fowler, 1958; Cameron, 1958). These branches included two new neutrino sources, the decay of ^7Be and ^8B, that yield neutrinos above the threshold energy of the $^{37}Cl - {}^{37}Ar$ absorption reaction. Furthermore, it was found that the neutrino capture cross section for ^{37}Cl is greatly enhanced by the presence of the analog and other excited states in ^{37}Ar (Bahcall, 1964). This fact implied that the chlorine experiment would be particularly sensitive to the energetic neutrinos from ^8B decay.

(Cosmic) Neutrino - astronomy

M. Koshiba - Nobel Prize 2002

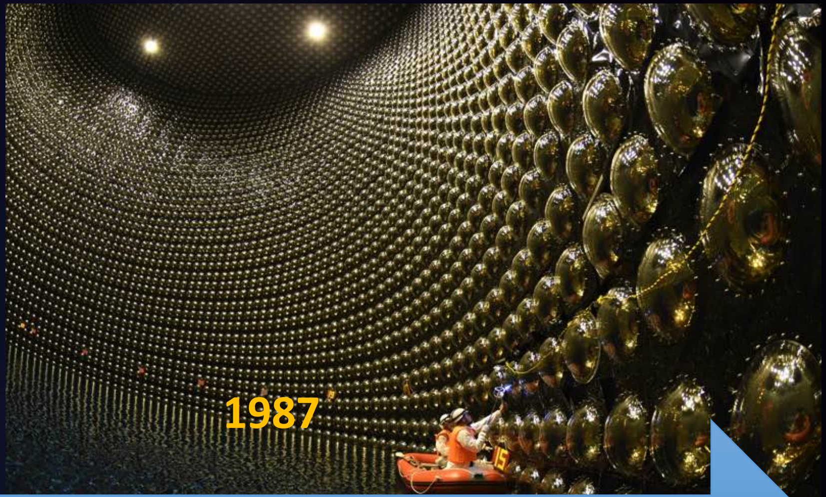

1604

1912

1962

1964

1964

1970s

1987

First observation of the SN neutrinos

K.S. Hirata et al. (Kamiokande-II Collaboration) Observation in the Kamiokande-II Detector of the Neutrino Burst from Supernova SN 1987a. Phys.Rev.D 38 (1988) 448-458

Gravitational Wave - astronomy

B.C. Barish, K.S. Thorne, R. Weiss - Nobel Prize 2017

1604

1912

1962

1964

1964

1970s

1987

2015

First observation GW150914

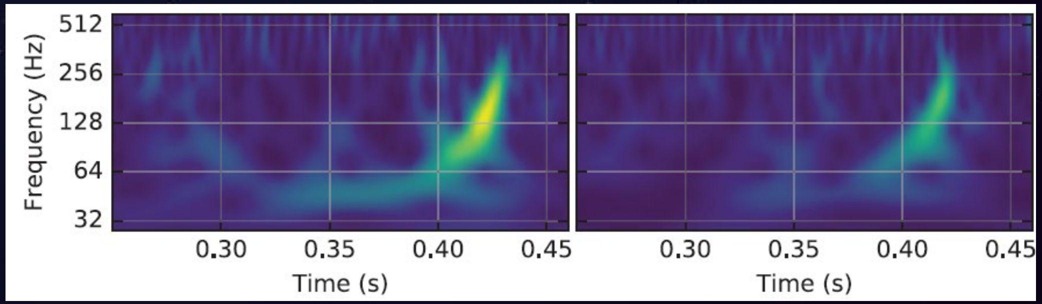

B. P. Abbott et al.* (LIGO Scientific Collaboration and Virgo Collaboration) Observation of Gravitational Waves from a Binary Black Hole Merger, PRL 116, 061102 (2016)

The Multimessenger Era

GCN (gcn.gsfc.nasa.gov): The Gamma-ray Coordinates Network (TAN: Transient Astronomy Network) includes: Optical, Radio, GeV/TeV Gamma-ray, neutrinos

CHIRP (chirp.sr.bham.ac.uk): Gravitational Waves

SNEWS (snews.bnl.gov): SuperNova Early Warning System

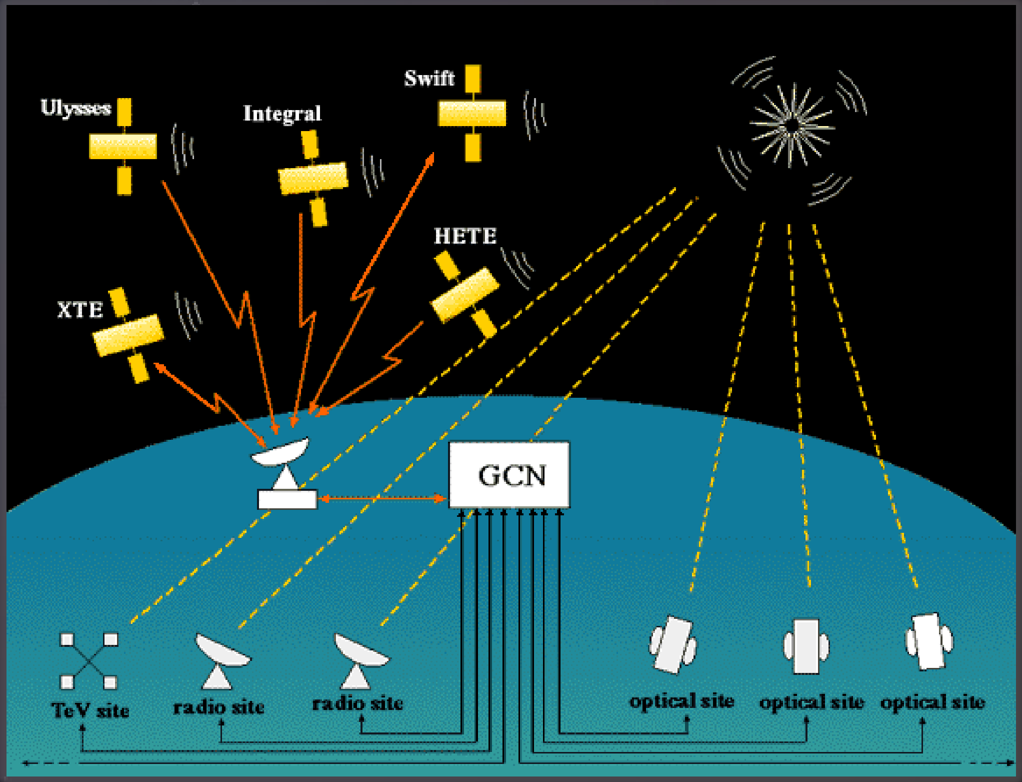

The Multimessenger Era - GW170817

6-th GW event observed, first corresponding to two neutron star coalescence, duration of approximately 100 seconds

The aftermath of this merger was seen by 70 observatories on 7 continents and in space, across the electromagnetic spectrum, marking a significant breakthrough for multi-messenger astronomy.

Independently, a short (~2 s duration) gamma-ray burst, GRB 170817A, was detected by the Fermi and INTEGRAL spacecraft beginning 1.7 seconds after the GW merger signal.

An astronomical transient designated AT 2017gfo (originally, SSS 17a) was found, 11 hours after the GW signal, in the galaxy NGC 4993 during a search of the region indicated by the GW detection. Observed by numerous telescopes, from radio to X-ray wavelengths, over the following days and weeks, has been explained as a fast-moving, rapidly-cooling cloud of neutron-rich material ejected from the neutron-star merger.

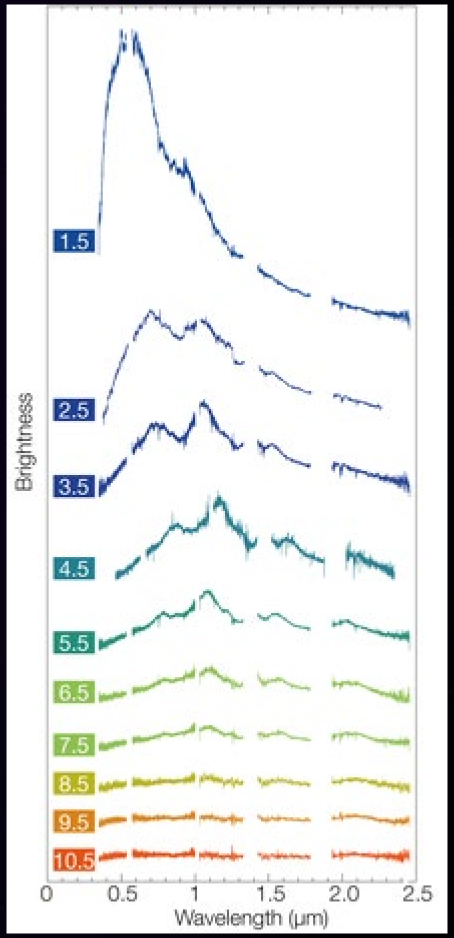

E.Amaldi, “From the Discovery of the Neutron to the Discovery of Nuclear Fission”, Phys. Rep., 111 (1-4), 1-331

The Neutrino(s)

1914 – J. Chadwick observes that the β rays have a continuous energy distribution

Verhandlungen der Deutschen Physikalischen Gesellschaft, 16 (1914) 383–391.

1930 – W. Pauli proposed the existence of a neutral particle with small mass

Open Letter to the Group of Radioactives at the Meeting in Tübingen, Dec. 4th, 1930

1932 – E. Fermi named the «neutrino» for the first time

1934 – E. Fermi description of the β-decay

E.Fermi,Tentativo di una teoria dei raggi β, Nuovo Cimento 11 (1934) 1-19;Versuch einer Theorie der β-Strahlen I, Zeit. f. Phys. 88 (1934) 161-171

$$\omega = \frac{2\pi}{\hbar} \left|H_{fi}\right|^2 \rho_f$$

$$H_{fi} = \frac{G_F}{V} M_{fi} = \frac{G_F}{V} \int \Psi_f \Psi_i d\tau$$

$$G_F = 1.166 \cdot 10^{-5}\ \mathrm{GeV}^{-2}$$

The Neutrino(s)

1937 – C.D. Anderson and S. Neddermeyer observed the first muon

S.H. Neddermeyer and C.D. Anderson, Note on the Nature of Cosmic-Ray Particles Phys. Rev. 51 (1937) 884

1953 – C.Cowan and F. Reines observed the first (anti-)neutrino

C. L. Cowan, F. Reines et al. Detection of the Free Neutrino: a Confirmation, Science, 124 (1956) 103–104

1957 – B. Pontecorvo speculated the neutrino oscillations

B. Pontecorvo, Sov.Phys.JETP 6 (1957) 429

1958 – M. Goldhaber et al. determined the helicity of the neutrino

M.Goldhaber, L.Grodzins and A.W.Sunyar, Phys.Rev. 109, 1015 (1958)

1962 – Direct observation of muon neutrino

G. Danby, J-M Gaillard, K. Goulianos, L.M. Lederman, N. Mistry, M. Schwartz and J. Steinberger, Phys. Rev. Lett. 9 (1962) 36

The Neutrino(s)

1989 – LEP determined the number of «light» neutrinos

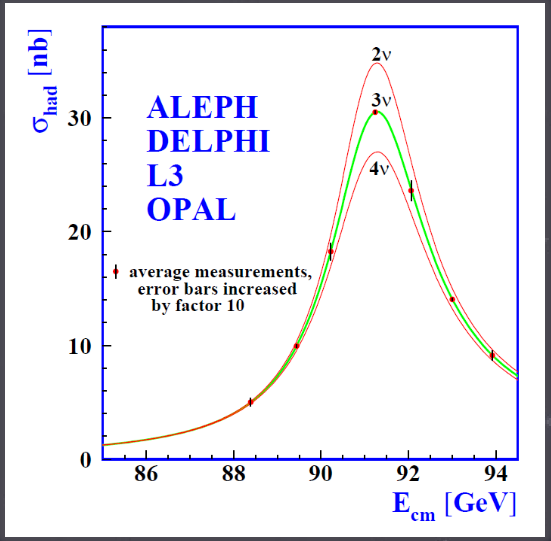

S. Schael et al. Precision electroweak measurements on the Z Resonance, Phys. Rept. 427, 257–454 (2006)

1998 – Confirmation of neutrino flavour oscillation

Y. Fukuda, et al. (Super-Kamiokande Collaboration) Evidence for Oscillation of Atmospheric Neutrinos Phys. Rev. Lett. 81 (1998) 1562–1567

2000 - Direct observation of tau neutrino

K. Kodama et al. (DONUT Collaboration, Observation of tau neutrino interactions, in Physics Letters B504 (2001) 218

The Neutrino Sources and Fluxes

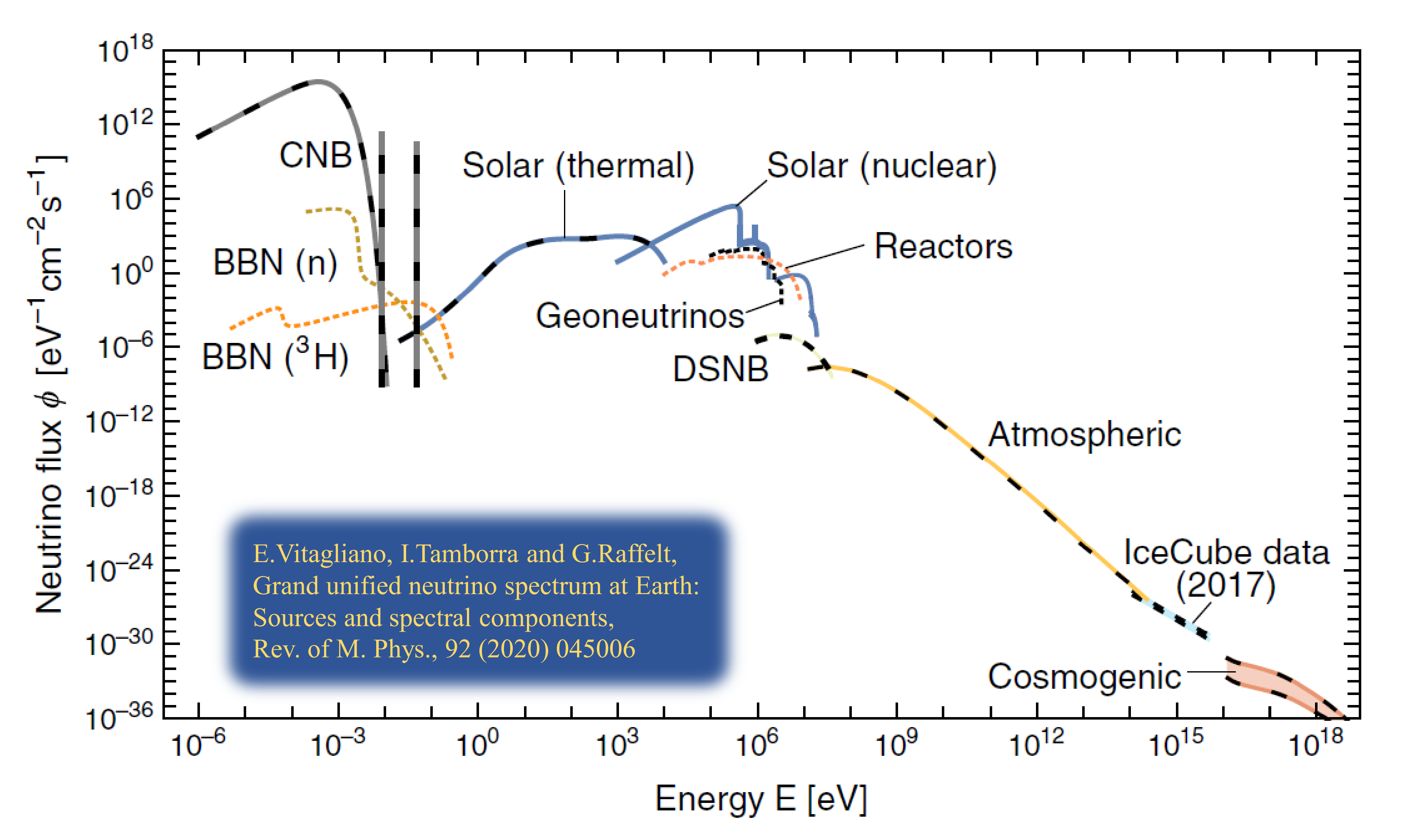

J.Formaggio and G.Zeller "From eV to EeV: Neutrino Cross Sections Across Energy Scales." Rev. of Mod. Phys. 84 (2012) 1307–1341.

The Neutrino Detection

The interaction with leptons and quarks is determined by the exchange of a Vector Boson

Charged current

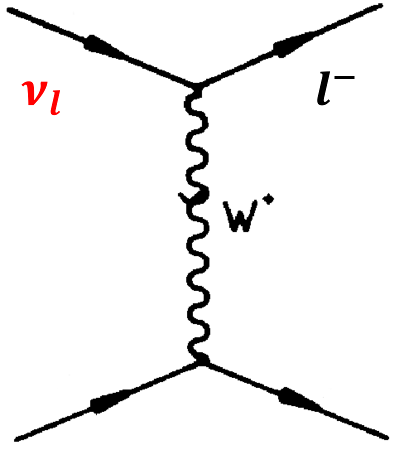

Only left-handed particles interact

Neutral current

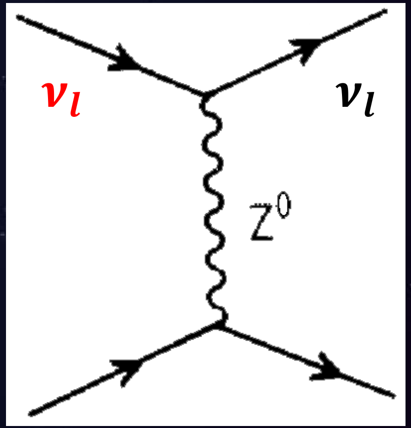

Left-handed and right-handed particles interact with different coupling

The Neutrino Detection

$$\nu_{\mu(\tau)} + e^- \rightarrow \nu_e + \mu^-(\tau^-)$$

$$E_{\mu\,min} = 1.08 \times 10^4 \text{ MeV}$$
$$E_{\tau\,min} = 3 \times 10^6 \text{ MeV}$$

$$\nu_e + e^- \rightarrow \nu_e + e^-$$

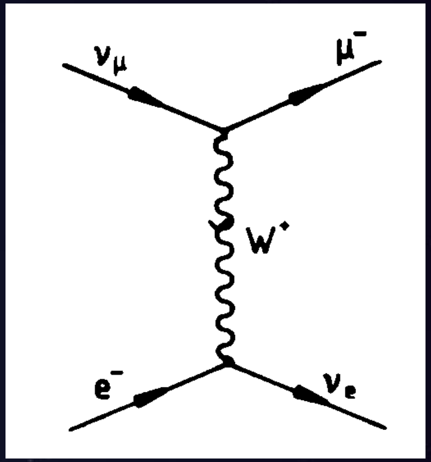

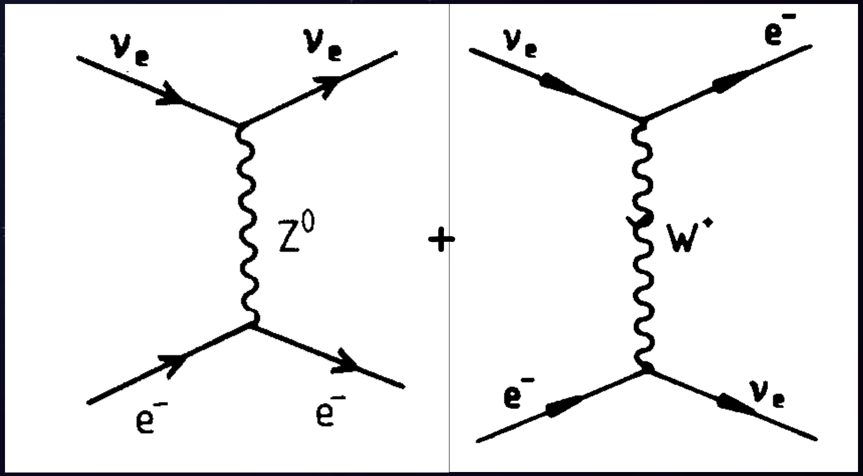

Scattering $\nu_\mu + e^- \to \mu^- + \nu_e$ - Building the Cross Section

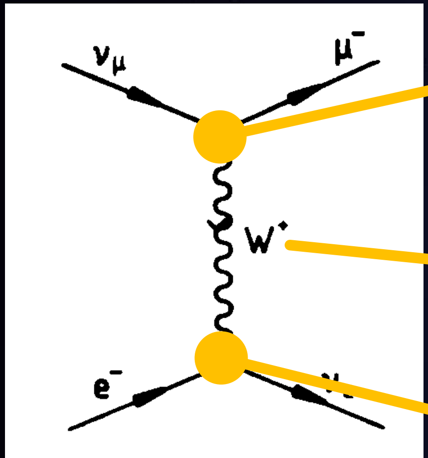

$$-i\frac{g}{\sqrt{2}}\gamma_\mu\frac{(1-\gamma_5)}{2}$$

$$-\frac{g^{\mu\nu}+\frac{q^\mu q^\nu}{M_W^2}}{q^2-M_W^2}$$

$$-i\frac{g}{\sqrt{2}}\gamma_\nu\frac{(1-\gamma_5)}{2}$$

$$F=\bar{u}(\boldsymbol{\mu})\left(-i\frac{g}{\sqrt{2}}\gamma_\mu\frac{(1-\gamma_5)}{2}\right)u(\boldsymbol{\nu_\mu})\times$$

$$\times\left(-\frac{g^{\mu\nu}+\frac{q^\mu q^\nu}{M_W^2}}{q^2-M_W^2}\right)\times$$

$$\times\,\bar{u}(\boldsymbol{\nu_e})\left(-i\frac{g}{\sqrt{2}}\gamma_\nu\frac{(1-\gamma_5)}{2}\right)u(\boldsymbol{e})$$

$$d\sigma\propto\frac{1}{2}\sum_{s,r}\sum_{s',r'}|F|^2$$

Scattering $\nu_\mu + e^- \rightarrow \mu^- + \nu_e$

$$g = \frac{e}{\sin\theta_W}$$

$$\frac{G_F}{\sqrt{2}} = \frac{g^2}{8M_W^2}$$

$$G_F = 1.166 \times 10^{-5}\ \mathrm{GeV}^{-2}$$

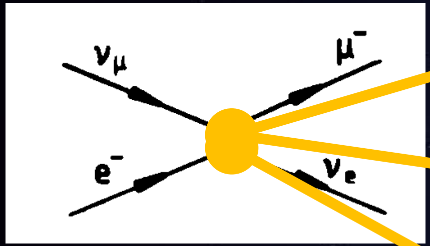

$$-i\frac{g}{\sqrt{2}}\gamma_\mu\frac{(1-\gamma_5)}{2}$$

$$\frac{g^{\mu\nu}}{M_W^2}$$

$$-i\frac{g}{\sqrt{2}}\gamma_\nu\frac{(1-\gamma_5)}{2}$$

$$F = \frac{\boldsymbol{g^2}}{\boldsymbol{8M_W^2}}\bar{u}(\boldsymbol{\mu})\gamma_\mu(1-\gamma_5)u(\boldsymbol{\nu_\mu})g^{\mu\nu}\bar{u}(\boldsymbol{\nu_e})\gamma_\nu(1-\gamma_5)u(\boldsymbol{e})$$

$$d\sigma \propto \frac{1}{2}\sum_{s,r}\sum_{s',r'}|F|^2 = \left(\frac{G_F^2}{2}\right)^2 N_{\mu\nu}E^{\mu\nu}$$

Average on the initial spin values

Sum over initial and final spin values

Elementary Particle Spin-½ *Weak* Tensor

$$\sigma = 2\frac{m_e G_F^2}{\pi}E_\nu$$

Scattering $\nu_x + e^-$ - Summary Cross Sections

$$\sigma_0 = 2\frac{m_e^2 G_F^2}{\pi} = 8.8 \times 10^{-45}\ \mathrm{cm}^2$$

$\nu_e + e^- \to \nu_e + e^-$	$\sigma = \sigma_0 \frac{\boldsymbol{E_\nu}}{m_e}\left[\left(\frac{1}{2}+\xi\right)^2 + \frac{1}{3}\xi^2\right]$	$\sigma = 0.55 \times \sigma_0 \frac{E_\nu}{m_e}$
$\bar{\nu}_e + e^- \to \bar{\nu}_e + e^-$	$\sigma = \sigma_0 \frac{\boldsymbol{E_\nu}}{m_e}\left[\frac{1}{3}\left(\frac{1}{2}+\xi\right)^2 + \xi^2\right]$	$\sigma = 0.23 \times \sigma_0 \frac{E_\nu}{m_e}$
$\nu_{\mu(\tau)} + e^- \to \nu_{\mu(\tau)} + e^-$	$\sigma = \sigma_0 \frac{\boldsymbol{E_\nu}}{m_e}\left[\left(\frac{1}{2}-\xi\right)^2 + \frac{1}{3}\xi^2\right]$	$\sigma = 0.09 \times \sigma_0 \frac{E_\nu}{m_e}$
$\nu_{\mu(\tau)} + e^- \to \nu_e + \mu^-(\tau^-)$	$\sigma = \sigma_0 \frac{\boldsymbol{E_\nu}}{m_e}$	$\sigma = \sigma_0 \frac{E_\nu}{m_e}$
$\bar{\nu}_{\mu(\tau)} + e^- \to \bar{\nu}_{\mu(\tau)} + e^-$	$\sigma = \sigma_0 \frac{\boldsymbol{E_\nu}}{m_e}\left[\frac{1}{3}\left(\frac{1}{2}+\xi\right)^2 + \xi^2\right]$	$\sigma = 0.08 \times \sigma_0 \frac{E_\nu}{m_e}$

$$\xi = \sin^2\theta_W$$

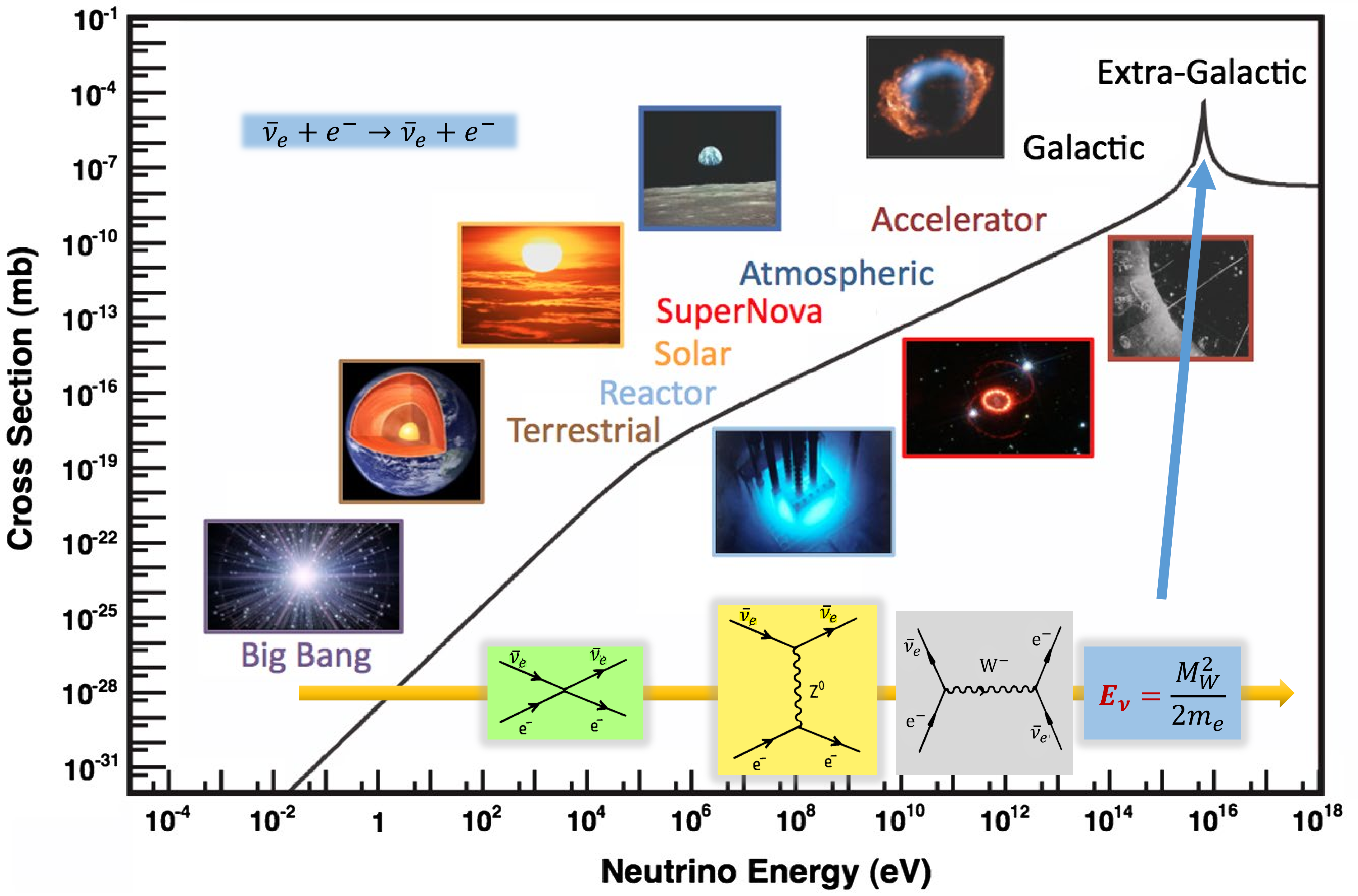

Cross Section (mb)
Neutrino Energy (eV)
10^{-1}
10^{-4}
10^{-7}
10^{-10}
10^{-13}
10^{-16}
10^{-19}
10^{-22}
10^{-25}
10^{-28}
10^{-31}
10^{-4}
10^{-2}
1
10^{2}
10^{4}
10^{6}
10^{8}
10^{10}
10^{12}
10^{14}
10^{16}
10^{18}
$\bar{\nu}_e + e^- \rightarrow \bar{\nu}_e + e^-$
Extra-Galactic
Galactic
Accelerator
Atmospheric
SuperNova
Solar
Reactor
Terrestrial
Big Bang
$\bar{\nu}_e$
$\bar{\nu}_e$
e^-
e^-
Z^0
W^-
$E_\nu = \frac{M_W^2}{2m_e}$

Scattering $\nu_x + e^-$ - Summary Cross Sections

A remarkable feature of neutrino-electron scattering is that it is highly directional.

The outgoing electron is emitted at very small angles with respect to the incoming neutrino direction.

$$E_e \theta_e^2 \leq 2m_e$$

This property has been widely used by the experiments observing the solar neutrino flux

Scattering $\nu_l + A \to l^- + X$

Low energy (few MeV)

only process of interest $\quad \boldsymbol{\nu_e} + {}^A_Z X \to \boldsymbol{e^-} + {}_{Z+1}^{\;\;A}X$

the process is connected to the beta decay via the principle of detailed balancing

cross section of the order $\sigma \approx 10^{-42}\ \mathrm{cm}^2$

threshold given by $E_{th} = M_{at}(A, Z+1) - M_{at}(A, Z)$

$$\nu_e + {}^{71}\mathrm{Ga} \to {}^{71}\mathrm{Ge} + e^- \quad 0.23\ \mathrm{MeV}$$

$$\nu_e + {}^{37}\mathrm{Cl} \to {}^{37}\mathrm{Ar} + e^- \quad 0.82\ \mathrm{MeV}$$

Scattering $\nu_l + A \rightarrow l^- + X$

Medium energy (1-100 MeV)

quasi elastic scattering on single nucleon

$$\boldsymbol{\nu_e} + \mathrm{n} \rightarrow \boldsymbol{e^-} + \mathrm{p}$$
$$(\boldsymbol{\bar{\nu}_e} + \mathrm{p} \rightarrow \boldsymbol{e^+} + \mathrm{n})$$

(for $\boldsymbol{\bar{\nu}_e}$ threshold given by $E_{th} = \frac{(m_n+m_e)^2-m_p^2}{2m_p} = 1.806\ \mathrm{MeV}$)

the process is connected to the neutron decay via the principle of detailed balancing

$$\bar{u}(\mathbf{p})\gamma_\mu(1 - g_A\gamma_5)u(\mathbf{n}) \qquad g_A \approx 1.26$$

cross section (free nucleon)

$$\sigma = 1.6 \times 10^{-44}(1 + 3g_A^2)\left(\frac{E_\nu}{\mathrm{MeV}}\right)^2\ \mathrm{cm}^2$$

Scattering $\nu_l + A \to l^- + X$

Medium energy (> GeV)

quasi elastic scattering on single nucleon

resonance production

deep inelastic scattering on single parton

$\nu_l + \mathrm{d} \to l^- + \mathrm{u}$

$(\bar{\nu}_l + \mathrm{u} \to l^+ + \mathrm{d})$

cross section (isoscalar target $\frac{\mathrm{p+n}}{2}$)

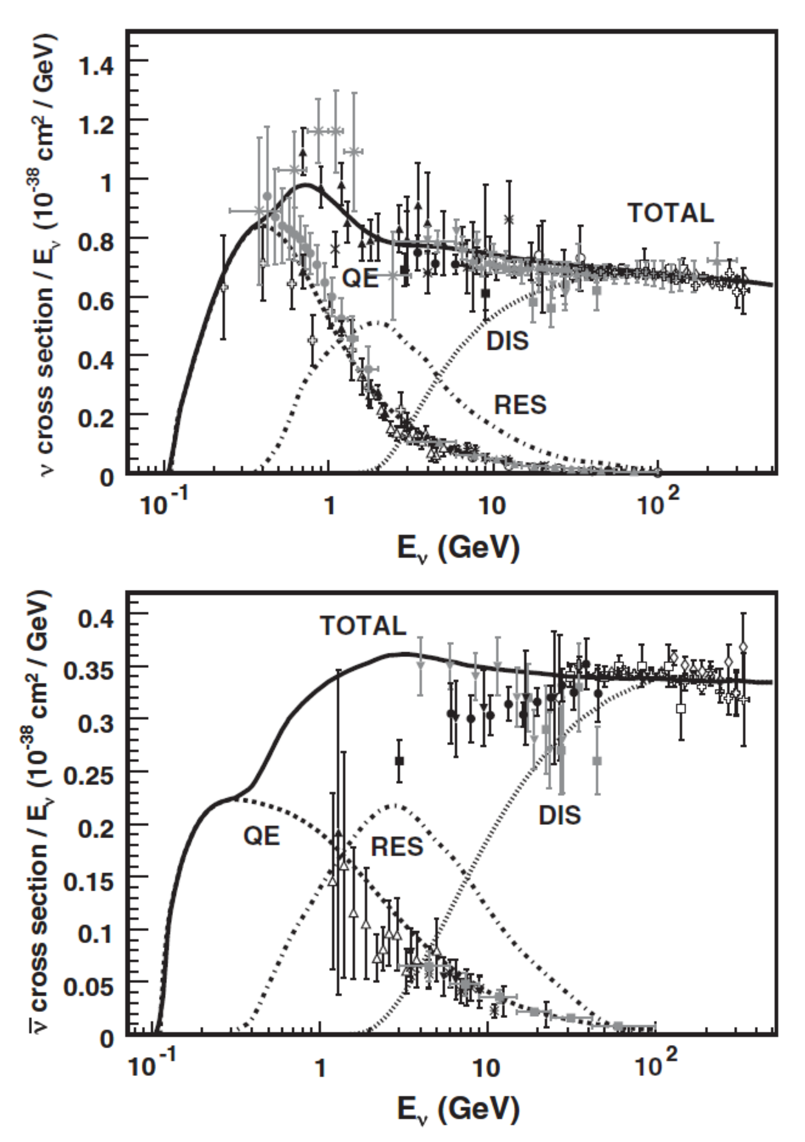

Scattering $\nu_l + A \to l^- + X$

Medium energy (> 20 GeV)

deep inelastic scattering on single parton

$\nu_l + \mathrm{d} \to l^- + \mathrm{u}$

$(\bar{\nu}_l + \mathrm{u} \to l^+ + \mathrm{d})$

cross section (isoscalar target $\frac{\mathrm{p+n}}{2}$)

$$\sigma(\nu_l \to l^-) = \frac{G_F^2}{\pi} M E_\nu \left[\langle x\rangle_q + \frac{1}{3}\langle x\rangle_{\bar{q}}\right]$$

$$\sigma(\bar{\nu}_l \to l^+) = \frac{G_F^2}{\pi} M E_\nu \left[\frac{1}{3}\langle x\rangle_q + \langle x\rangle_{\bar{q}}\right]$$

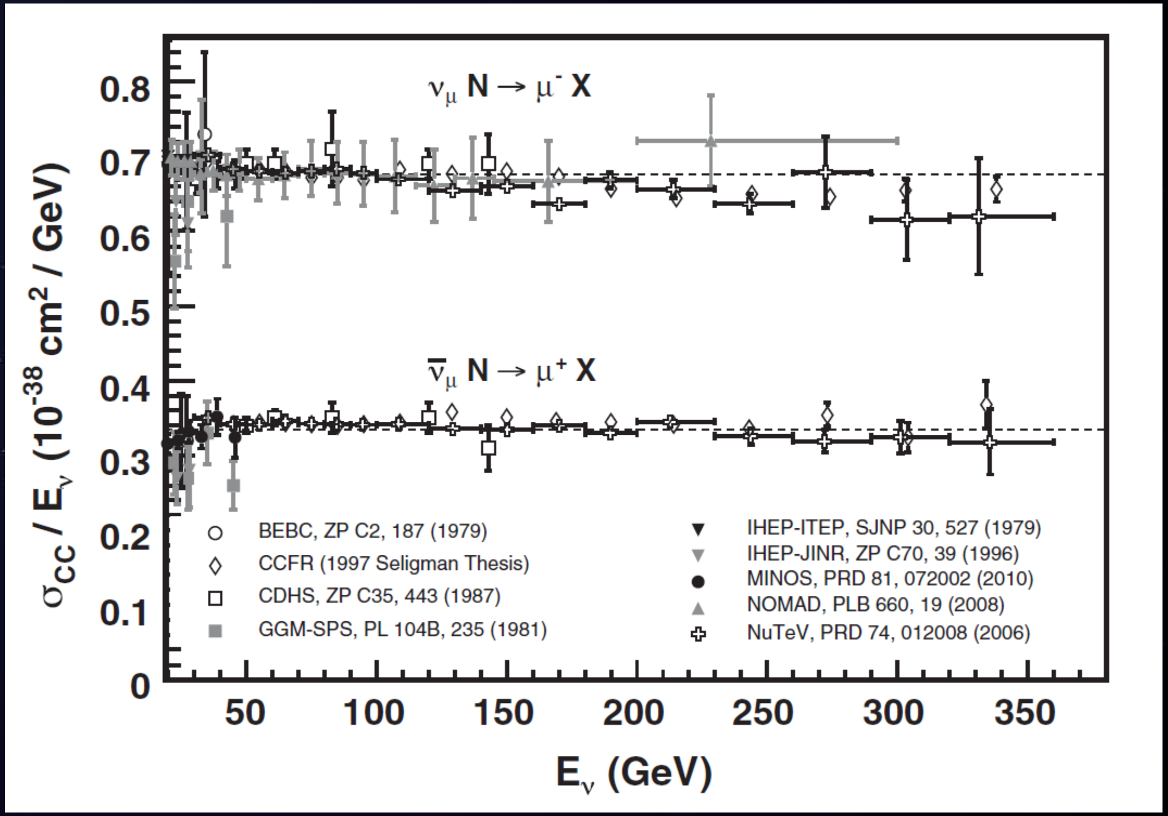

Scattering $\nu_l + A \to l^- + X$

Medium energy (> 0.5 TeV)

deep inelastic scattering on single parton

but the Vector Meson no longer dominates

$$\sigma(\nu_l \to l^-) = 5.53 \cdot 10^{-36} \left(\frac{E_\nu}{1\ \mathrm{GeV}}\right)^{0.363}$$

At $E_{\bar{\nu}} \approx 10^4$ TeV dominates the resonant process

$$\bar{\nu}_e + e^- \to W^-$$

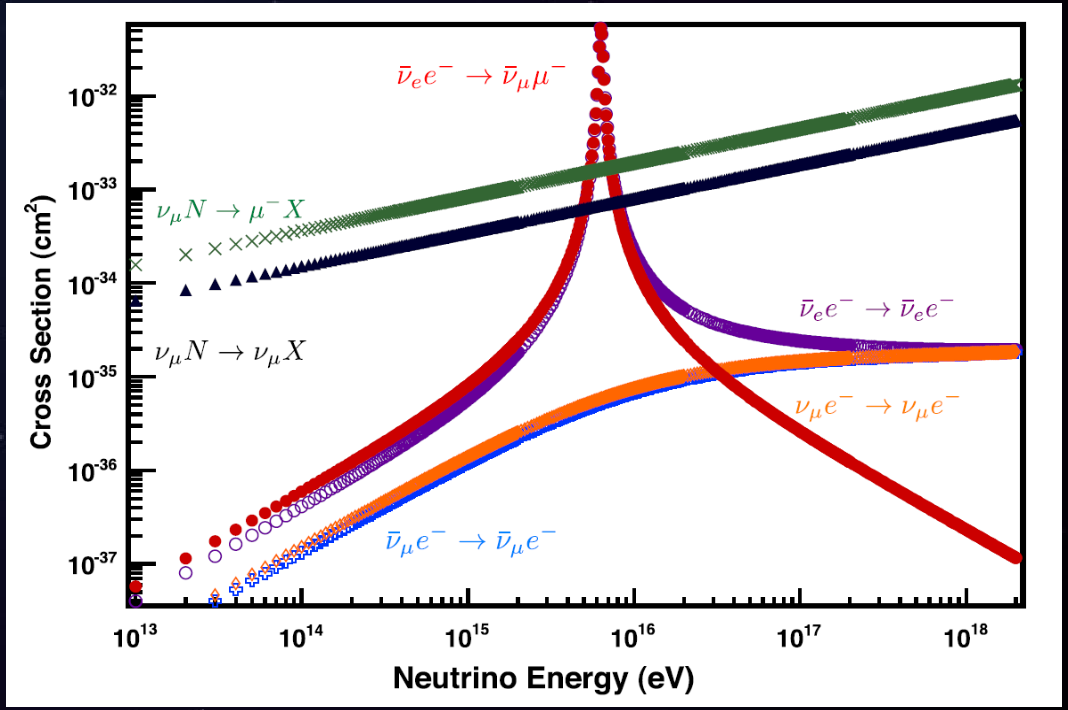

Part 1 - Final Consideration

New technologies offer the unique opportunity to study the Nature through new windows

Large field of view and timing necessary for Multimessenger Astronomy

Experimental challenge

- neutrino detection
- statistics
- energy measurement
- direction reconstruction

Part 1 - Final Consideration

Neutrino detection

energy transfer to ionizing particle

cross section small

Conversion rate $= \left(\int \frac{d\Phi_\nu}{dE_\nu} \cdot \sigma(E_\nu) \cdot dE_\nu\right) \cdot S \cdot N_{A\nu} \cdot \frac{\rho x}{A} = \Phi_\nu \cdot \langle\sigma\rangle \cdot N_{A\nu} \cdot \frac{\rho}{A} \cdot V_{det}$

Statistics

C. L. Cowan, F. Reines et al. Detection of the Free Neutrino: a Confirmation, Science, 124 (1956) 103–104

$Savannah\ River$

$\Phi_{\bar{\nu}} = 10^{17}\ \mathrm{s}^{-1}\mathrm{cm}^{-2}$

$\sigma = 6 \cdot 10^{-44}\ \mathrm{cm}^{-2}$

$V_{det} = 2 \cdot 10^{5}\ \mathrm{cm}^{3}$

$\bar{\boldsymbol{\nu}}_{\boldsymbol{e}} + \mathrm{p} \rightarrow \boldsymbol{e}^{+} + \mathrm{n}$

conversion rate $\sim \mathrm{s}^{-1}$

The Neutrino Mass

The neutrino masses are small and the absolute scale is still unknown

$$\delta m^2_{sol} = m_2^2 - m_1^2 = 7.5 \times 10^{-5}\ \mathrm{eV}^2$$

$$\delta m^2_{atm} = m_3^2 - m_{12}^2 = \pm 2.45 \times 10^{-3}\ \mathrm{eV}^2$$

The eigenstates of the interaction Hamiltonian are different from the eigenstates of the free Hamiltonian

Eigenstates are connected by the unitary matrix U_{li}

$$\nu_l = \sum_i U_{li} \nu_i$$

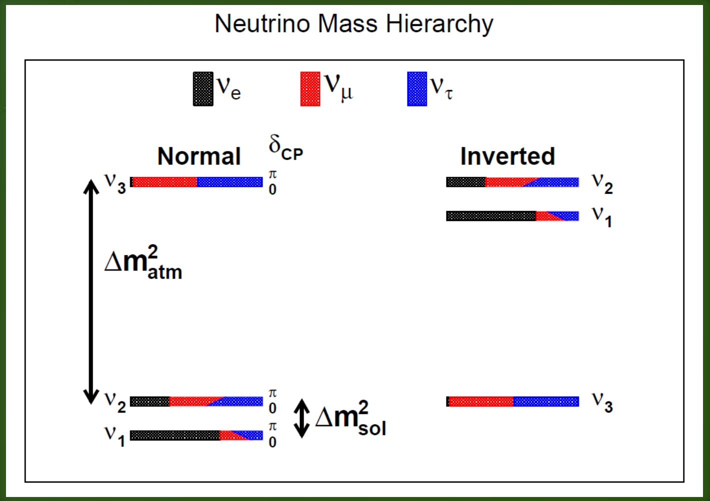

The Neutrino Oscillations

PMNS matrix (Pontecorvo, Maki, Nakagawa and Sakata): three angles and one CP phase

$$U_{li} = \begin{pmatrix} 1 & 0 & 0 \\ 0 & c_{23} & s_{23} \\ 0 & -s_{23} & c_{23} \end{pmatrix} \cdot \begin{pmatrix} c_{13} & 0 & s_{13}e^{-i\delta_{CP}} \\ 0 & 1 & 0 \\ -s_{13}e^{i\delta_{CP}} & 0 & c_{13} \end{pmatrix} \cdot \begin{pmatrix} c_{12} & s_{12} & 0 \\ -s_{12} & c_{12} & 0 \\ 0 & 0 & 1 \end{pmatrix}$$

$$\theta_{12} = 33.48^{+0.77}_{-0.74}$$
$$\theta_{23} = 42.2^{+0.1}_{-0.1}$$
$$\theta_{12} = 8.52^{+0.20}_{-0.21}$$

$$U = \begin{pmatrix} \cos\theta & \sin\theta \\ -\sin\theta & \cos\theta \end{pmatrix}$$

$$P_{\nu_l \to \nu_{l'}} = 1 - \sin^2 2\theta \cdot \sin^2\left(\pi \frac{L}{L_{osc}}\right)$$

$$L_{osc} = \frac{4\pi E_\nu}{\delta m^2} = 2.48 \frac{E_\nu/_{\mathrm{GeV}}}{\delta m^2/_{eV^2}}\ \mathrm{m}$$

E_ν (GeV)	L_{osc} 1 → 2 (m)	L_{osc} 2 → 3 (m)
10^{-3}	33	1
1	$3.3 \cdot 10^4$	10^3
10^3	$3.3 \cdot 10^7$	10^6
10^6	$3.3 \cdot 10^{10}$	10^9

A.Yu.Smirnov," The MSW Effect and Matter Effects in Neutrino Oscillations", Physica Scripta T121 (2005) 57-64

The Neutrino Oscillations

Neutrino flavour oscillation in matter differs from oscillation in vacuum

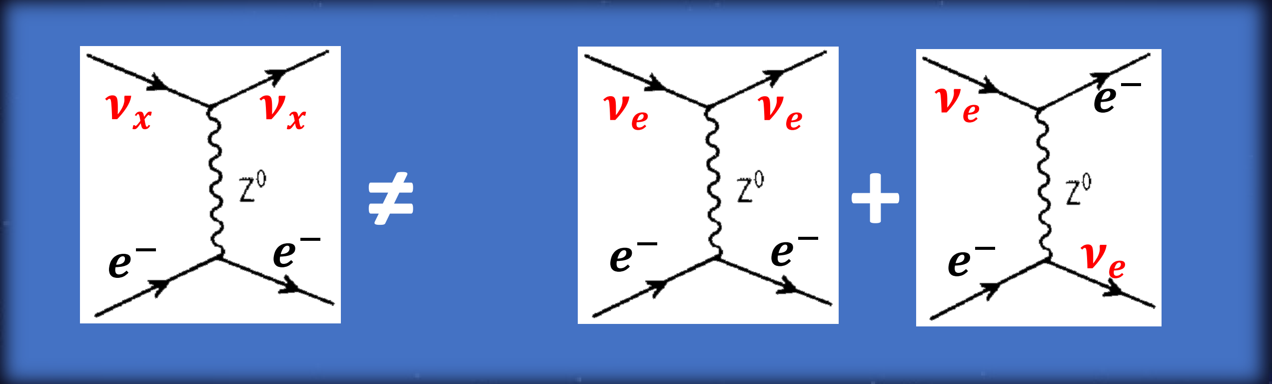

Coherent elastic forward scattering, similarly to optics, generates a phase difference, a refractive index, or equivalently, a neutrino effective mass.

The **MSW** (Mikheyev-Smirnov-Wolfenstein) effect is the adiabatic or partially adiabatic neutrino flavor conversion in medium with varying density

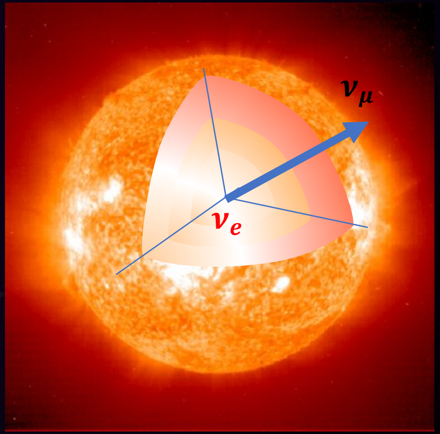

Solar Neutrinos

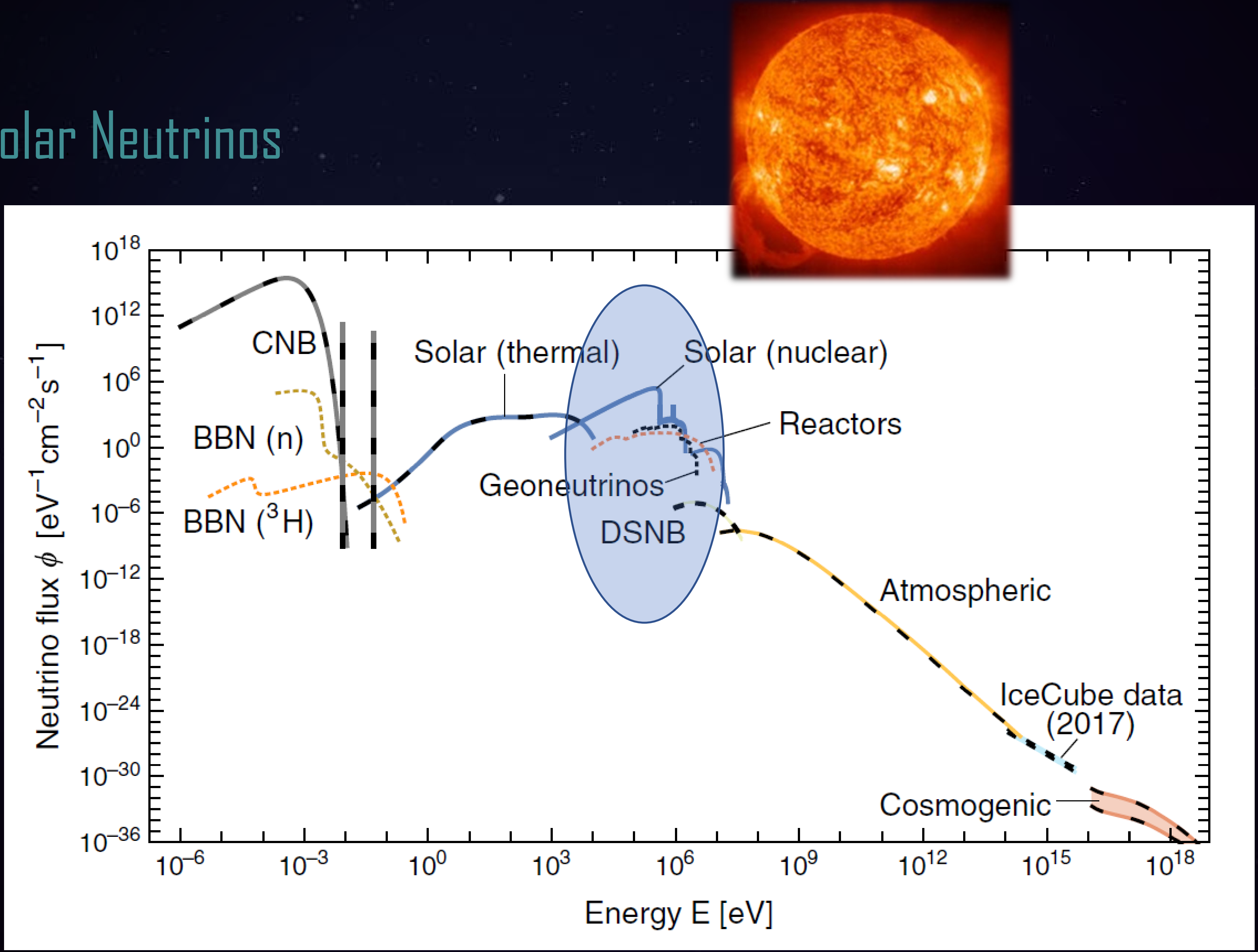

Solar Neutrinos

Solar Standard Model (**SSM**)
J.N.Bahcall and M.H.Pinsonneault
Rev.Mod.Phys. 67(1995)781

A – deuteron production

$\mathrm{p}+\mathrm{p}\to \mathrm{e}^{+}+\nu_e+\mathrm{d}$	99.6%	continuous spectrum
$\mathrm{p}+\mathrm{p}+\mathrm{e}^{-}\to \nu_e+\mathrm{d}$	0.4%	monoenergetic

B – ^{3}He production

$$\mathrm{d}+\mathrm{p}\to\gamma+{}^{3}\mathrm{He}$$

C – ^{4}He production

$^{3}\mathrm{He}+{}^{3}\mathrm{He}\to 2\mathrm{p}+{}^{4}\mathrm{He}$		85%	
$^{3}\mathrm{He}+{}^{4}\mathrm{He}\to\gamma+{}^{7}\mathrm{Be}$	$^{7}\mathrm{Be}+\mathrm{e}^{-}\to\nu_e+{}^{7}\mathrm{Li}\quad {}^{7}\mathrm{Li}+\mathrm{p}\to 2\,{}^{4}\mathrm{He}$	15%	monoenergetic
	$^{7}\mathrm{Be}+\mathrm{p}\to\gamma+{}^{8}\mathrm{B}\searrow 2\,{}^{4}\mathrm{He}+\mathrm{e}^{+}+\nu_e$	0.019%	continuous spectrum
$^{3}\mathrm{He}+\mathrm{p}\to \mathrm{e}^{+}+\nu_e+{}^{4}\mathrm{He}$		$2.4\cdot 10^{-5}$	continuous spectrum

Sola Neutrinos - CNO

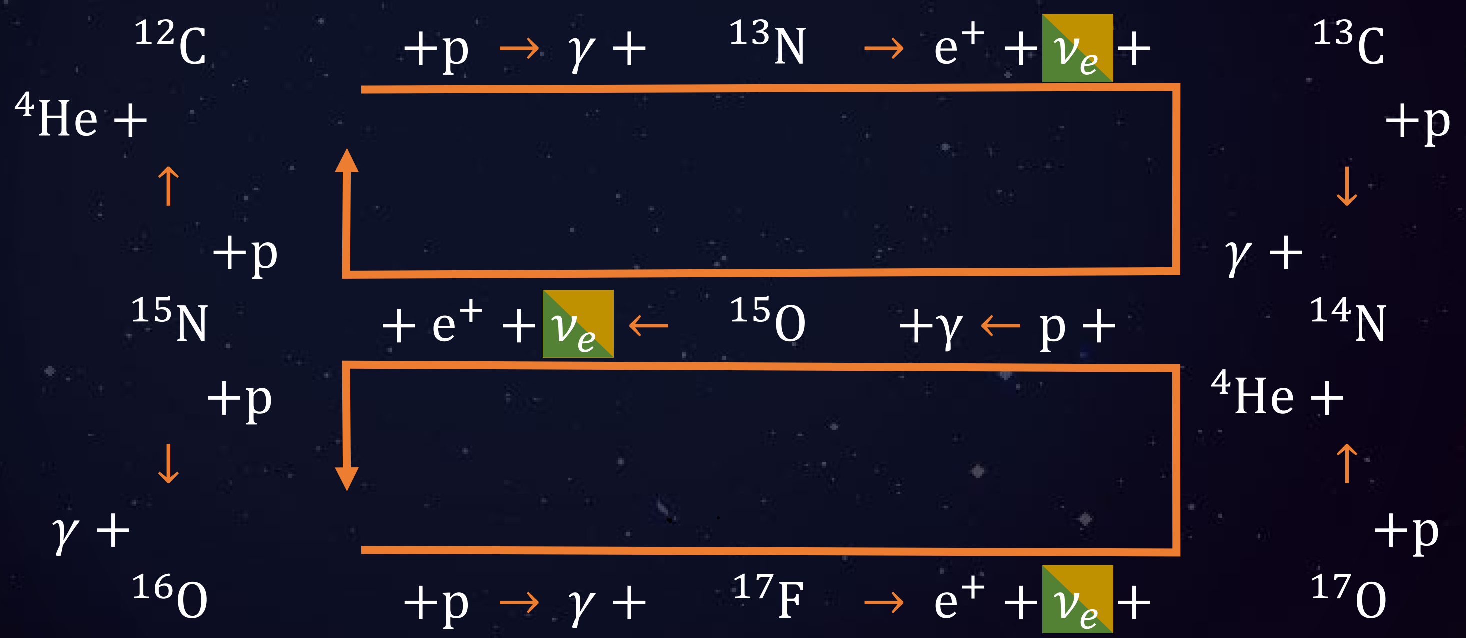

Solar Neutrinos

Channel	Flux	Reaction	E_{av} MeV	E_{max} MeV	Flux at Earth GS98	AGSS09	Observed	Units
pp Chains (β^+)	Φ_{pp}	$p + p \to d + e^+ + \nu_e$	0.267	0.423	5.98 ±0.6%	6.03 ±0.5%	$5.971^{+0.62\%}_{-0.55\%}$	10^{10} cm^{-2} s^{-1}
	Φ_B	$^8B \to {}^8Be^* + e^+ + \nu_e$	6.735 ± 0.036	∼ 15	5.46 ±12%	4.50 ±12%	$5.16^{+2.5\%}_{-1.7\%}$	10^6 cm^{-2} s^{-1}
	Φ_{hep}	$^3He + p \to {}^4He + e^+ + \nu_e$	9.628	18.778	0.80 ±30%	0.83 ±30%	$1.9^{+63\%}_{-47\%}$	10^4 cm^{-2} s^{-1}
pp Chains (EC)	Φ_{Be}	$e^- + {}^7Be \to {}^7Li + \nu_e$ $e^- + {}^7Be \to {}^7Li^* + \nu_e$	0.863 (89.7%) 0.386 (10.3%)		4.93 ±6%	4.50 ±6%	$4.80^{+5.9\%}_{-4.6\%}$	10^9 cm^{-2} s^{-1}
	Φ_{pep}	$p + e^- + p \to d + \nu_e$	1.445		1.44 ±1%	1.46 ±0.9%	$1.448^{+0.90\%}_{-0.90\%}$	10^8 cm^{-2} s^{-1}
CNO Cycle (β^+)	Φ_N	$^{13}N \to {}^{13}C + e^+ + \nu_e$	0.706	1.198	2.78 ±15%	2.04 ±14%	< 13.7	10^8 cm^{-2} s^{-1}
	Φ_O	$^{15}O \to {}^{15}N + e^+ + \nu_e$	0.996	1.732	2.05 ±17%	1.44 ±16%	< 2.8	10^8 cm^{-2} s^{-1}
	Φ_F	$^{17}F \to {}^{17}O + e^+ + \nu_e$	0.998	1.736	5.29 ±20%	3.26 ±18%	< 8.5	10^6 cm^{-2} s^{-1}
CNO Cycle (EC)	Φ_{eN}	$^{13}N + e^- \to {}^{13}C + \nu_e$	2.220		2.20 ±15%	1.61 ±14%	—	10^5 cm^{-2} s^{-1}
	Φ_{eO}	$^{15}O + e^- \to {}^{15}N + \nu_e$	2.754		0.81 ±17%	0.57 ±16%	—	10^5 cm^{-2} s^{-1}
	Φ_{eF}	$^{17}F + e^- \to {}^{17}O + \nu_e$	2.758		3.11 ±20%	1.91 ±18%	—	10^3 cm^{-2} s^{-1}

E.Vitagliano, I.Tamborra and G.Raffelt,
Rev. of M. Phys., 92 (2020) 045006

$$4p \to {}^4He + 2e^+ + 2\nu_e \qquad Q = 26.73\ \mathrm{MeV}$$

$$\langle E(2\nu)\rangle = 0.59\ \mathrm{MeV}$$

$$L_\odot = 2.39 \times 10^{39}\ \mathrm{MeV}/\mathrm{s}$$

$$L_\nu = 2 \times \frac{L_\odot}{Q - \langle E(2\nu)\rangle} = 1.83 \times 10^{38}\ \nu/\mathrm{s}$$

$$\Phi_\nu = 6.51 \times 10^{10}\ \nu/\mathrm{cm}^2 \cdot \mathrm{s}$$

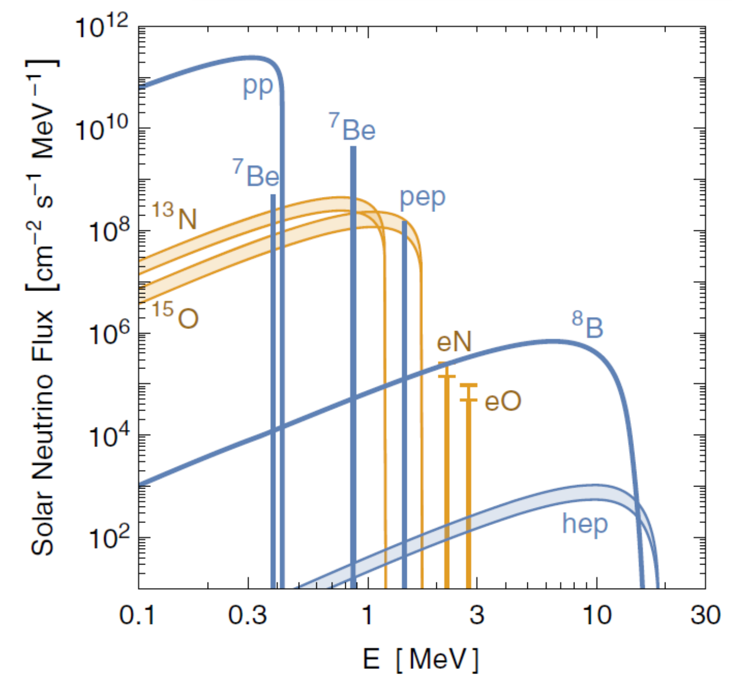

Solar Neutrinos – 1^ Puzzle

Homestake (1970-1994):

C_2Cl_4 mass: 6.15×10^5 kg

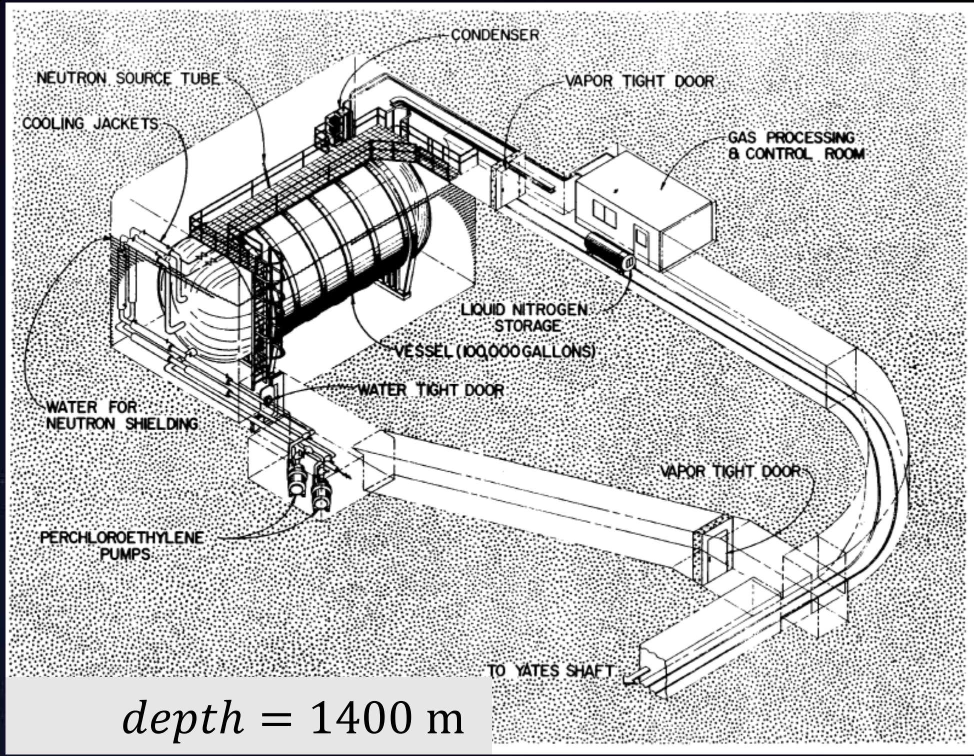

$depth = 1400$ m

B.T. Cleveland et al. Measurement of the Solar Electron Neutrino Flux with the Homestake Chlorine Detector, 1998 ApJ 496 505

Solar Neutrinos – 1^ Puzzle

Homestake (1970-1994):

C_2Cl_4 mass: 6.15×10^5 kg

process: $\nu_e + {}^{37}\mathrm{Cl} \rightarrow {}^{37}\mathrm{Ar} + e^-$ $\quad \tau_{\mathrm{Ar}} = 50$ d

108 individual observations in 25 years

Threshold at $E_\nu = 814$ keV

Sensitivity to ^{7}Be and ^{8}B neutrinos

1° solar neutrinos puzzle

Measured flux: 2.56±0.22 SNU

Expected flux: 7.6±1.3 SNU

$1\ SNU = 10^{-36}\ \mathrm{events}/\mathrm{atoms \cdot s}$

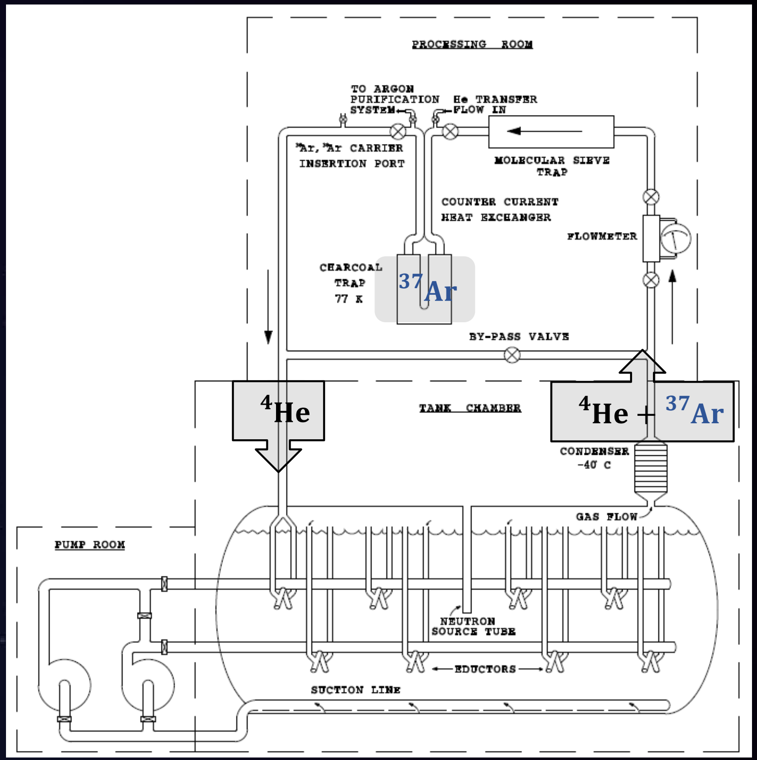

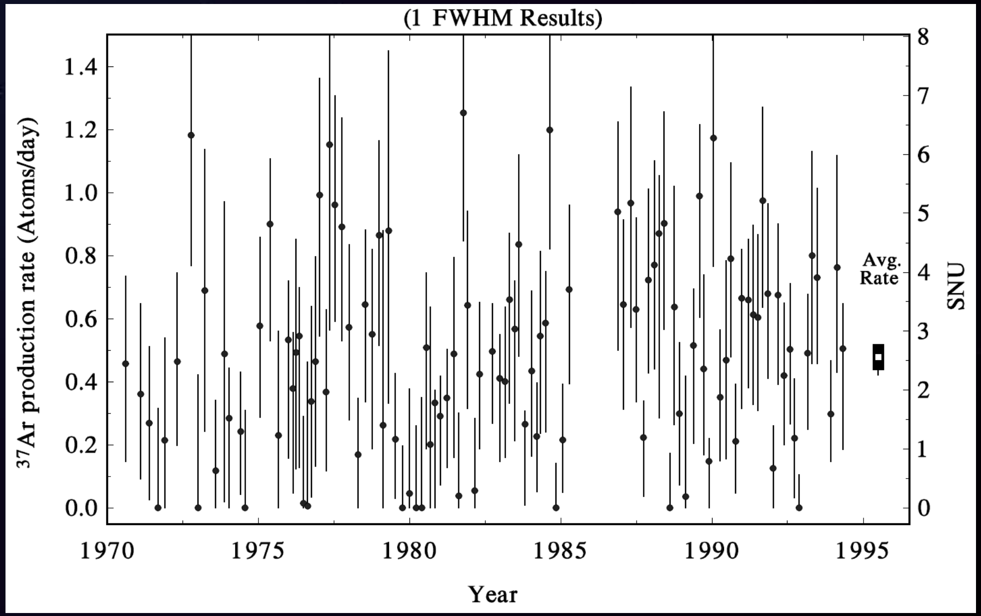

Solar Neutrinos – 2^ Puzzle

Kamiokande II (1987-1988):

H_2O mass: 2.1×10^6 kg + 958 PMTs

SuperKamiokande (1996-today):

H_2O mass: 3.2×10^7 kg + 11000 PMTs

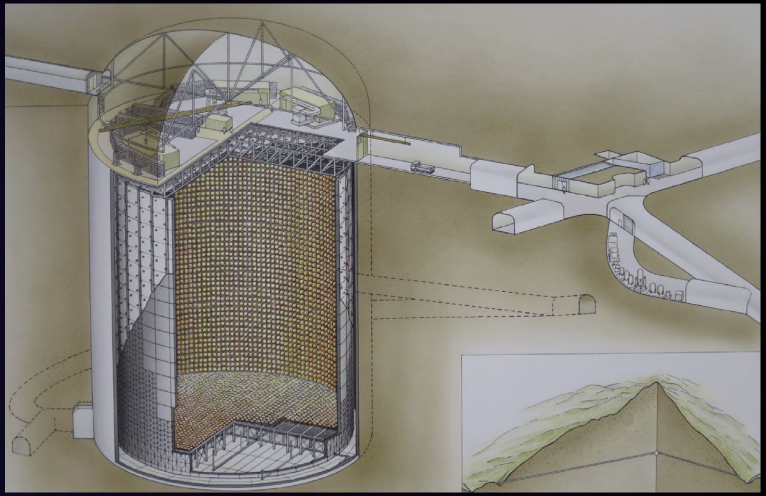

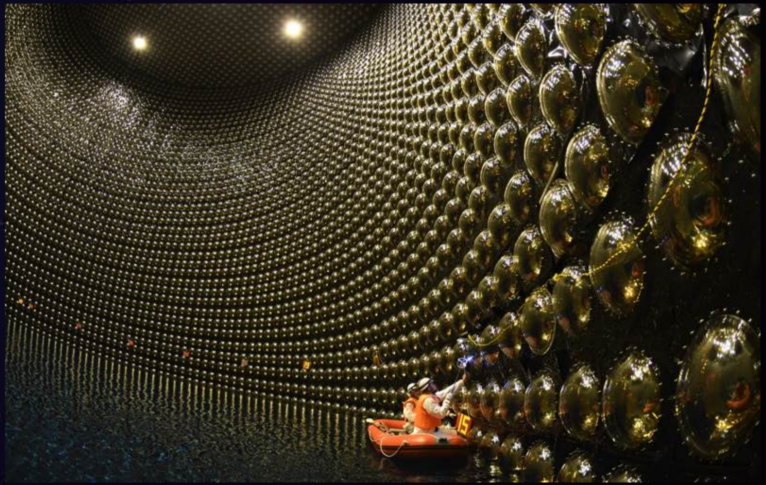

K.S. Hirata et al. (Kamiokande-II Collaboration) Observation of ^8B solar neutrinos in the Kamiokande-II detector. Phys. Rev. Lett. 63 (1989) 16–19

Solar Neutrinos – 2^ Puzzle

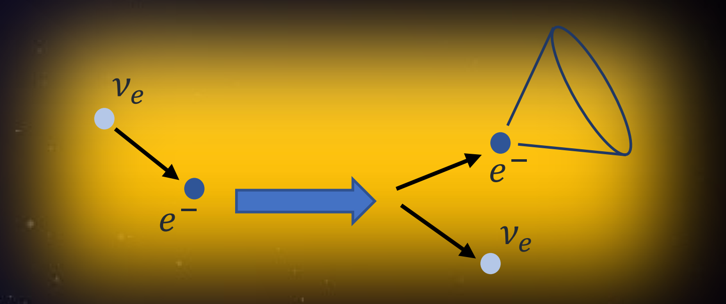

Kamiokande II (1987-1988):

H_2O mass: 2.1×10^6 kg + 958 PMTs

SuperKamiokande (1996-today):

H_2O mass: 3.2×10^7 kg + 11000 PMTs

process: $\nu_e + e^- \rightarrow \nu_e + e^-$

Detects the Cherenkov light emitted by the recoiling electrons

Threshold at $E_\nu = 7.6$ MeV determined by the detected Ch. Light amount

Sensitivity to ^{8}B neutrinos

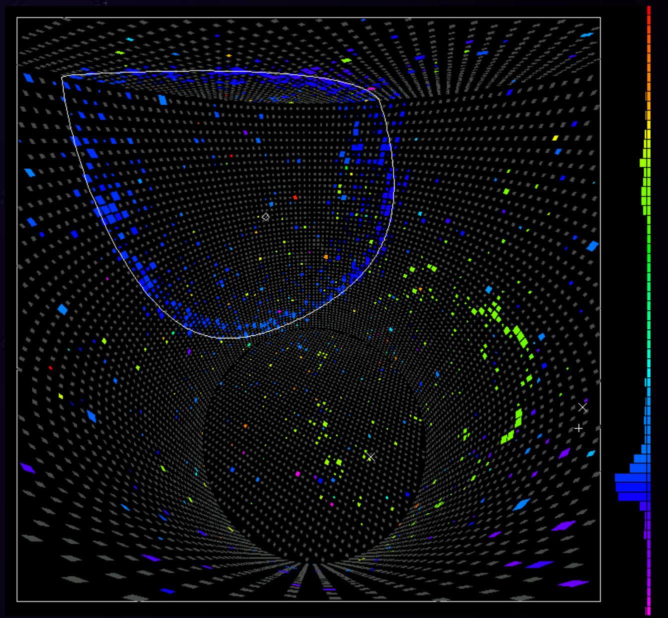

2° solar neutrinos puzzle

Measured flux: 0.46 of the expected flux

Solar Neutrinos – 3^ Puzzle

Gallex/GNO@LNGS (1991-2003):
$GaCl_2$ mass: 3.0×10^4 kg

SAGE@Baksan (INR-Caucaso) (mid ‘90s):
$GaCl_2$ mass: 5.6×10^4 kg

process: $\nu_e + {}^{71}\mathrm{Ga} \rightarrow {}^{71}\mathrm{Ge} + e^- \quad \tau_{\mathrm{Ge}} = 16.5\ \mathrm{d}$

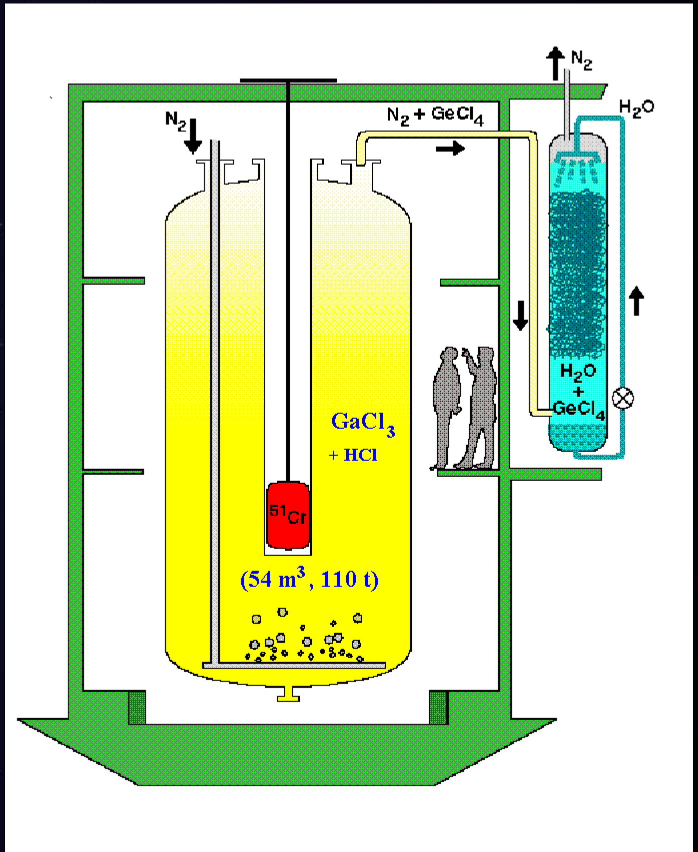

Threshold at $E_\nu = 233\ \mathrm{keV}$

Sensitivity to pp neutrinos

3° solar neutrinos puzzle

Measured flux: 76±8 SNU

Expected flux: 128±8 SNU

W. Hampel et al. (GALLEX Collaboration) GALLEX solar neutrino observation: Results for GALLEX IV. Phys. Lett. B 447 (1999) 127–133.

J.N. Abdurashitov et al. (SAGE Collaboration) Measurement of the solar neutrino capture rate with gallium metal. III. Results for the 2002–2007 data taking period. Phys. Rev. C 80 (2009) 015807.

Solar Neutrinos

SNO:

D_2O $(+NaCl)$ mass: 10^6 kg

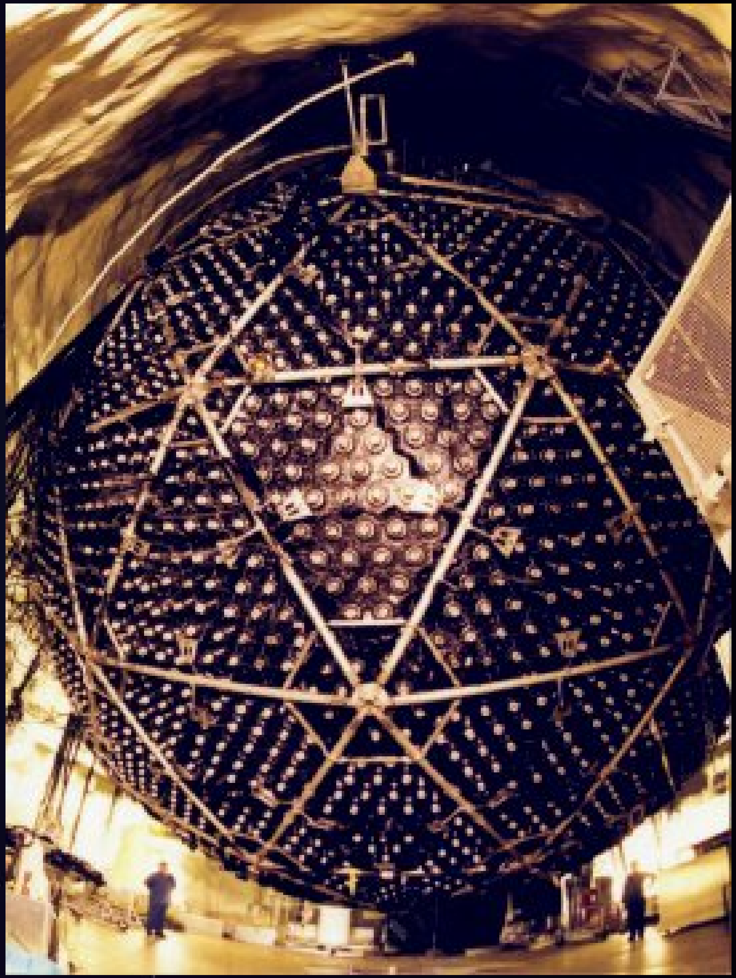

S.N. Ahmed et al. (SNO Collaboration) Measurement of the total active ^8B solar neutrino flux at the sudbury neutrino observatory with enhanced neutral current sensitivity. Phys. Rev. Lett. 92 (2004) 181301

Solar Neutrinos

SNO:

D_2O ($+NaCl$) mass: 10^6 kg

processes:

$$\nu_e + \mathrm{d} \rightarrow \mathrm{p} + \mathrm{p} + e^-$$

$$\nu_\mathrm{x} + \mathrm{d} \rightarrow \nu_\mathrm{x} + \mathrm{p} + \mathrm{n}$$ followed by $\mathrm{n} + {}^{35}\mathrm{Cl} \rightarrow {}^{36}\mathrm{Cl} + \gamma s$

Detects the Cherenkov light

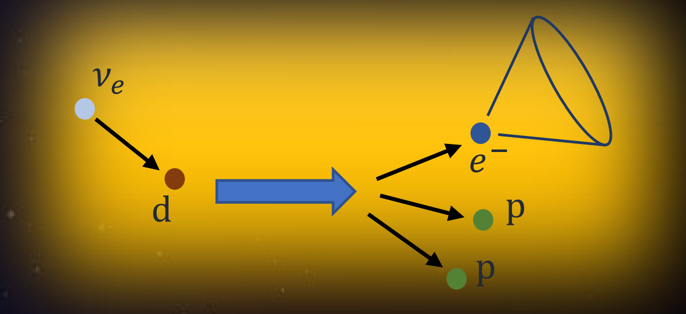

Threshold at $E_\nu = 5$ MeV

Sensitivity to ^{8}B neutrinos

Confirmed the Super-K result

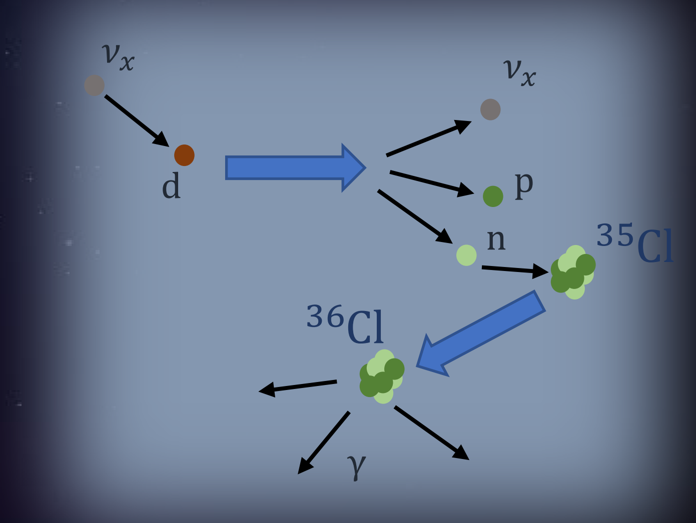

The Solar Neutrino Puzzle

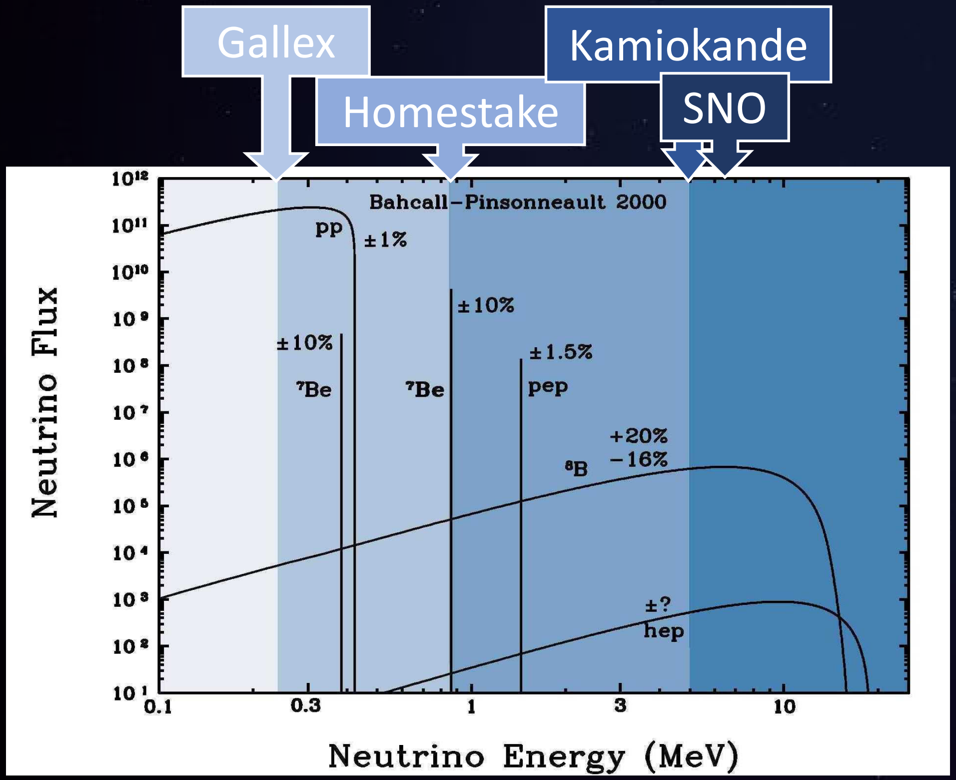

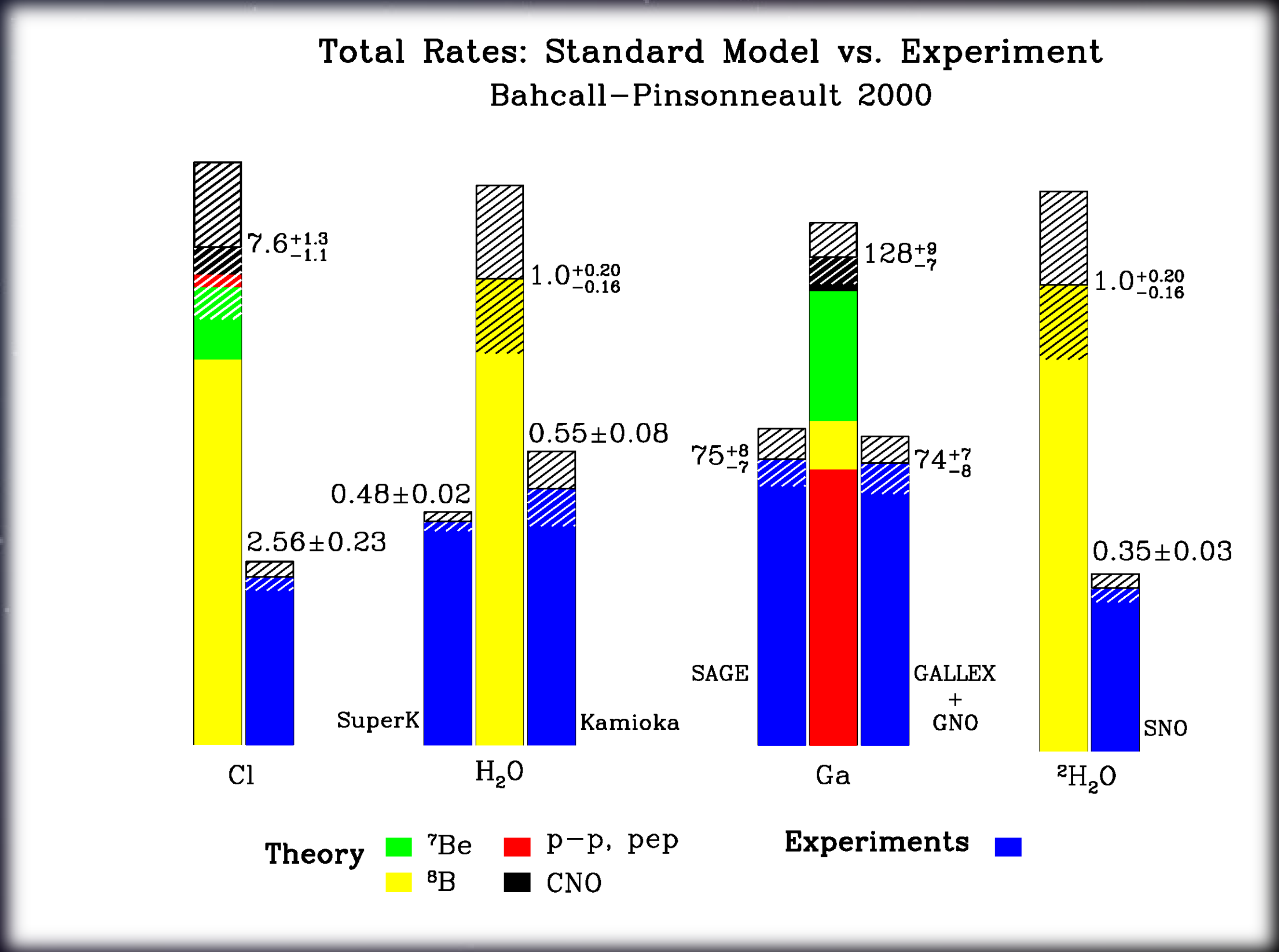

The Solution to the Solar Neutrino Puzzle

SNO:

Observed for the first time signals from ν_x

processes:

$$\nu_e + \mathrm{d} \rightarrow \mathrm{p} + \mathrm{p} + e^-$$

$$\nu_\mathrm{x} + \mathrm{d} \rightarrow \nu_\mathrm{x} + \mathrm{p} + \mathrm{n}$$ followed by $\mathrm{n} + {}^{35}\mathrm{Cl} \rightarrow {}^{36}\mathrm{Cl} + \gamma s$

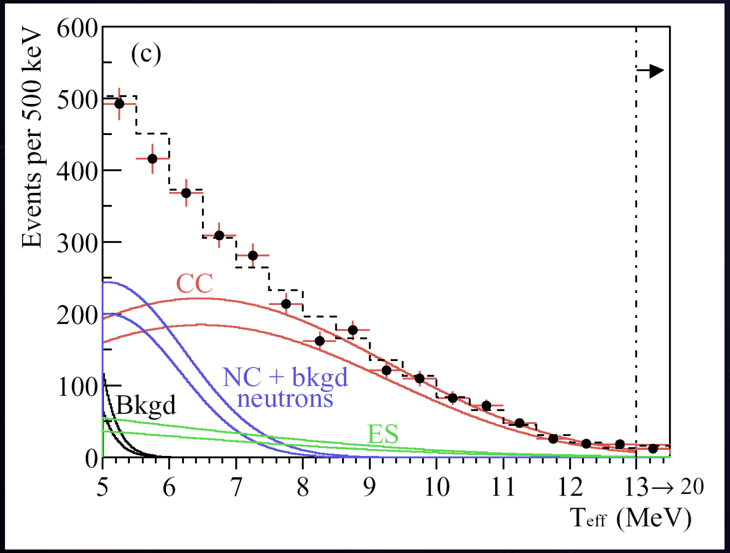

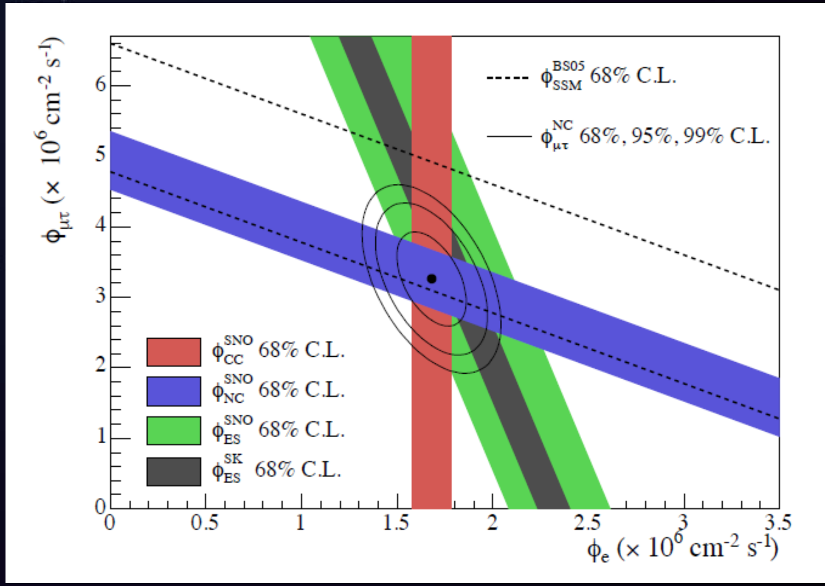

Neutrinos from CNO

BOREXINO@LNGS (2007-today):

Liquid scintillator mass: 10^5 kg

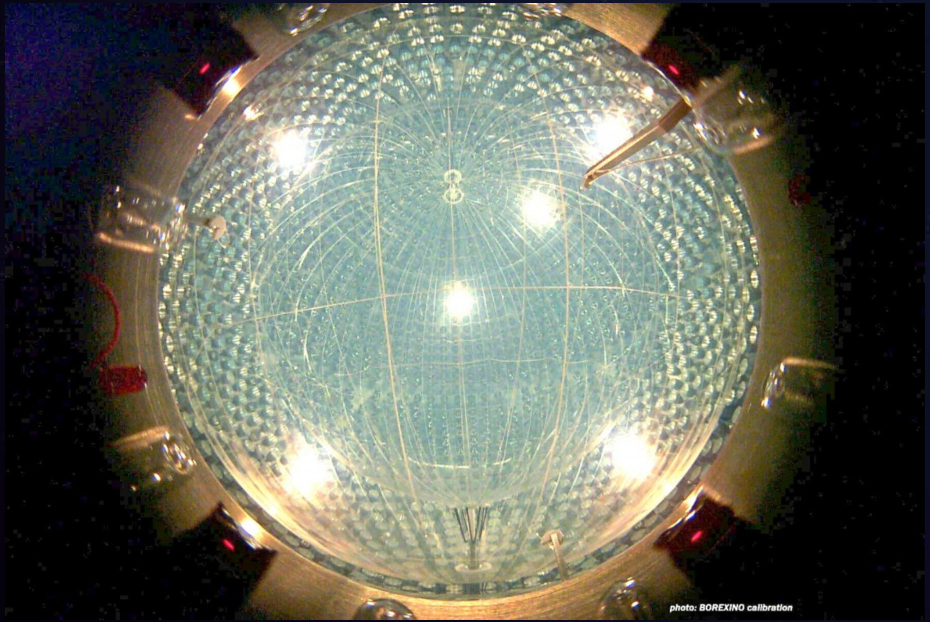

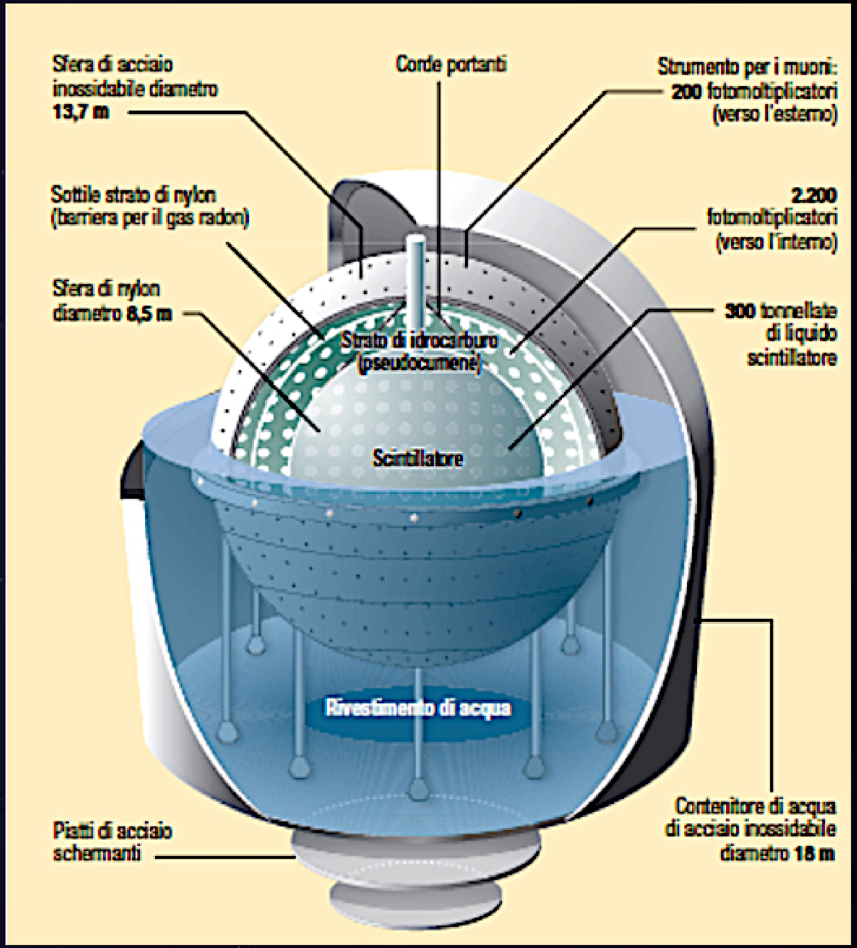

Neutrino from CNO

BOREXINO@LNGS (2007-today):

Liquid scintillator mass: 10^5 kg

processes:

$$\nu_x + e^- \rightarrow \nu_x + e^-$$

Threshold at $E_\nu = 0.19$ MeV

Sensitivity to all solar neutrinos

The Borexino Collaboration., Agostini, M., Altenmüller, K. et al. Comprehensive measurement of pp-chain solar neutrinos. Nature 562, 505–510 (2018)

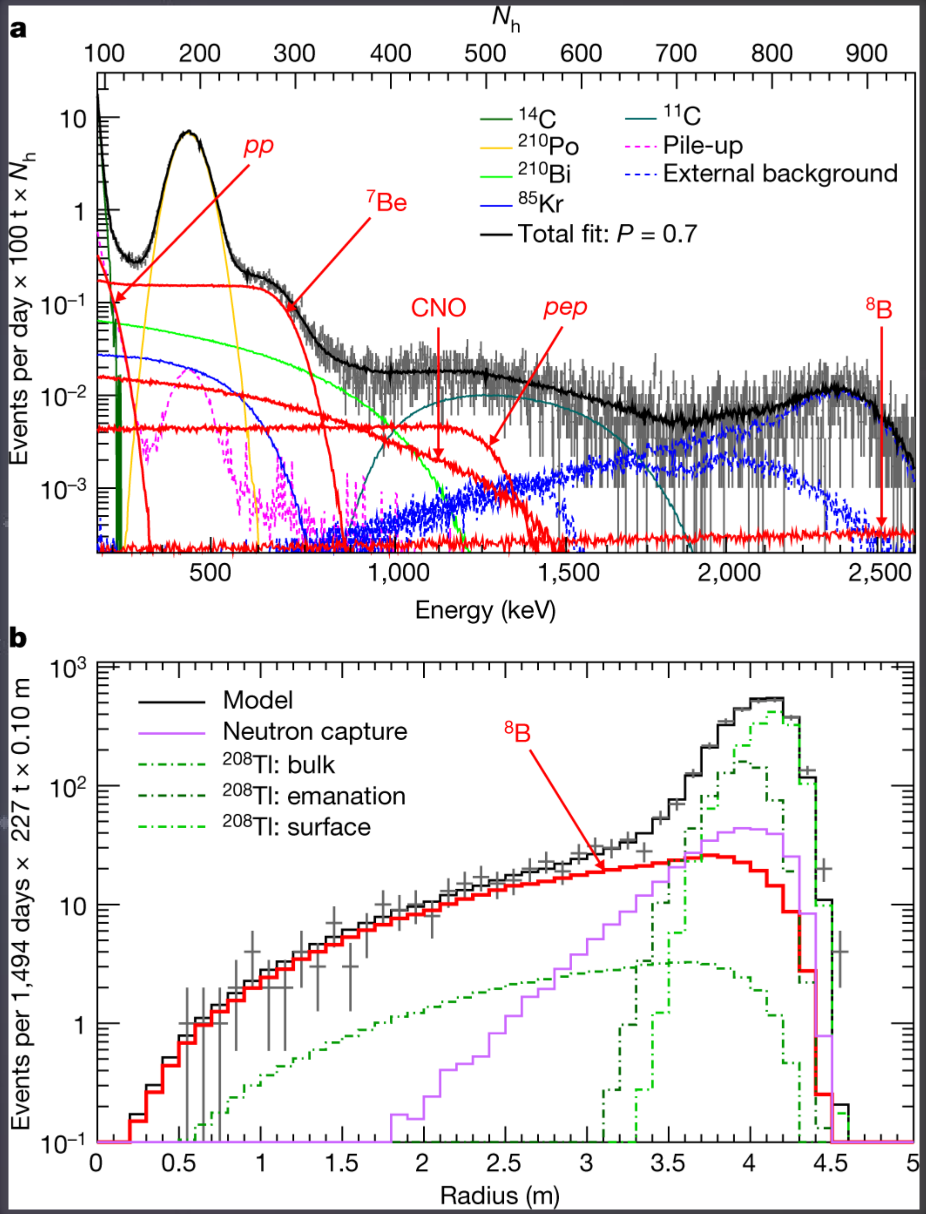

Neutrino from CNO

BOREXINO@LNGS (2007-today):

Liquid scintillator mass: 10^5 kg

processes:

$$\nu_x + e^- \rightarrow \nu_x + e^-$$

Threshold at $E_\nu = 0.19$ MeV

Sensitivity to all solar neutrinos

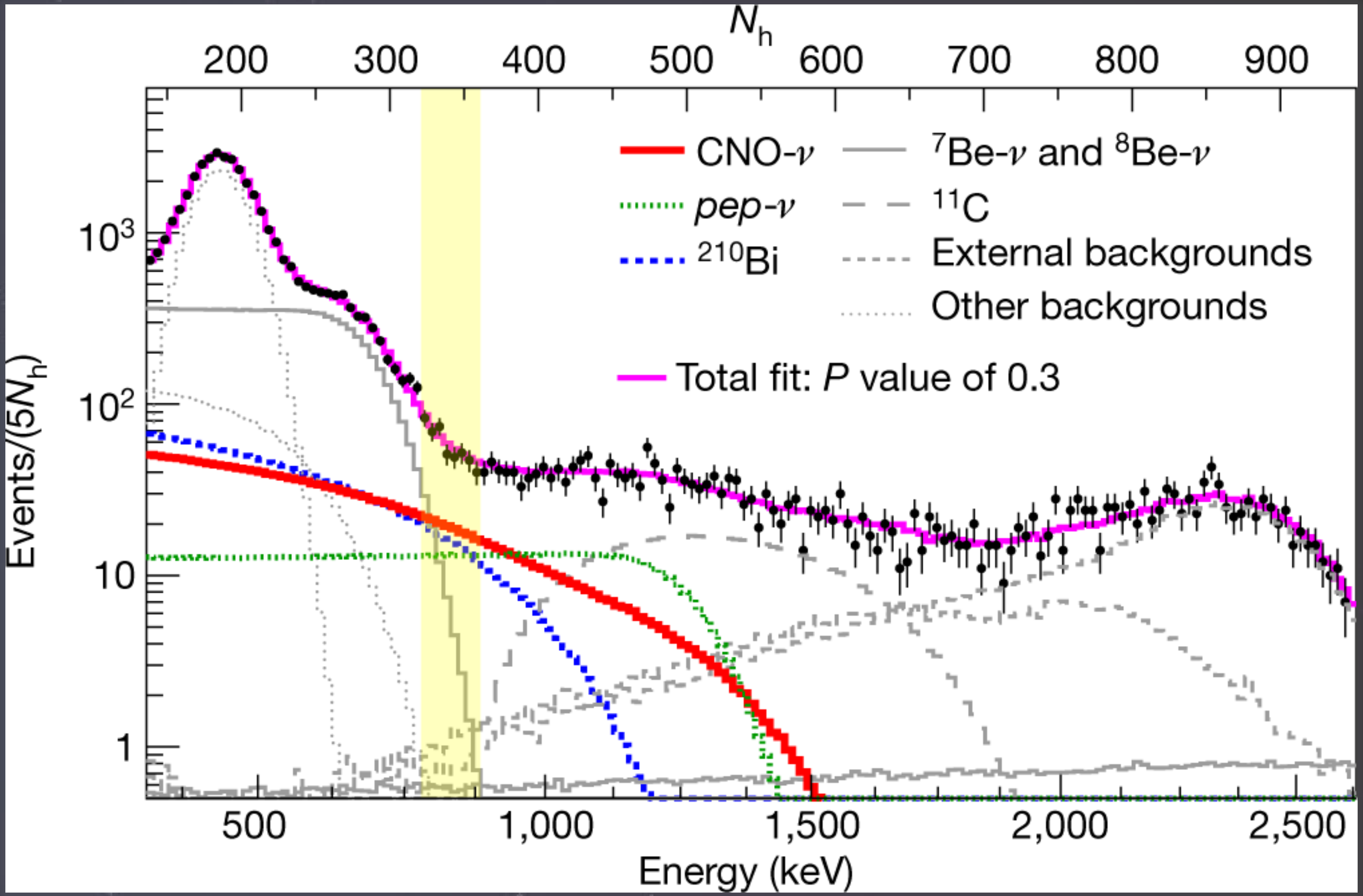

The Borexino Collaboration., Agostini, M., Altenmüller, K. et al. Experimental evidence of neutrinos produced in the CNO fusion cycle in the Sun. Nature 587, 577–582 (2020).

High Energy Neutrinos

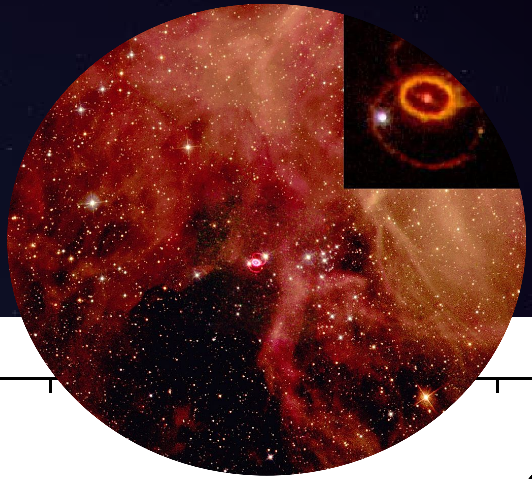

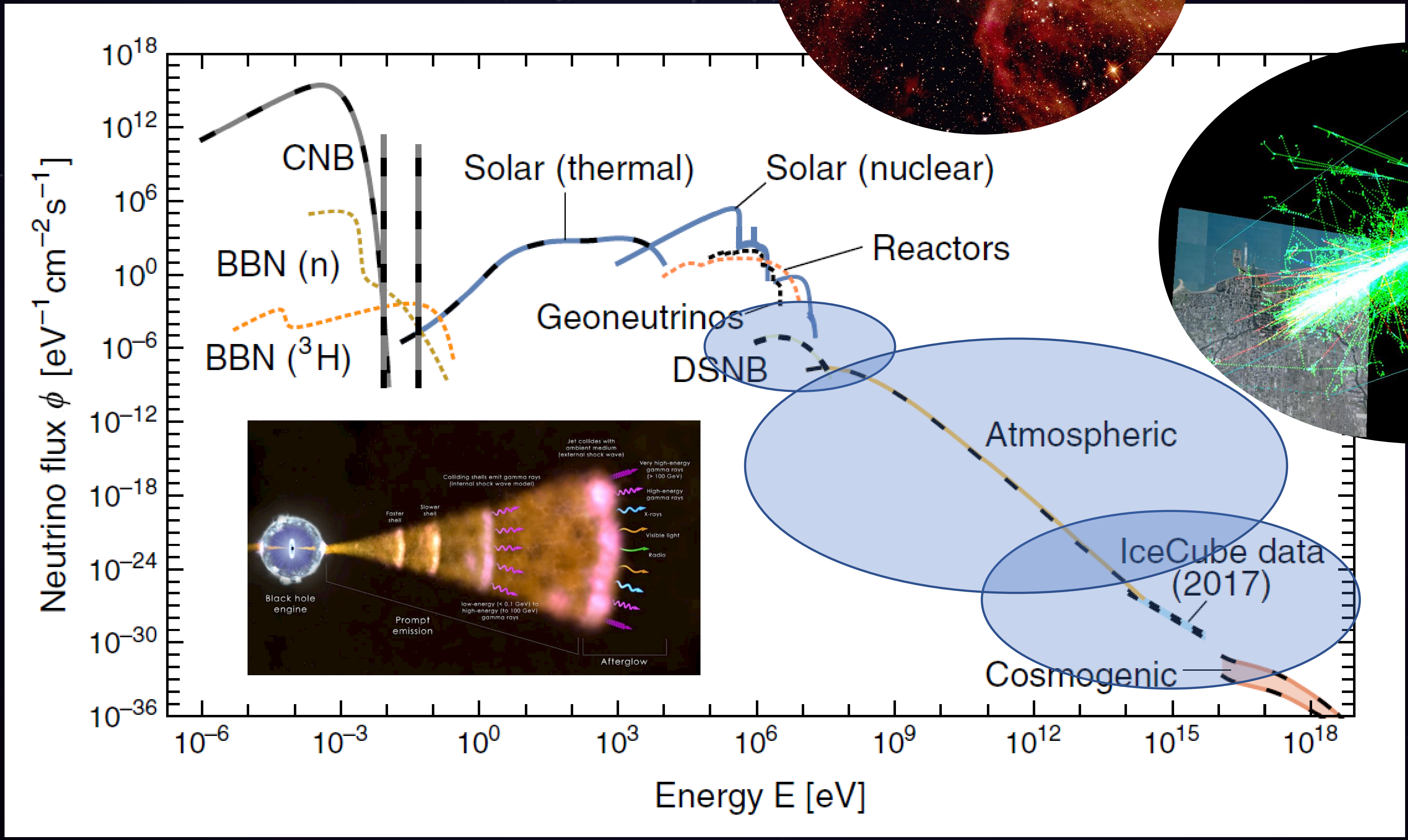

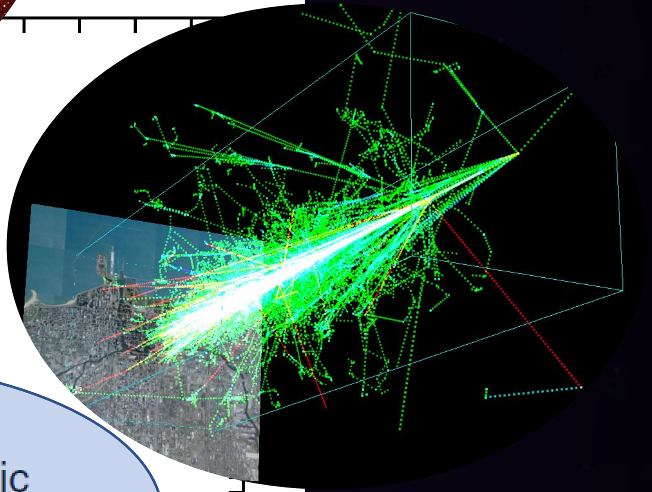

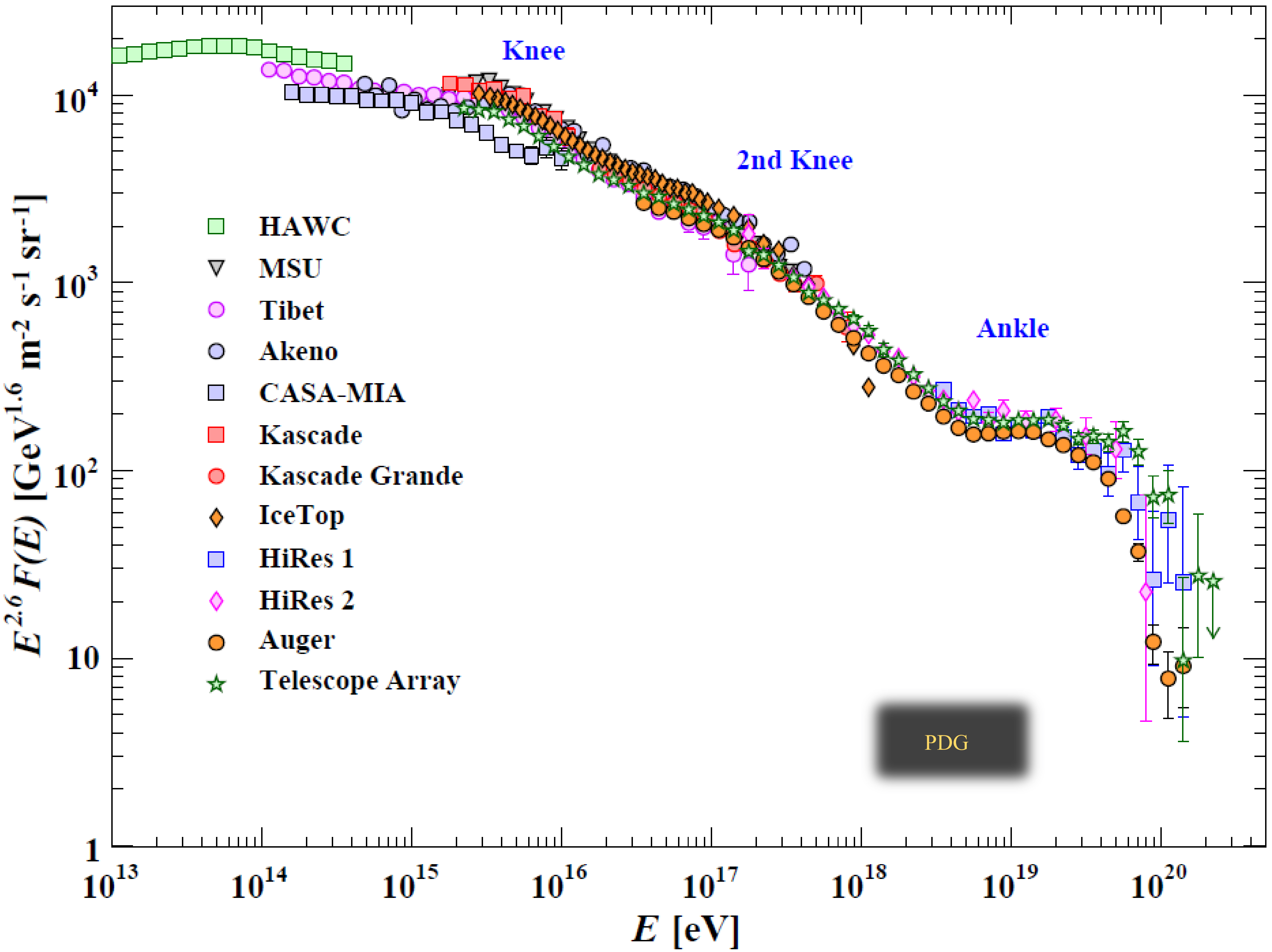
Knee
2nd Knee
Ankle
HAWC
MSU
Tibet
Akeno
CASA-MIA
Kascade
Kascade Grande
IceTop
HiRes 1
HiRes 2
Auger
Telescope Array
PDG
$E^{2.6}F(E)$ [GeV$^{1.6}$ m^{-2} s^{-1} sr^{-1}]
E [eV]
1
10
10^2
10^3
10^4
10^{13}
10^{14}
10^{15}
10^{16}
10^{17}
10^{18}
10^{19}
10^{20}

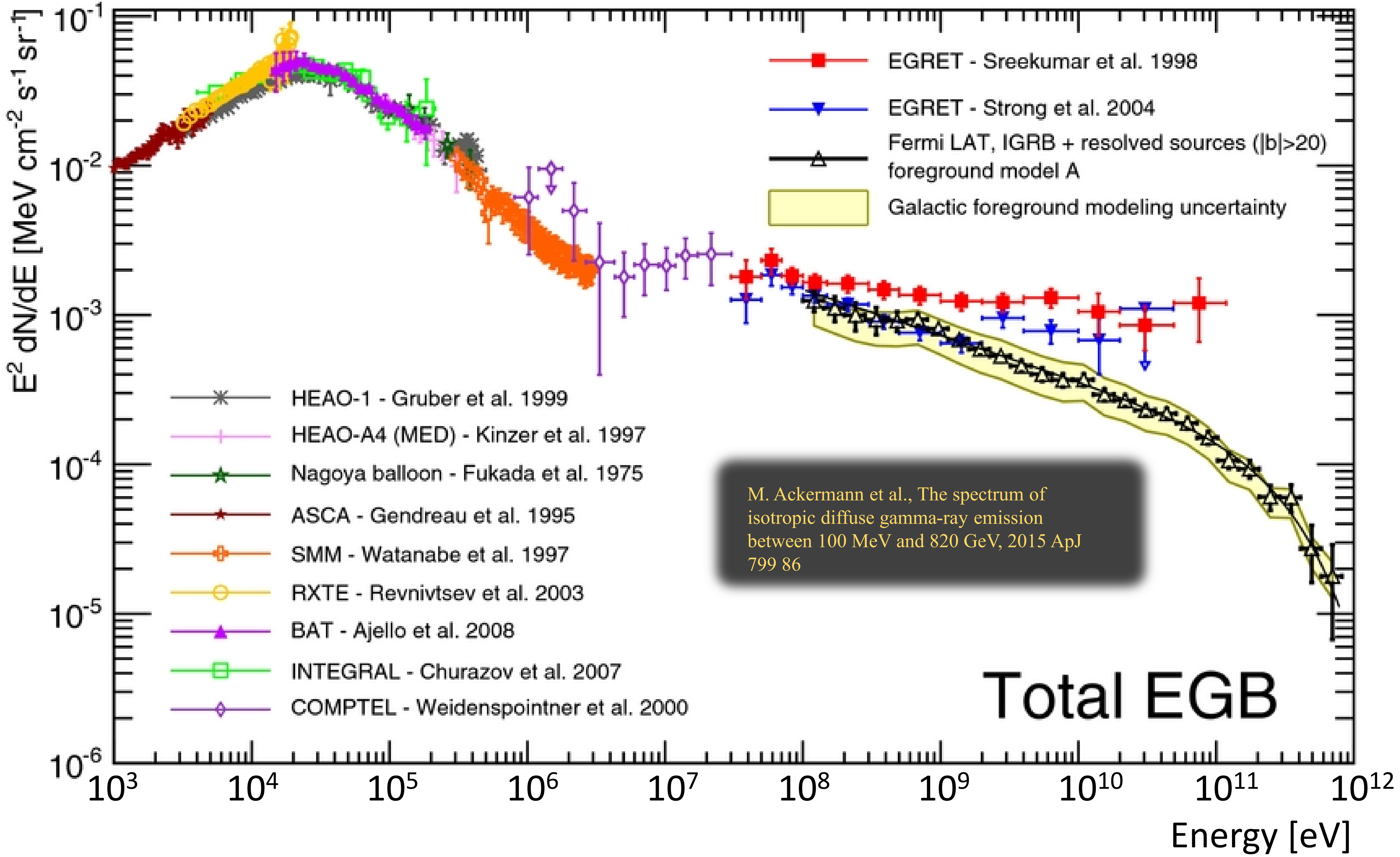

E^2 dN/dE [MeV cm^-2 s^-1 sr^-1]
EGRET - Sreekumar et al. 1998
EGRET - Strong et al. 2004
Fermi LAT, IGRB + resolved sources (|b|>20) foreground model A
Galactic foreground modeling uncertainty
HEAO-1 - Gruber et al. 1999
HEAO-A4 (MED) - Kinzer et al. 1997
Nagoya balloon - Fukada et al. 1975
ASCA - Gendreau et al. 1995
SMM - Watanabe et al. 1997
RXTE - Revnivtsev et al. 2003
BAT - Ajello et al. 2008
INTEGRAL - Churazov et al. 2007
COMPTEL - Weidenspointner et al. 2000
M. Ackermann et al., The spectrum of isotropic diffuse gamma-ray emission between 100 MeV and 820 GeV, 2015 ApJ 799 86
Total EGB
Energy [eV]

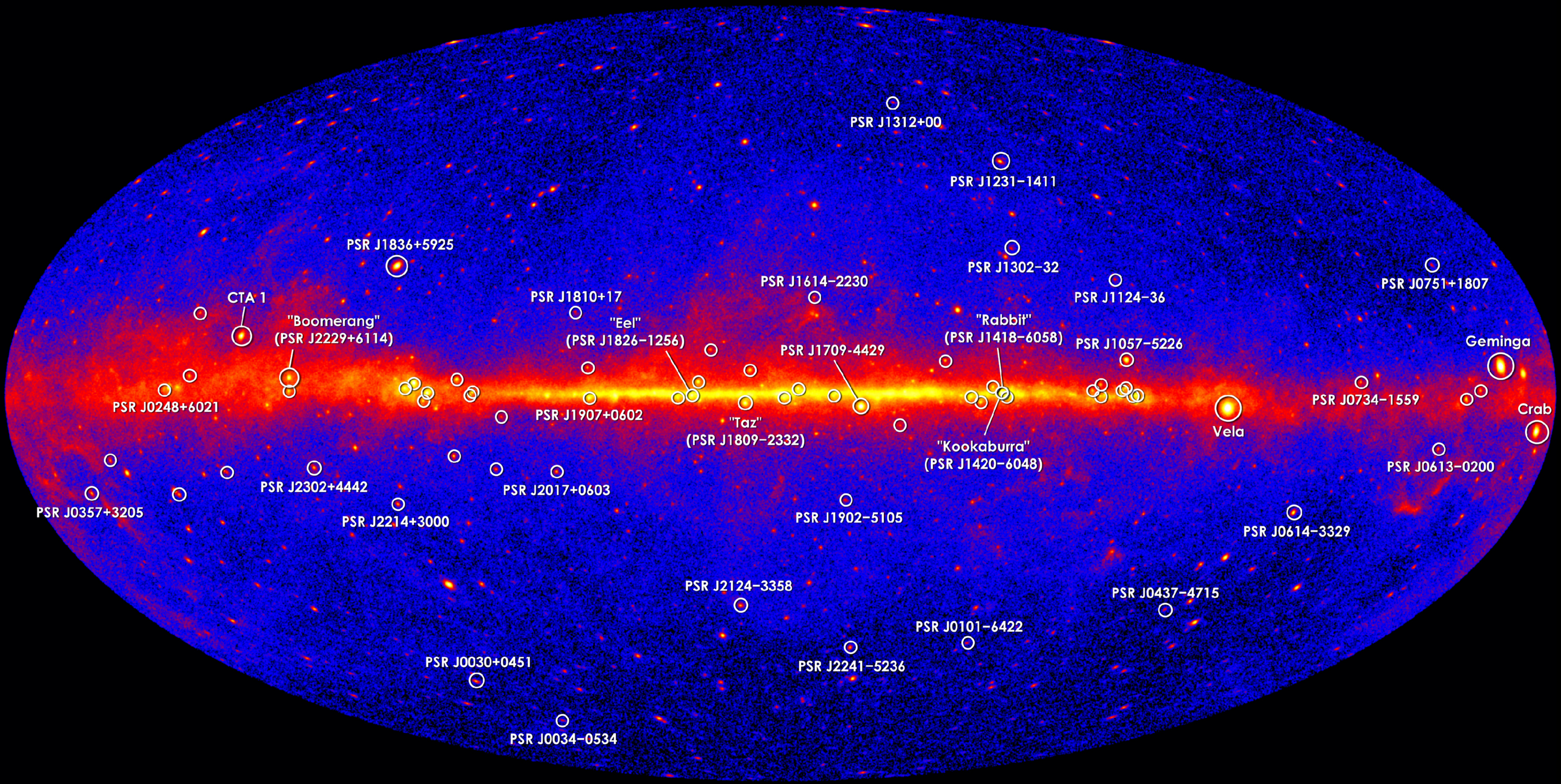

NASA/DOE/Fermi LAT Collaboration

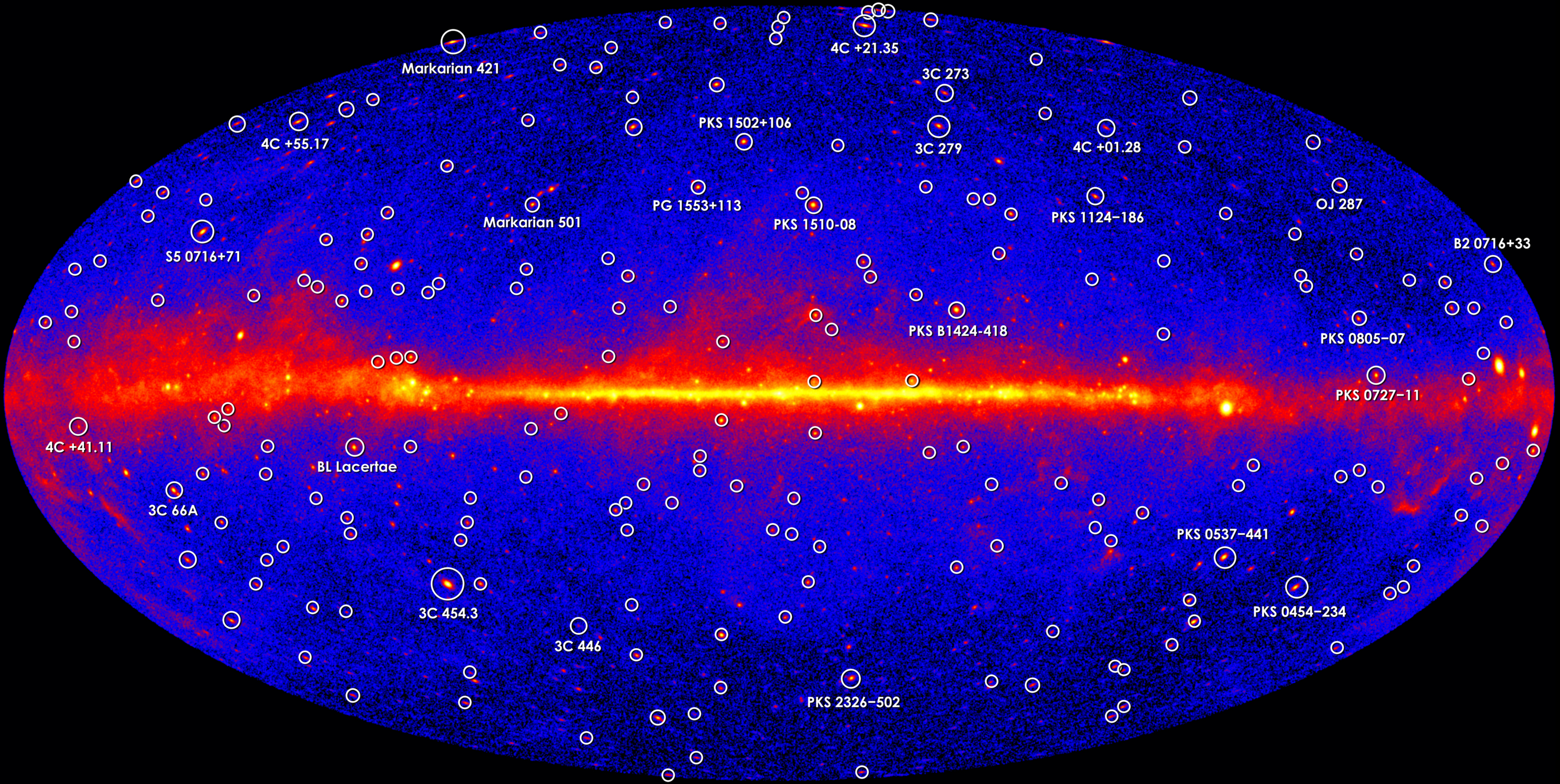

NASA/DOE/Fermi LAT Collaboration

The Neutrino Cosmic-Ray Connection

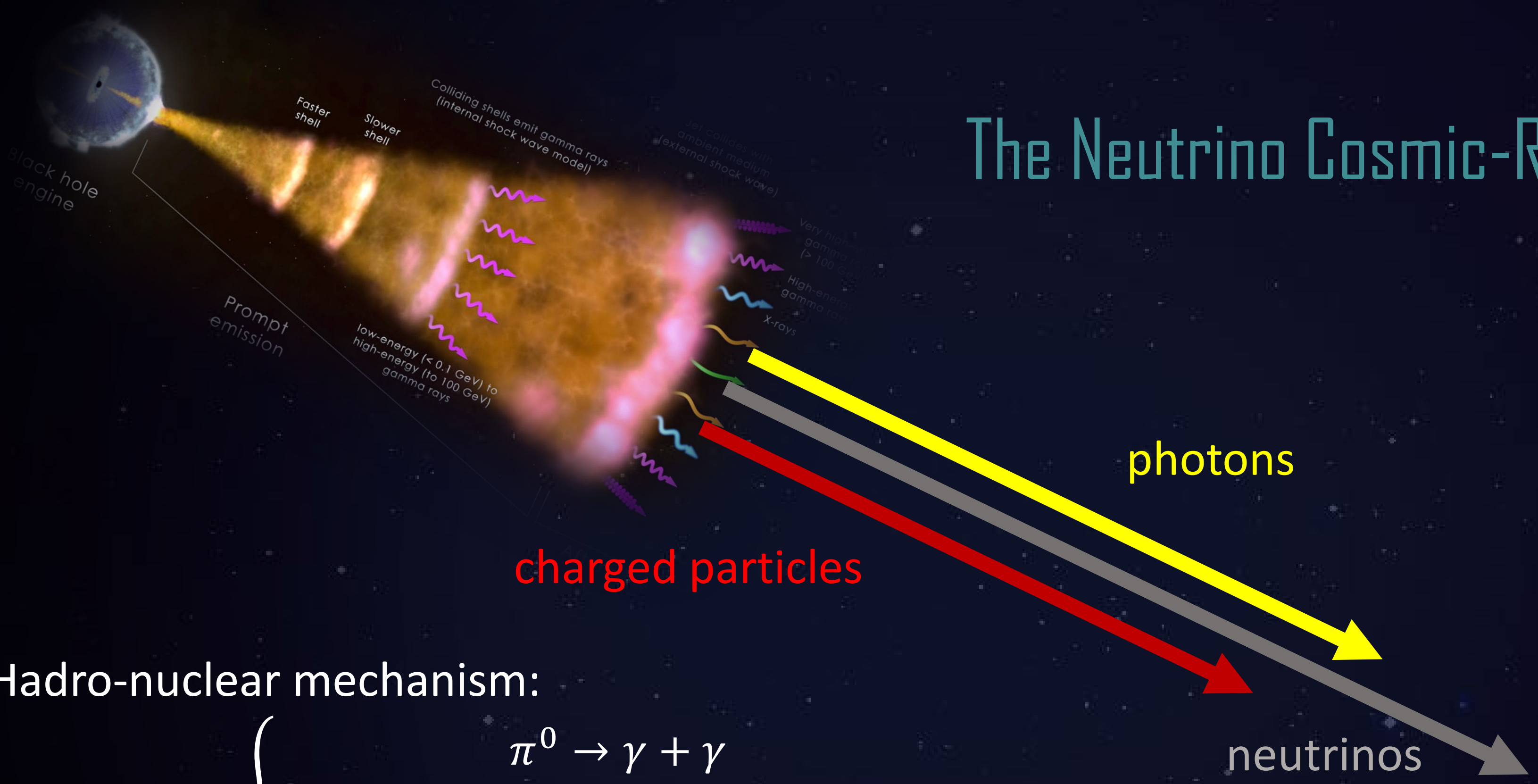

Hadro-nuclear mechanism:

$$\mathrm{p} + \mathrm{p} \rightarrow \begin{cases} \pi^0 \rightarrow \gamma + \gamma \\ \pi^+ \rightarrow \mu^+ + \nu_\mu \rightarrow e^+ + \boldsymbol{\nu_e} + \boldsymbol{\bar{\nu}_\mu} + \boldsymbol{\nu_\mu} \\ \pi^- \rightarrow \mu^- + \bar{\nu}_\mu \rightarrow e^- + \boldsymbol{\bar{\nu}_e} + \boldsymbol{\nu_\mu} + \boldsymbol{\bar{\nu}_\mu} \end{cases}$$

Photo-hadronic mechanism:

$$\gamma + \mathrm{p} \rightarrow \Delta^+ \rightarrow \begin{cases} \mathrm{p} + \pi^0 \rightarrow \mathrm{p} + \gamma + \gamma \\ \mathrm{n} + \pi^+ \rightarrow \mathrm{n} + \mu^+ + \nu_\mu \rightarrow \mathrm{n} + e^+ + \boldsymbol{\nu_e} + \boldsymbol{\bar{\nu}_\mu} + \boldsymbol{\nu_\mu} \end{cases}$$

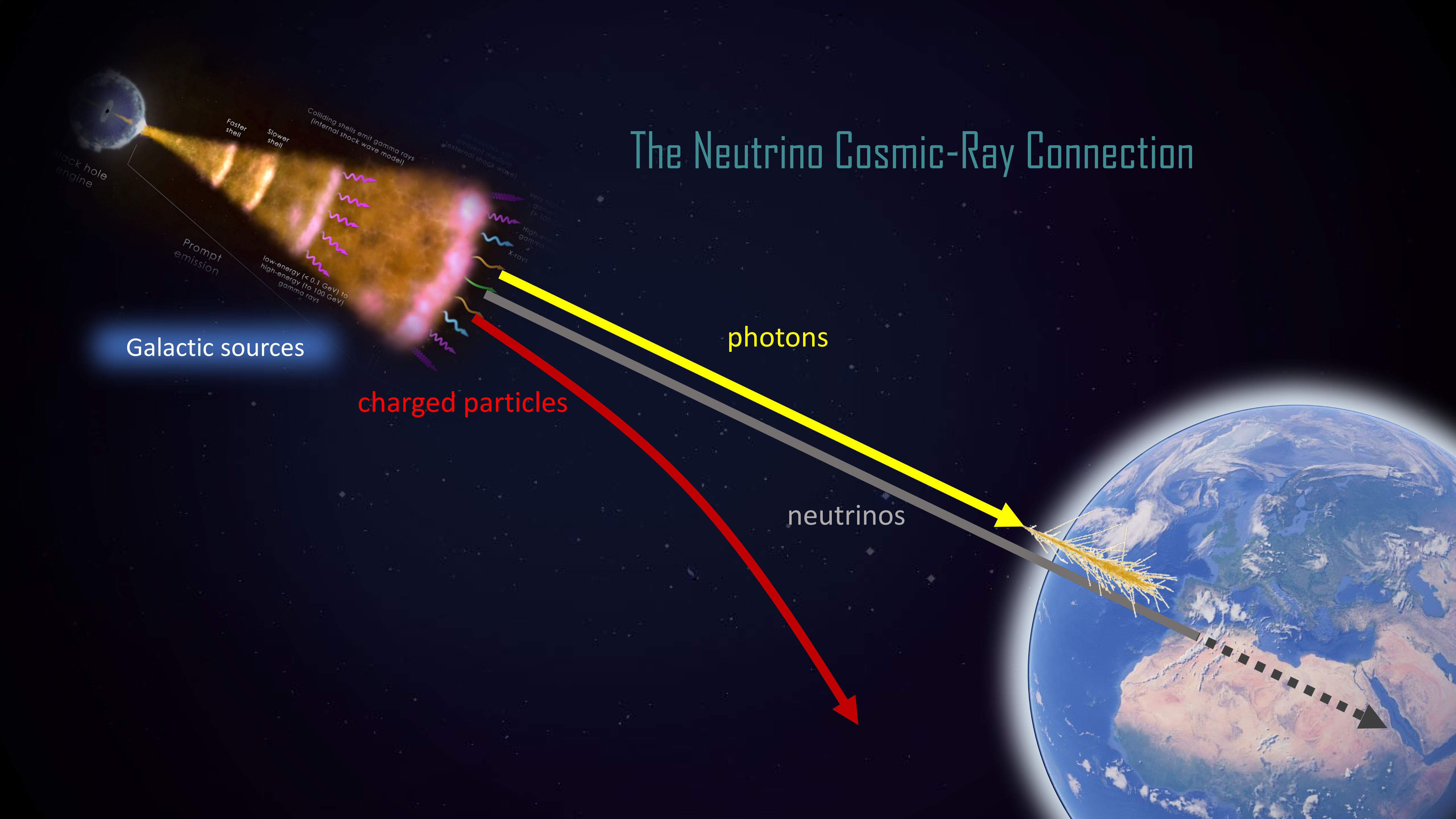
The Neutrino Cosmic-Ray Connection
Faster shell
Slower shell
Colliding shells emit gamma rays (internal shock wave model)
Black hole engine
Prompt emission
low-energy (< 0.1 GeV) to high-energy (to 100 GeV) gamma rays
X-rays
Galactic sources
photons
charged particles
neutrinos

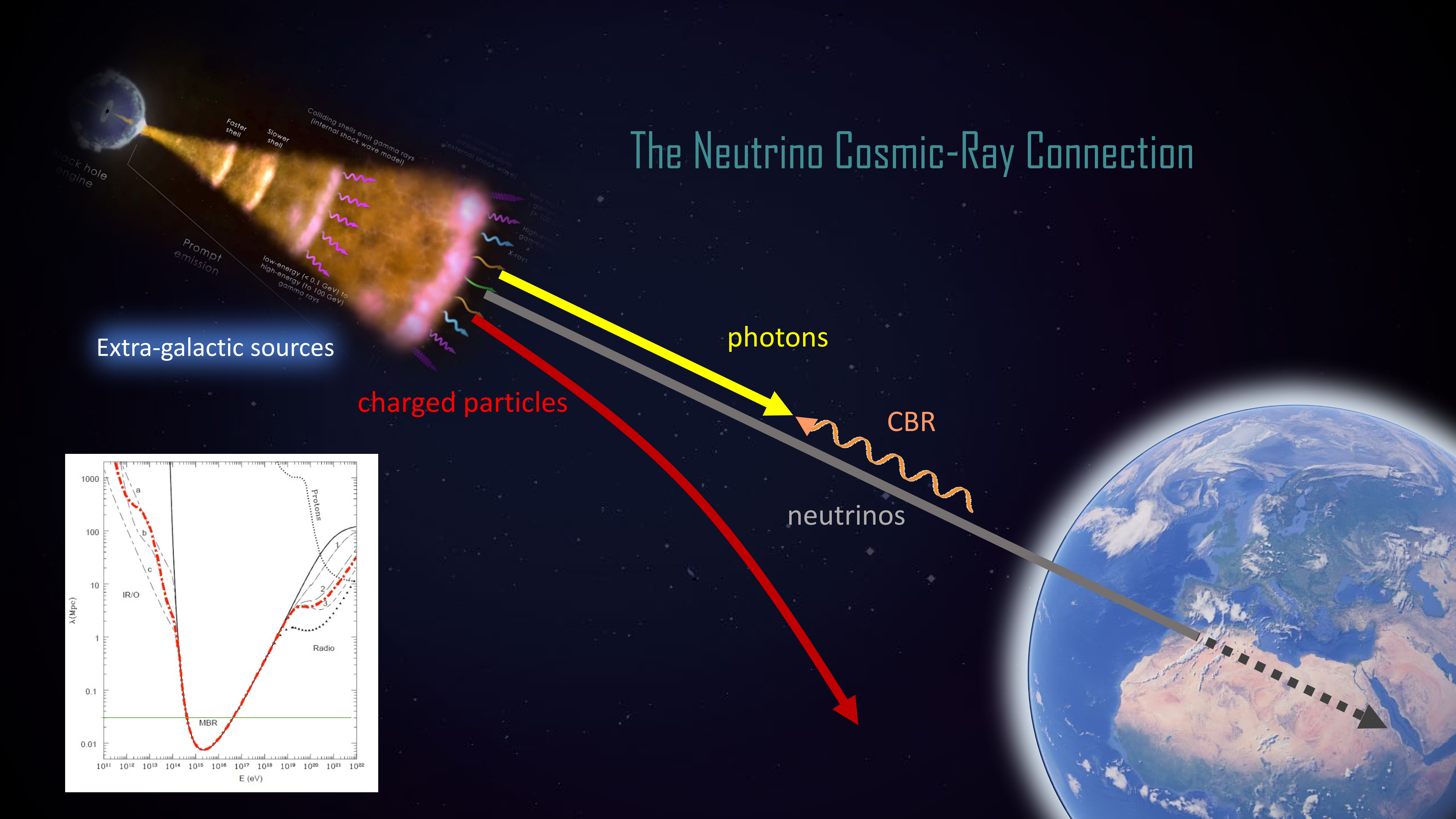

The Neutrino Cosmic-Ray Connection
Black hole engine
Faster shell
Slower shell
Colliding shells emit gamma rays (internal shock wave model)
Prompt emission
low-energy (< 0.1 GeV) to high-energy (to 100 GeV) gamma rays
X-rays
Extra-galactic sources
photons
charged particles
CBR
neutrinos
Protons
IR/O
Radio
MBR
λ (Mpc)
E (eV)

High Energy Neutrinos

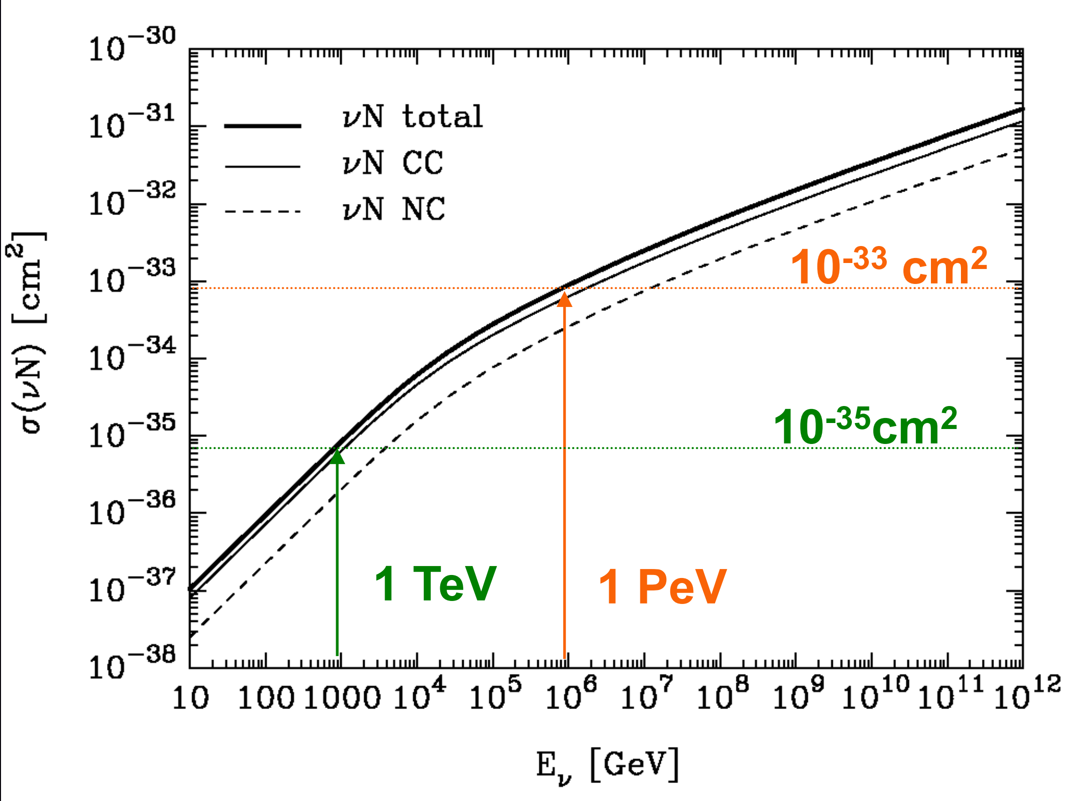

Savannah River $\qquad \bar{\boldsymbol{\nu}}_{\boldsymbol{e}} + \mathrm{p} \rightarrow \boldsymbol{e}^{+} + \mathrm{n} \qquad E_\nu \approx 4$ MeV

$\Phi_{\bar{\nu}} = 10^{17}\ \mathrm{s}^{-1}\mathrm{cm}^{-2}$

$\sigma = 6 \cdot 10^{-44}\ \mathrm{cm}^{-2}$

$V_{det} = 2 \cdot 10^{5}\ \mathrm{cm}^{3}$ $\qquad$ conversion rate $\approx 1\ \mathrm{s}^{-1}$

Kamiokande II $\qquad \boldsymbol{\nu}_{\boldsymbol{e}} + \boldsymbol{e}^{-} \rightarrow \boldsymbol{\nu}_{\boldsymbol{e}} + \boldsymbol{e}^{-} \qquad E_\nu \approx 8$ MeV

$\Phi_{\nu} = 7 \cdot 10^{5}\ \mathrm{s}^{-1}\mathrm{cm}^{-2}$

$\sigma = 1.5 \cdot 10^{-43}\ \mathrm{cm}^{-2}$

$V_{det} = 2.1 \cdot 10^{9}\ \mathrm{cm}^{3}$ $\qquad$ conversion rate $\approx 1\ \mathrm{h}^{-1}$

High energy neutrinos $\qquad \boldsymbol{\nu}_{\boldsymbol{l}} + \boldsymbol{A} \rightarrow \boldsymbol{l} + \boldsymbol{X} \qquad E_\nu \approx 1$ TeV

$\Phi_{\nu} = 10^{-6}\ \mathrm{s}^{-1}\mathrm{cm}^{-2}$

$\sigma = 8 \cdot 10^{-36}\ \mathrm{cm}^{-2}$

$\boldsymbol{V_{det} = 10^{15}\ cm^{3}}$ $\qquad$ conversion rate $\approx 2\ \mathrm{h}^{-1}$

High energy neutrinos $\qquad \boldsymbol{\nu}_{\boldsymbol{l}} + \boldsymbol{A} \rightarrow \boldsymbol{l} + \boldsymbol{X} \qquad E_\nu \approx 1$ PeV

$\Phi_{\nu} = 10^{-13}\ \mathrm{s}^{-1}\mathrm{cm}^{-2}$

$\sigma = 10^{-33}\ \mathrm{cm}^{-2}$

$\boldsymbol{V_{det} = 10^{15}\ cm^{3}}$ $\qquad$ conversion rate $\approx 0.1\ \mathrm{d}^{-1}$

Toward the Construction of a Neutrino Observatory

Perchè, secondo l'opinion mia,
A chi vuol una cosa ritrovare,
Bisogna adoperar la fantasia,
E giocar d'invenzione e 'ndovinare;

Galileo Galilei (1590)
Contro il portar la toga

Because, according to my opinion, to those who want to discover something, it is necessary to use the ***imagination****, and to play with* ***innovation*** *and* ***intuition****;*

Neutrino Detection Principle

$\nu_e + N \rightarrow e^- + X$

one electromagnetic shower and one hadronic shower

energy deposited close to the neutrino interaction point

☑ High energy resolution

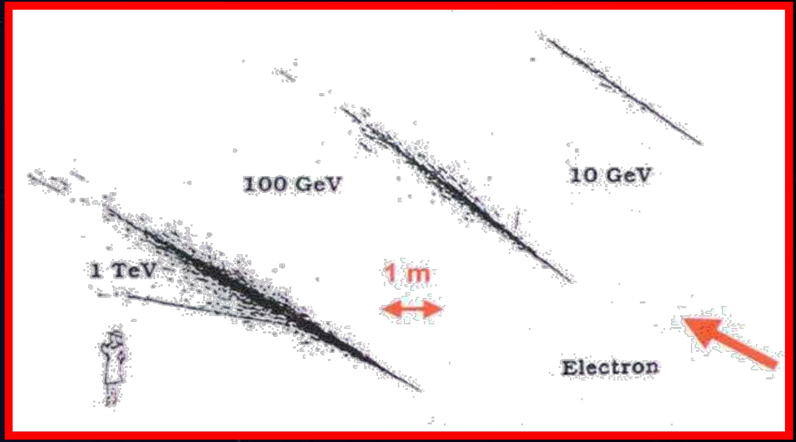

$\nu_\mu + N \rightarrow \mu + X$

one minimum ionizing particle and one hadronic shower

energy deposited along the muon path (!)

☑ High angular resolution

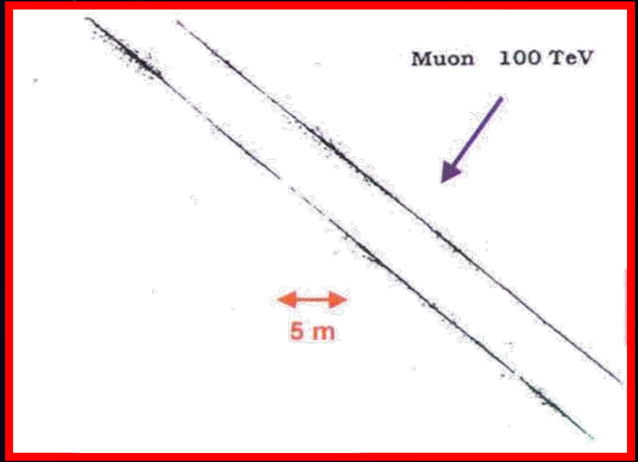

Neutrino Detection Principle

Muons have long range in water

$$R_\mu\left(E_\mu \approx 300\ \mathrm{GeV}\right) \approx 1\ \mathrm{km}$$

Muons radiation energy losses are strongly suppressed due to high mass

Detection of HE astrophysical neutrinos is achieved through CC neutrino interaction

Neutrino astronomy requires reconstruction of direction and energy of the reaction products (charged leptons)

$$\langle\theta\rangle \approx \frac{1.5^\circ}{\sqrt{E_\nu\ [\mathrm{TeV}]}}$$

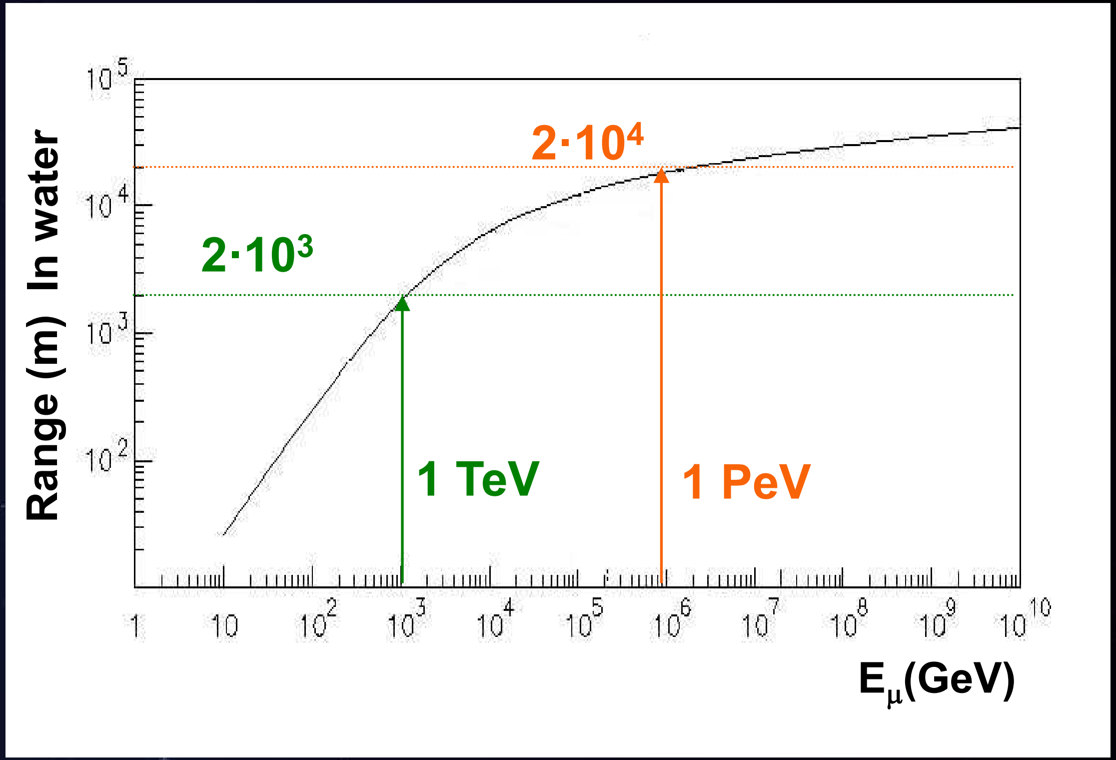

Neutrino Detection Principle

Due to the long muon range the target volume is much bigger than the detector instrumented volume

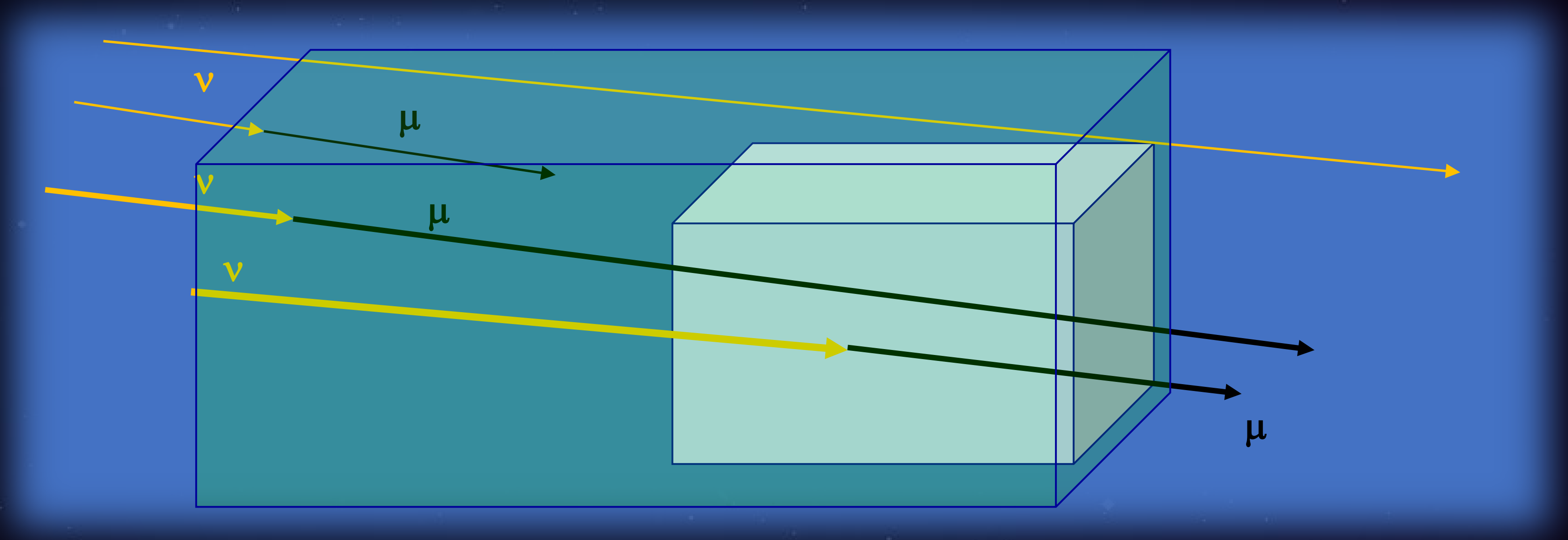

A 1 km^3 detector is *sufficient* to obtain reasonable counting rate

Neutrino Detection Principle

Large water volumes can be find in seas, lakes or ice

If the detector is located in depth, water acts also as shielding

Detection of muon already creates a problem:

muon are produced from interaction of primary cosmic ray with the atmosphere, mainly from decay of charged pions:

$$\pi^+ \to \mu^+ + \nu_\mu$$

Only upward muons are originated from neutrinos !

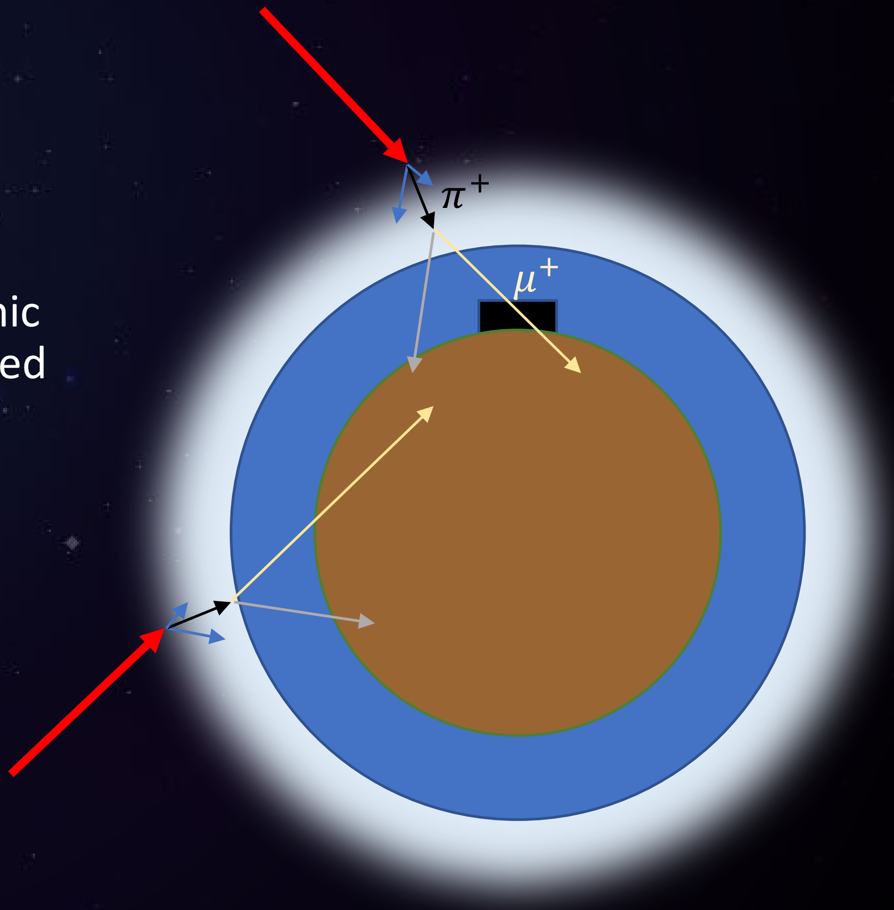

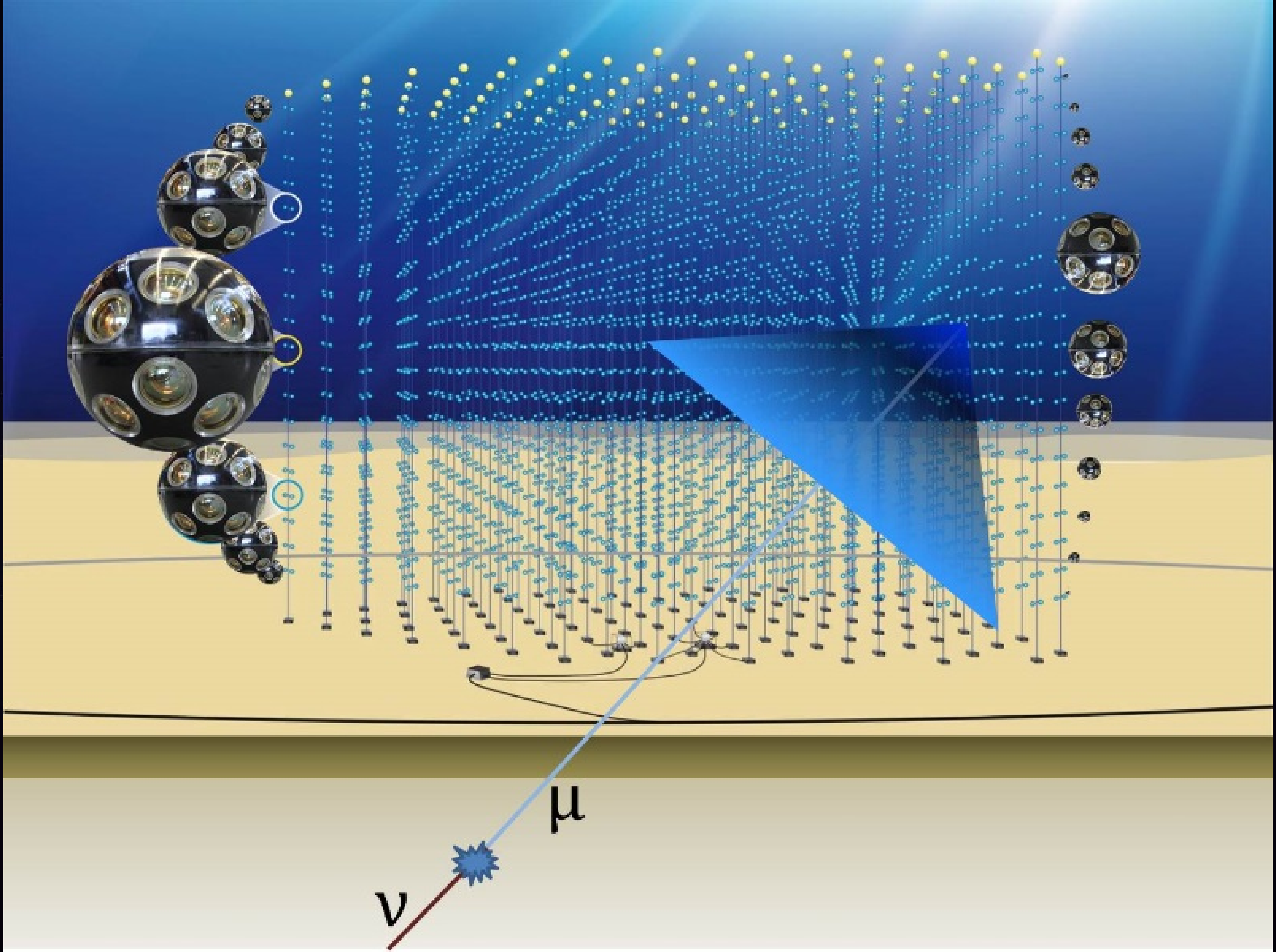
μ
ν

Muonic Neutrino Detection Principle

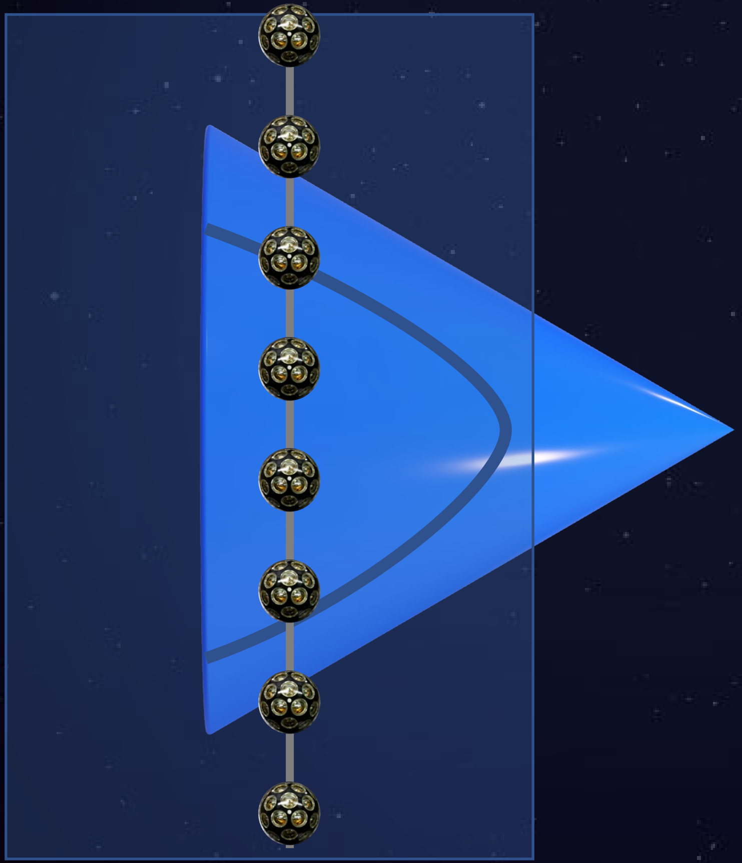

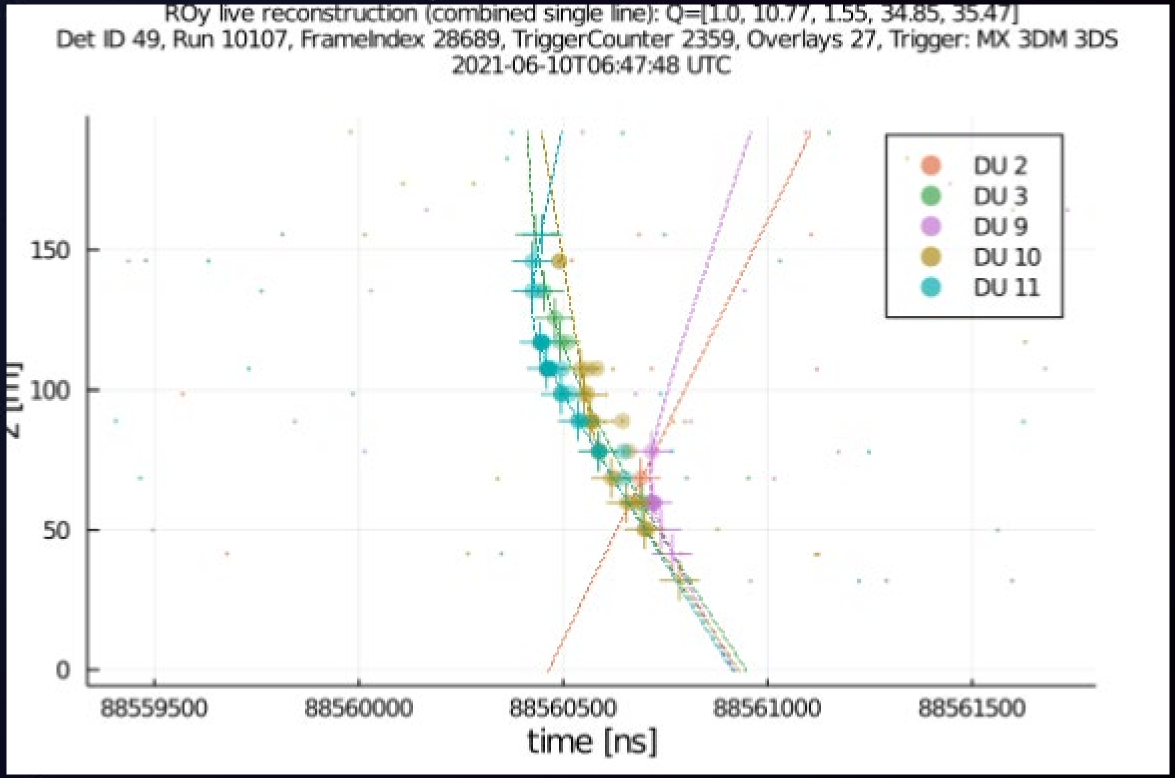

C.Spiering “Towards high-energy neutrino astronomy. A historical review” Eur. Phys. J. H 37, 515–565 (2012)

A Short Chronology of NeuTel History

1960 – M.Markov and I.Zheleznykh evaluated possible neutrino flux from the Crab nebula and outlined the limit in detection rate of a «conventional» underground neutrino detector

1970 - First proposal for an underwater neutrino detector DUMAND (Deep Underwater Muon and Neutrino Detector)

1995 - DUMAND project canceled, but his legacy generated all present detectors

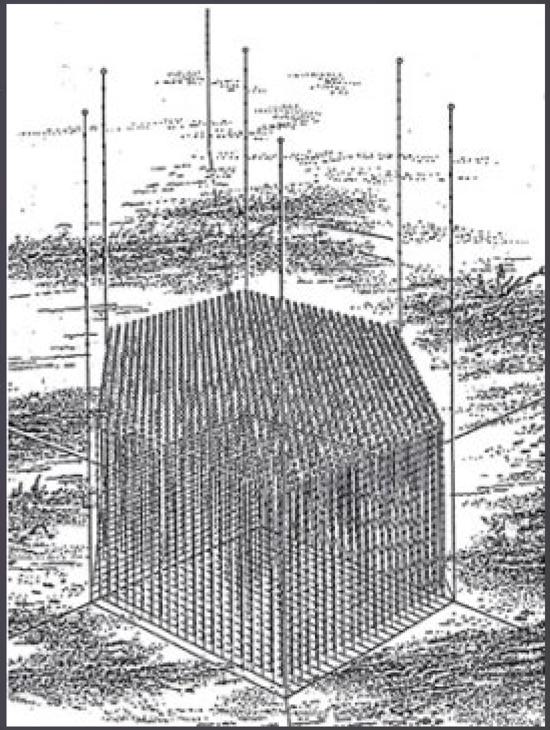

A Short Chronology of NeuTel History

1960 – M.Markov and I.Zheleznykh evaluated possible neutrino flux from the Crab nebula and outlined the limit in detection rate of a «conventional» underground neutrino detector

1970 - First proposal for an underwater neutrino detector DUMAND (Deep Underwater Muon and Neutrino Detector)

1995 - DUMAND project canceled, but his legacy generated all present detectors

1980 - The «Russian DUMAND» (NT200) was proposed in Baikal Lake

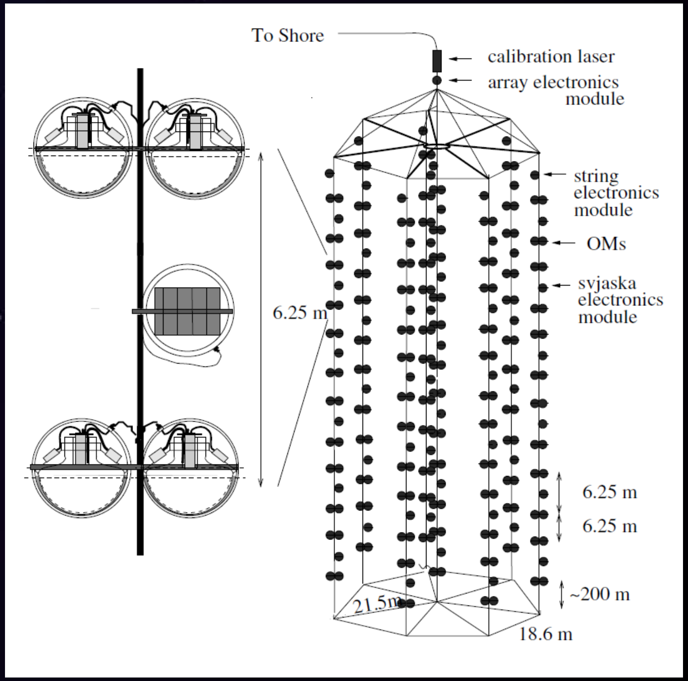

A Short Chronology of NeuTel History – South Pole

1988 - The neutrino detector at the South Pole was presented at the first «Venice Workshop on Neutrino Telescopes»

1990 - The construction of AMANDA started at South Pole

AMANDA remained in operation 9 years

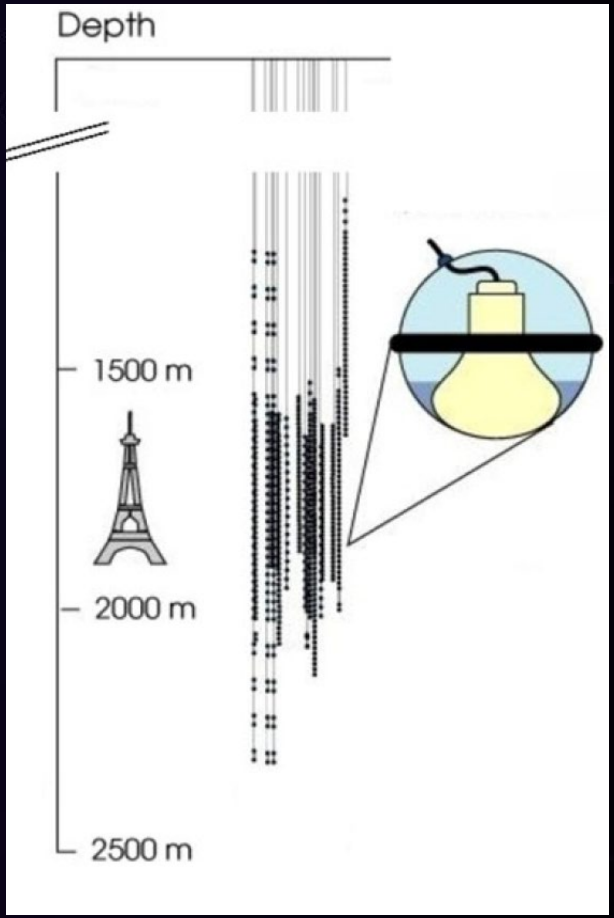

A Short Chronology of NeuTel History – South Pole

1988 - The neutrino detector at the South Pole was presented at the first «Venice Workshop on Neutrino Telescopes»

1990 - The construction of AMANDA started at South Pole

AMANDA remained in operation 9 years

1999 - The ICECube proposal submitted to NSF

2005 - First string of ICE deployed

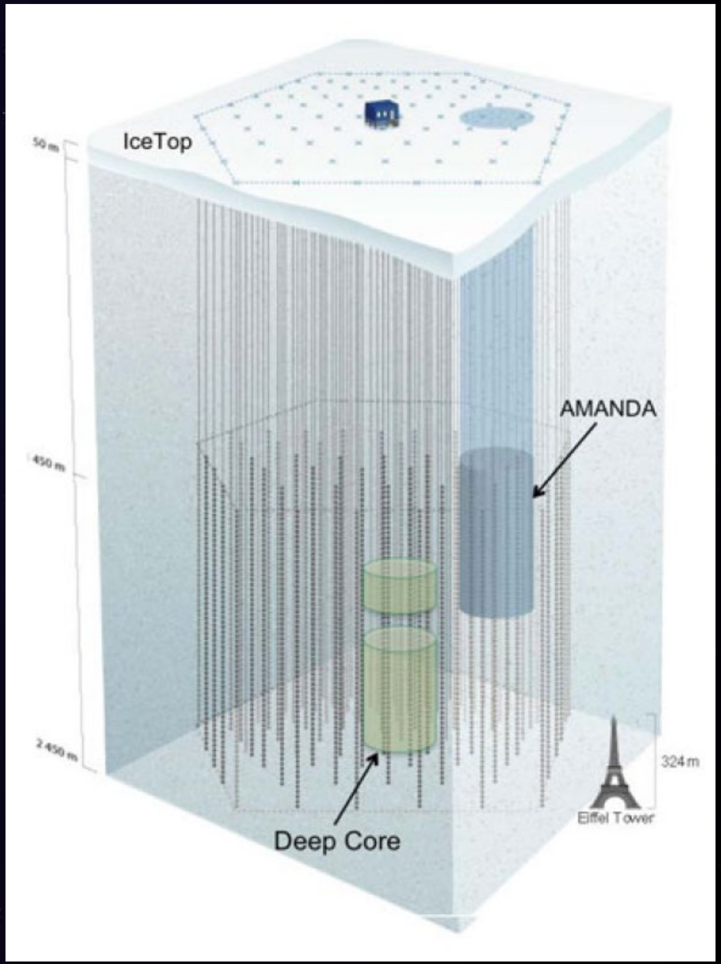

A Short Chronology of NeuTel History – Mediterranean Sea

1993 – The first neutrino detector in the Mediterranean Sea is proposed (NESTOR)

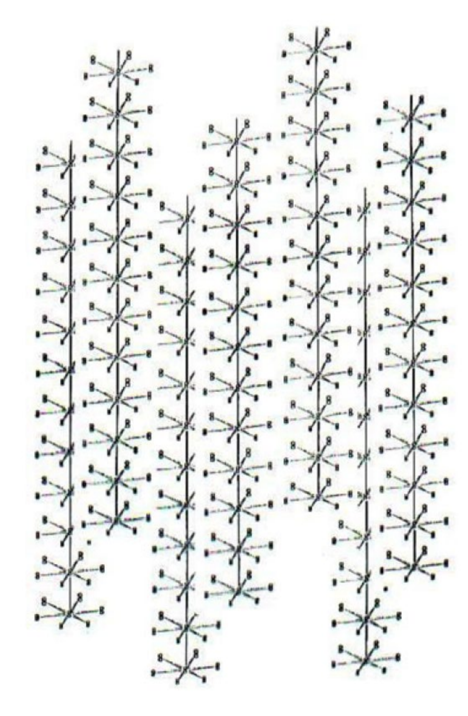

A Short Chronology of NeuTel History – Mediterranean Sea

1993 – The first neutrino detector in the Mediterranean Sea is proposed (NESTOR)

1997 - Definition of the ANTARES project

installation in 2008-2009

presently in operation

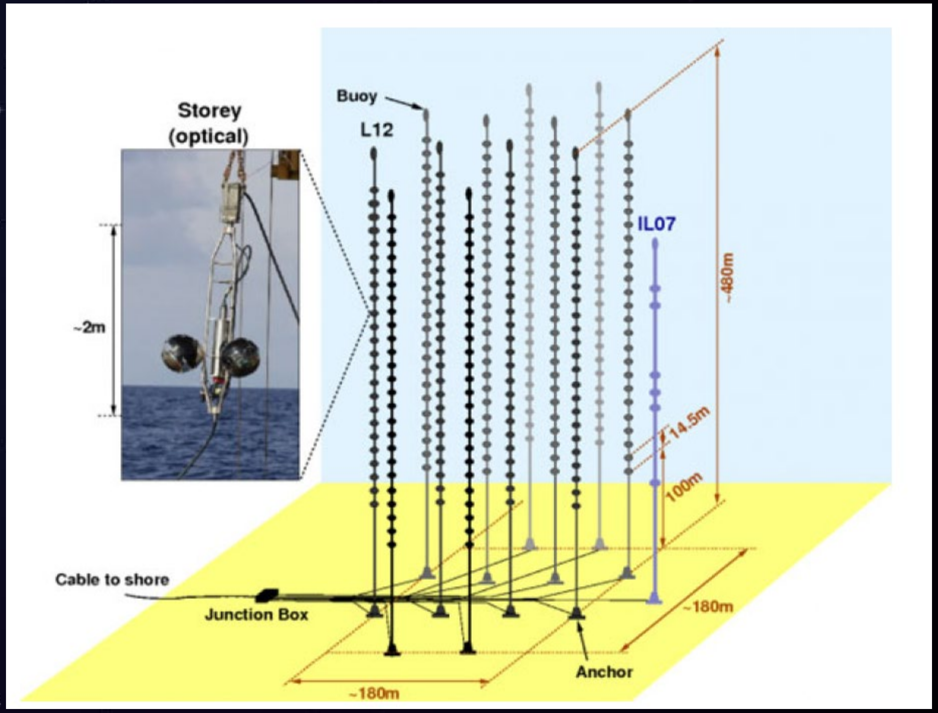

1998 - Presentation of the NEMO project

2008 - The three Mediterranean Iniziative converge and Definition of the Conceptual Design Report of KM3NeT is presented

2016 - Letter of Intent for KM3NeT 2.0

S. Adrián-Martínez et al “Letter of intent for KM3NeT 2.0” 2016 J. Phys. G: Nucl. Part. Phys. 43 084001

VLVnT 2021 - Very Large Volume Neutrino Telescope Workshop Valencia, 18 - 21 May 2021

Current Status

	OM	PMT/OM	Strings	OM/String	Height	Depth	Present size	Link
IceCube	5160	1x10"	86	60	1000	2500	1 km^3	icecube.wisc.edu
GVD	4032	1x10"	112 (14x8)	36	525	1300	under construction	baikalgvd.jinr.ru
KM3NeT	4140	32x2.5"	230 (2x115)	18	600	3500	under construction	www.km3net.org
ANTARES	900	3x10"	12	25	350	2500	0.035 km^3	antares.in2p3.fr

Atmospheric Neutrinos

A.Albert et al "Measurement of the atmospheric ν_e and ν_μ energy spectra with the ANTARES neutrino telescope" arXiv:2101.12170v2 [hep-ex]

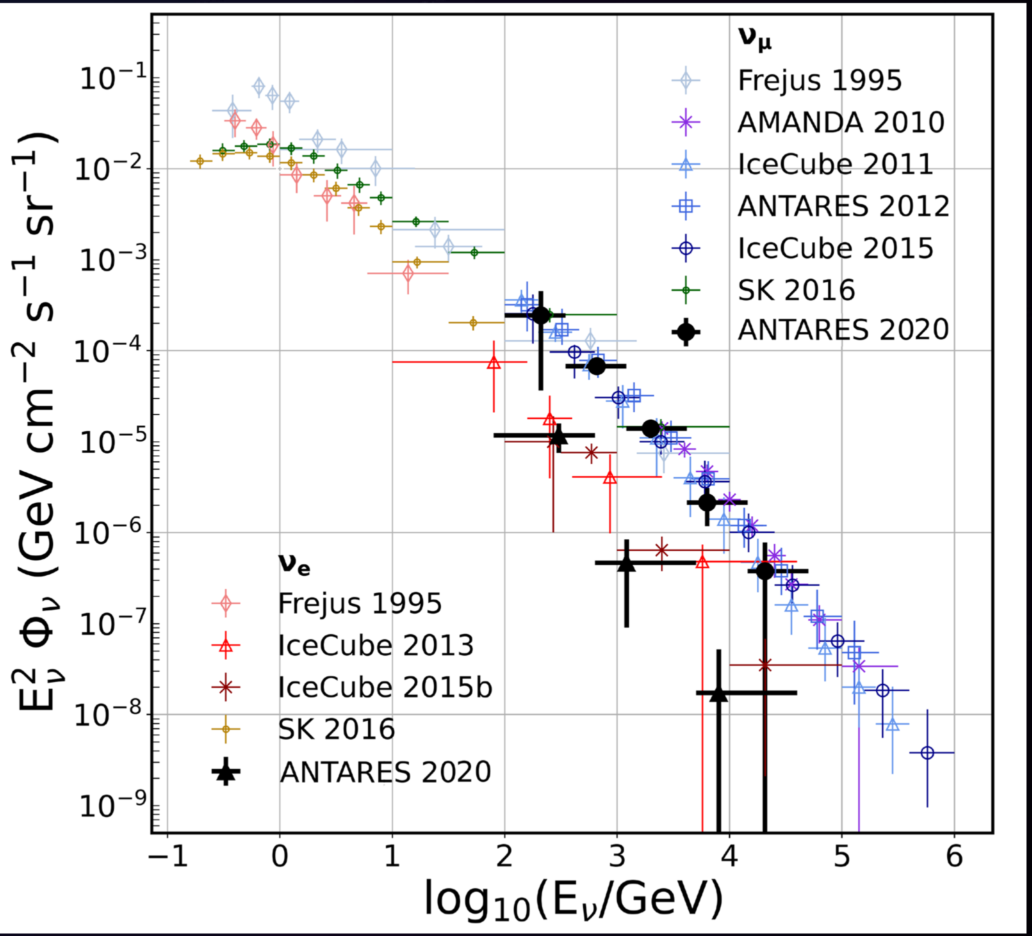

First Evidence of High Energy Cosmic Neutrinos

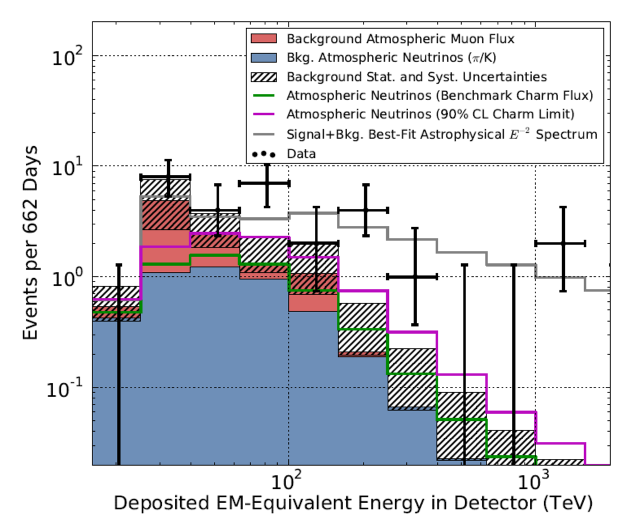

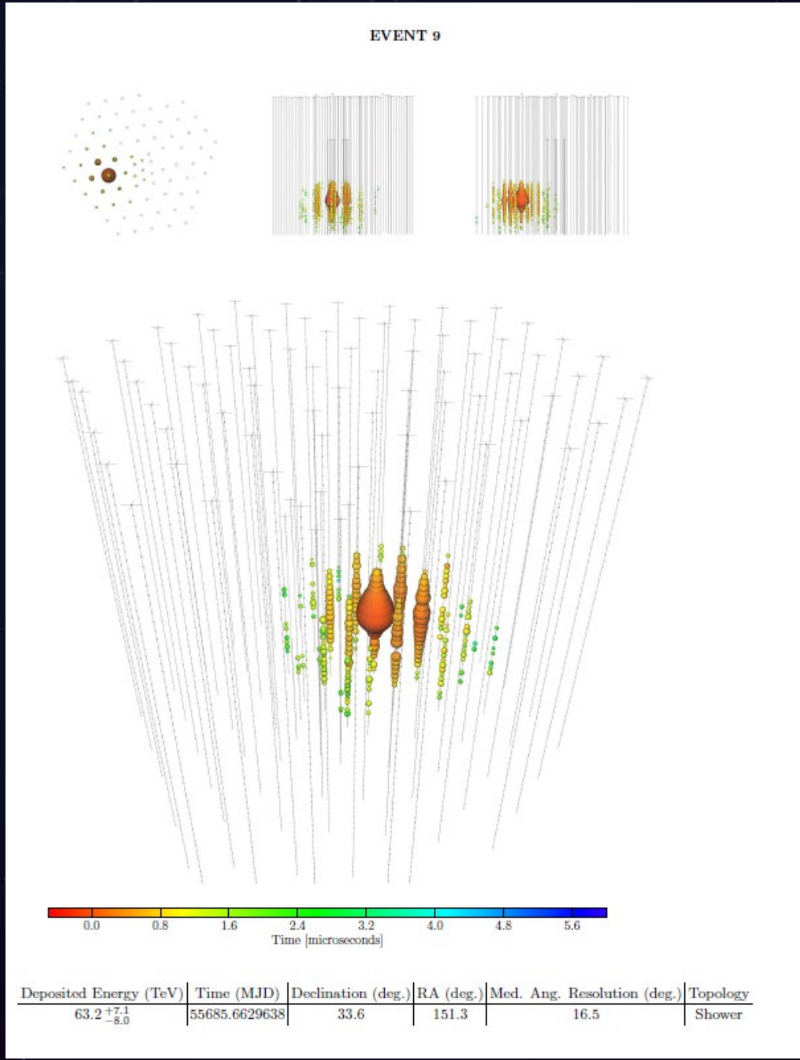

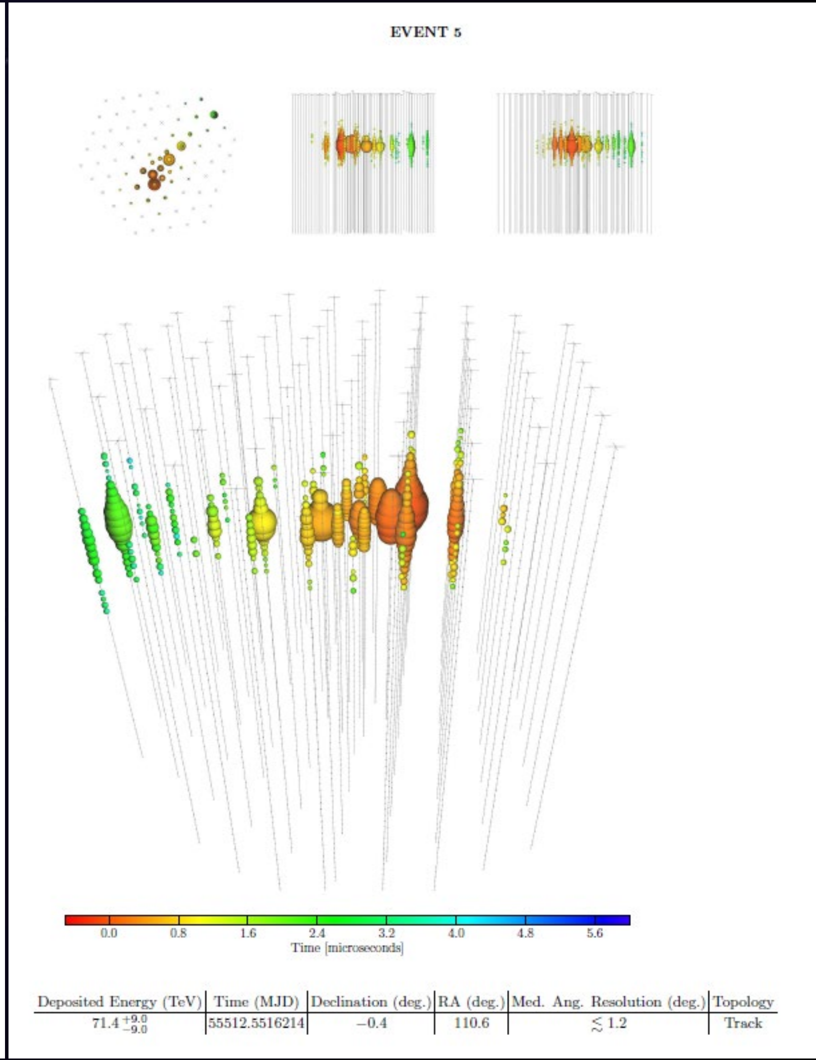

IceCube Collaboration "Evidence for High-Energy Extraterrestrial Neutrinos at the IceCube Detector" Science 342 (2013) 1242856

The Technology – IceCube/South Pole

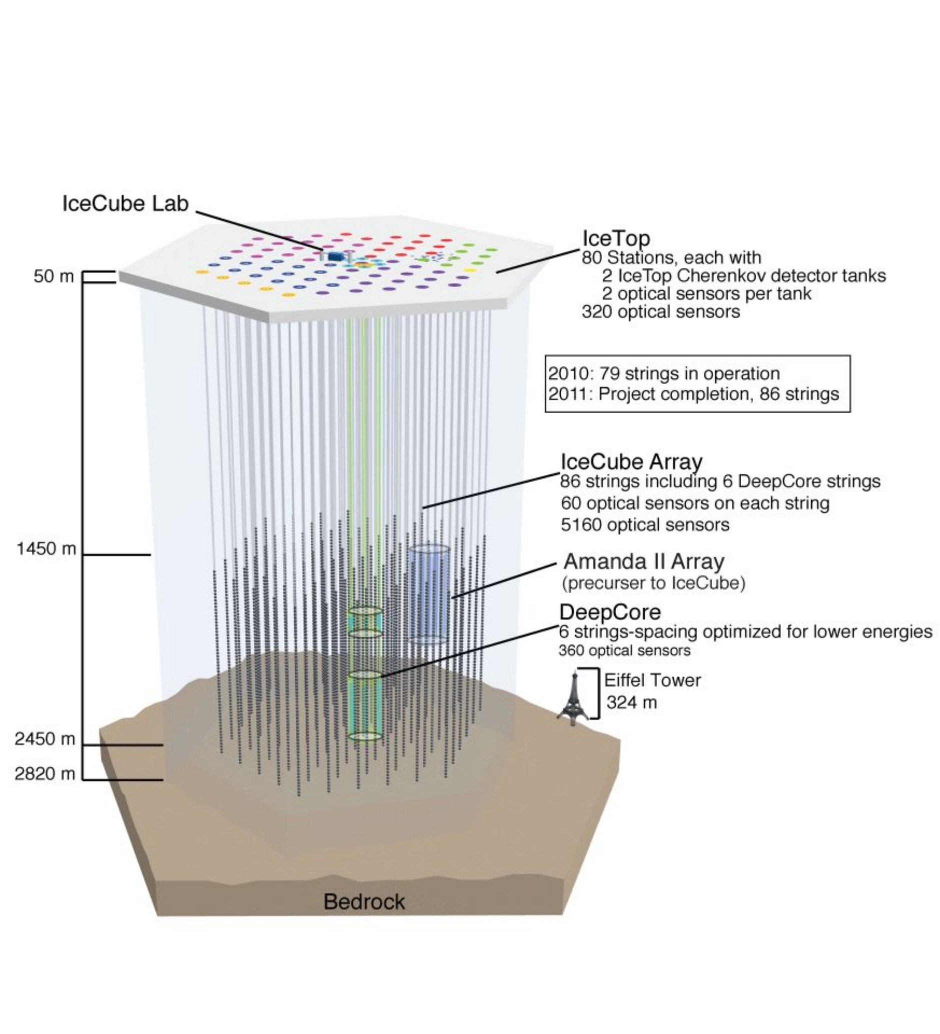

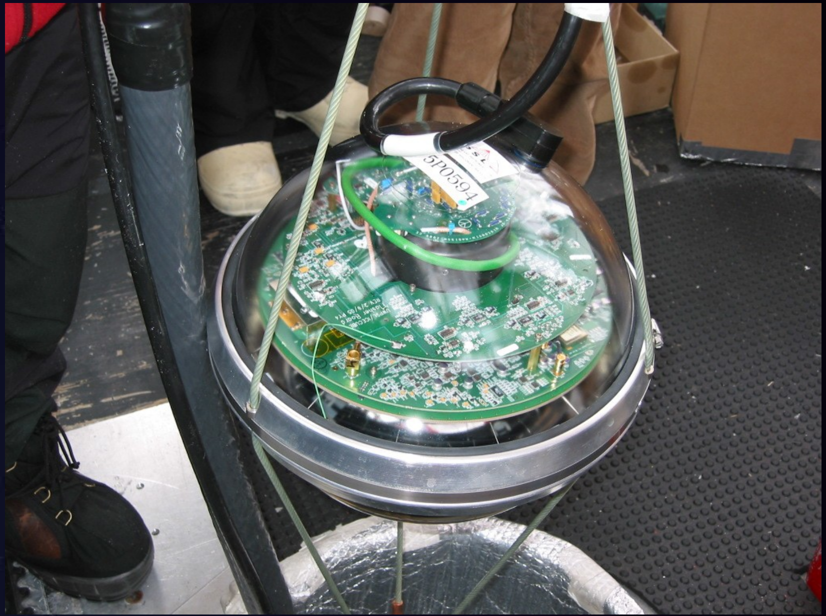

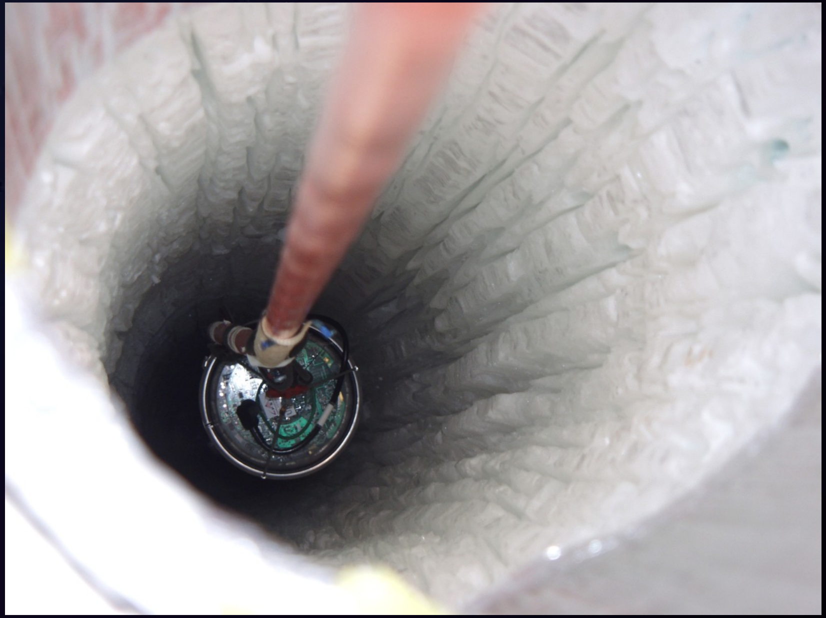

The Technology – GVD/Baikal

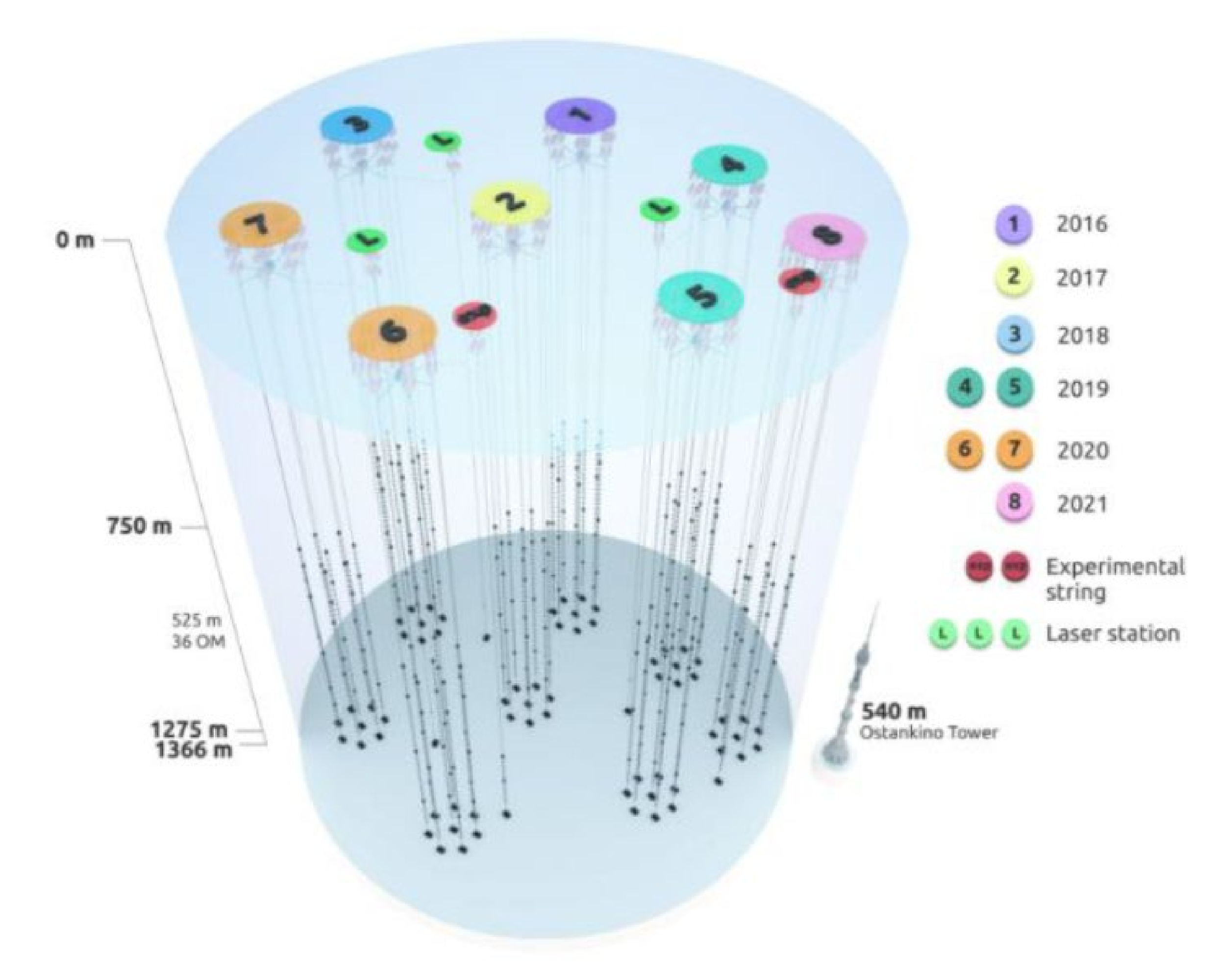

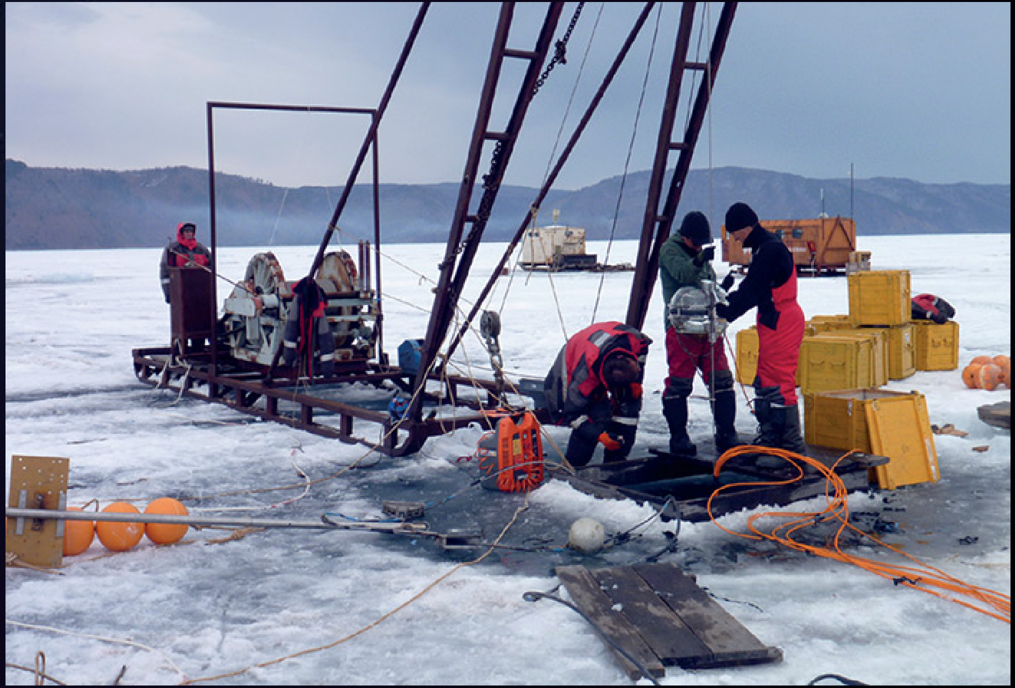

The Technology – KM3NeT/Mediterranean Sea

Basic requirement: a durable, reliable and not-expensive technology

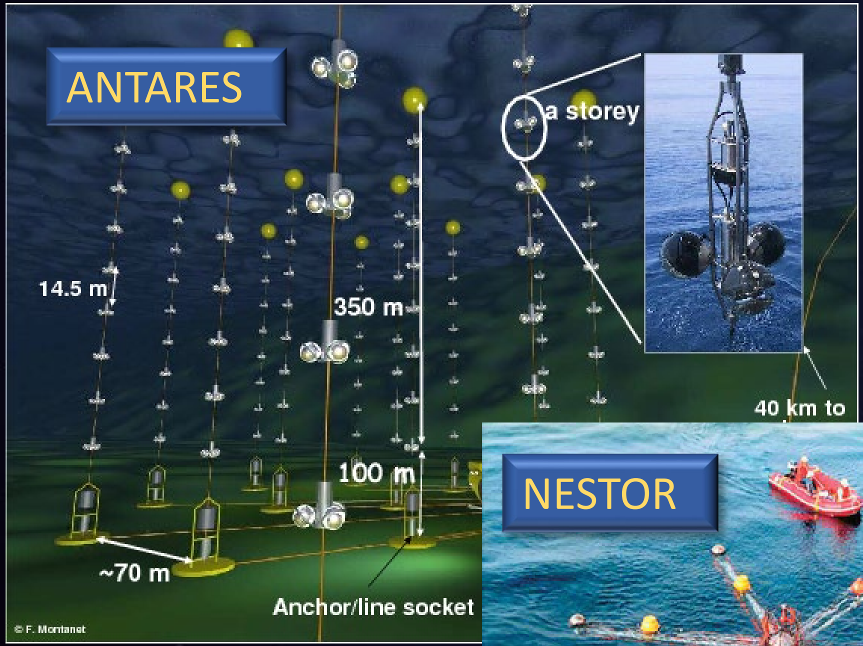

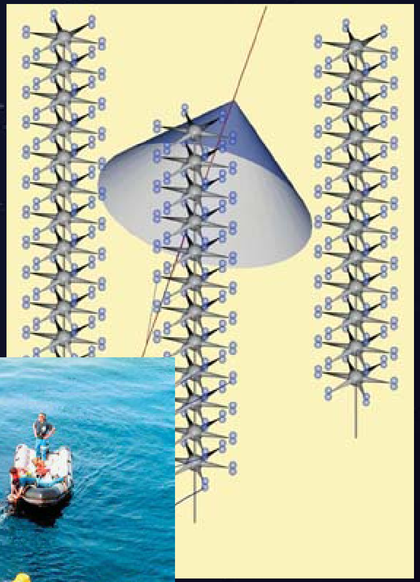

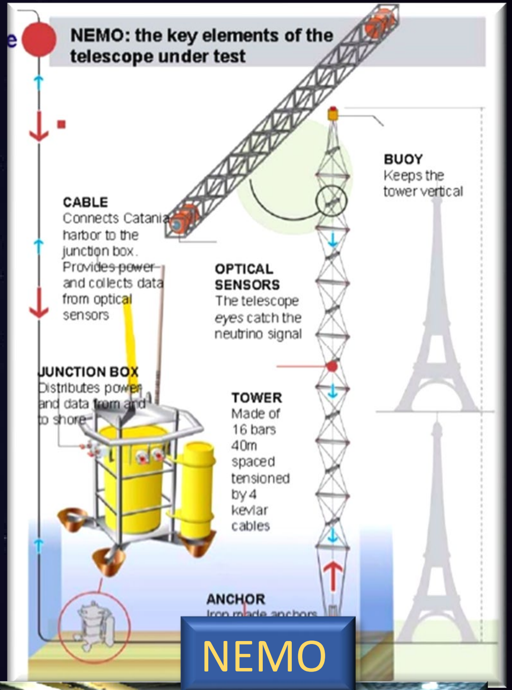

KM3NeT - The Detection Unit

18 DOM integrated on vertical slender strings supported by two parallel Dynema ropes

DOM counts Cherenkov photons

Strings arranged on the LOM, mounted on the anchor and ready for deployment

KM3NeT – The Detector Size

Astroparticle
Research
with **C**osmics
In the **A**byss

ARCA (off shore Capo Passero, It @ 3500 m depth)

ORCA (off shore Toulon, Fr @2500 m depth)

Oscillation
Research
with **C**osmics
In the **A**byss

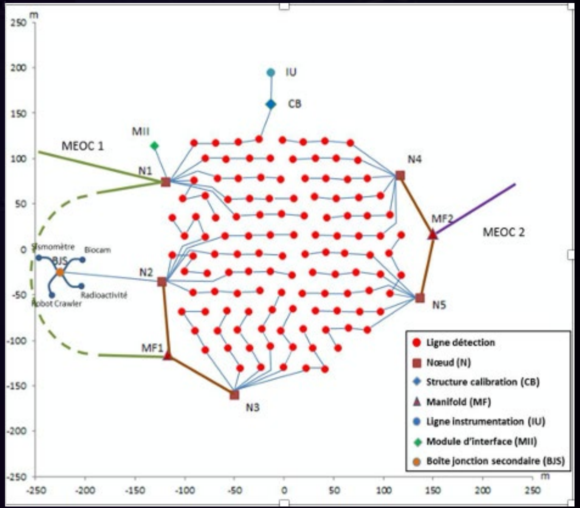

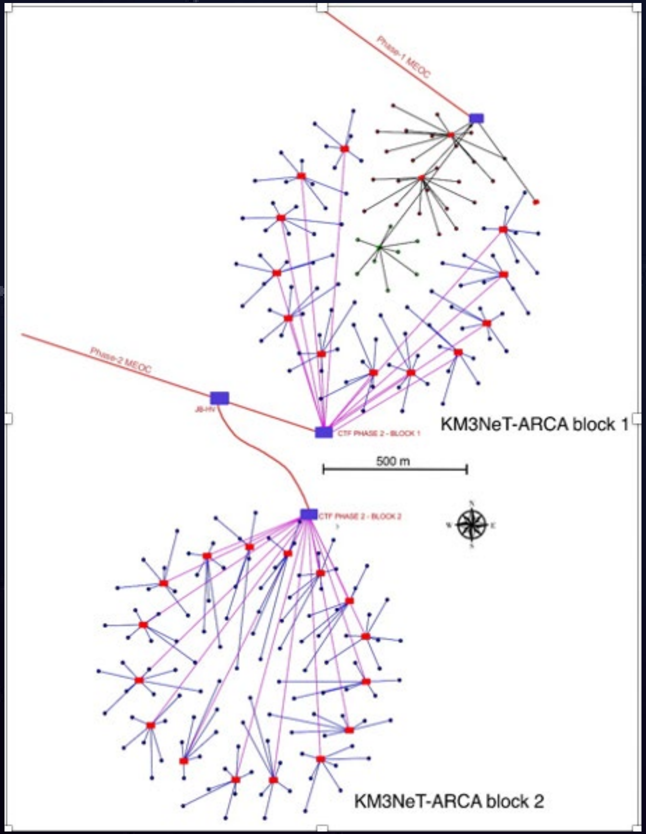

	ARCA	ORCA
Location	Italy	France
DU distance	90 m	20 m
DOM spacing	36 m	9 m
Instrumented mass	2*500 Mton	5.7 Mton

KM3NeT - The Physics Program

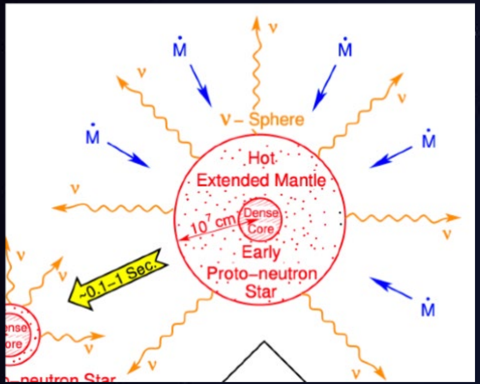

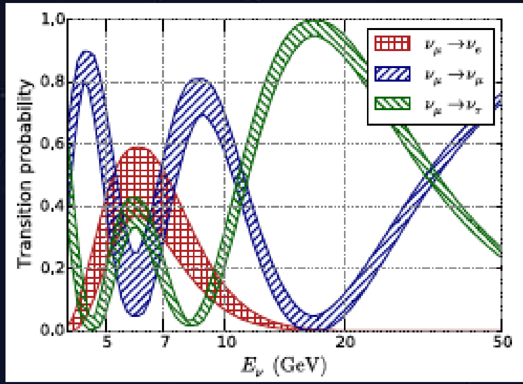

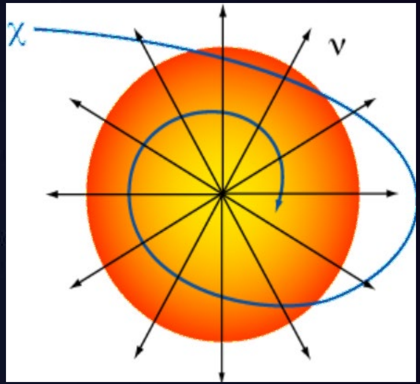

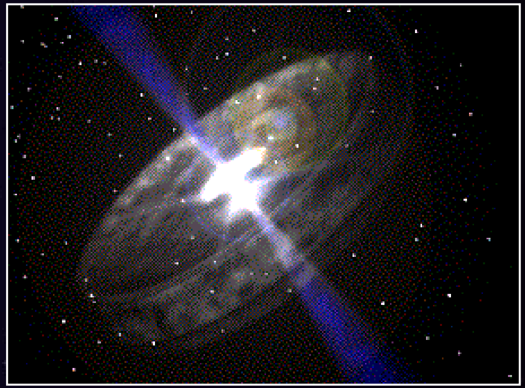

Low Energy	Medium Energy	High Energy
MeV < E_ν < 100 GeV	10 GeV < E_ν < 1 TeV	E_ν > 1 TeV

Supernovae

ν Oscillations

Dark matter
Monopoles, Nuclearites

Cosmic ν
Origin and production mechanism of HE CR

KM3NeT- ORCA KM3NeT- ARCA

+ oceanography, biology, seismology,...

Neutrinos from Supernova

In a typical CCSN, an amount of energy as large as 3 x 10^{53} erg can be released mainly through the emission of a burst of neutrinos having a mean energy in the 10-20MeV range.

Supernovae emits neutrinos and anti-neutrinos, mainly electron-type

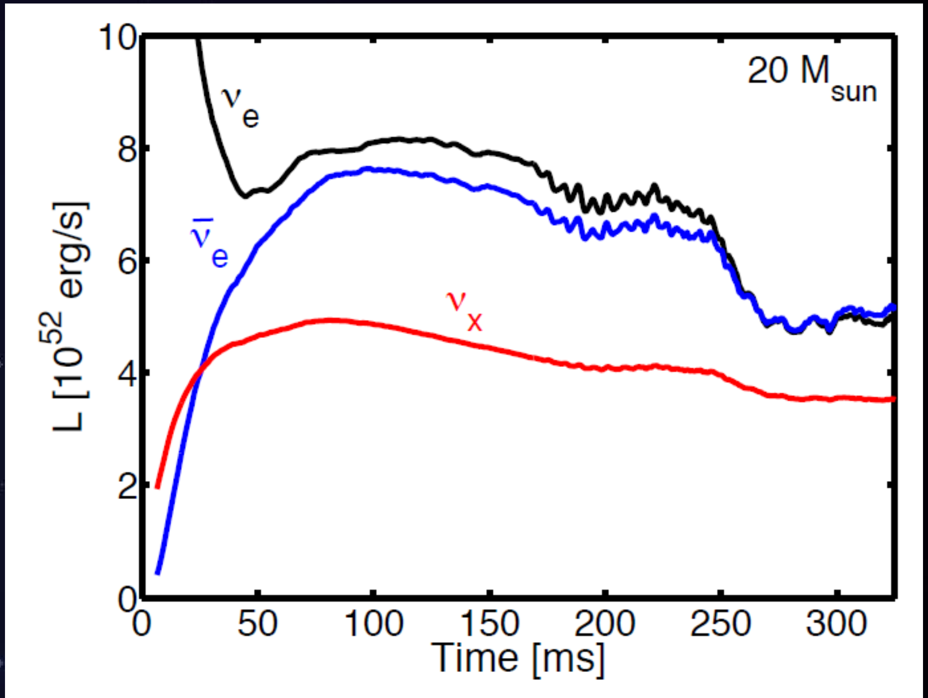

Neutrinos from Supernova – KM3NeT

S.Aiello et al. "The KM3NeT potential for the next core-collapse supernova observation with neutrinos", submitted to Eur. Phys. J. C

In a typical CCSN, an amount of energy as large as 3 x 10^{53} erg can be released mainly through the emission of a burst of neutrinos having a mean energy in the 10-20 MeV range.

Anti-neutrinos interacts via

$$\bar{\boldsymbol{\nu}}_{\boldsymbol{e}} + \mathrm{p} \rightarrow \boldsymbol{e}^{+} + \mathrm{n}$$

Positrons are detected via Cherenkov light

Multiplicity = $\sum PMT$ in a single DOM

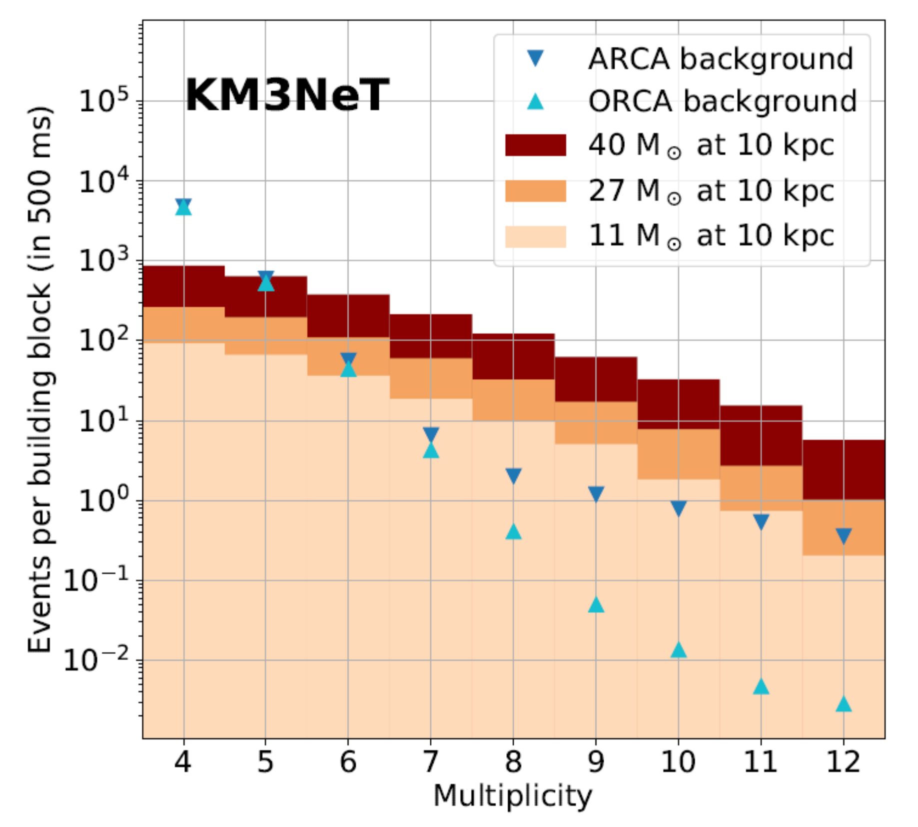

Neutrinos from Supernova – KM3NeT

S.Aiello et al. "The KM3NeT potential for the next core-collapse supernova observation with neutrinos", submitted to Eur. Phys. J. C

In a typical CCSN, an amount of energy as large as 3 x 10^{53} erg can be released mainly through the emission of a burst of neutrinos having a mean energy in the 10-20MeV range.

Anti-neutrinos interacts via

$$\bar{\nu}_e + \mathrm{p} \rightarrow e^{+} + \mathrm{n}$$

Positrons are detected via Cherenkov light

Multiplicity = $\sum PMT$ in a single DOM

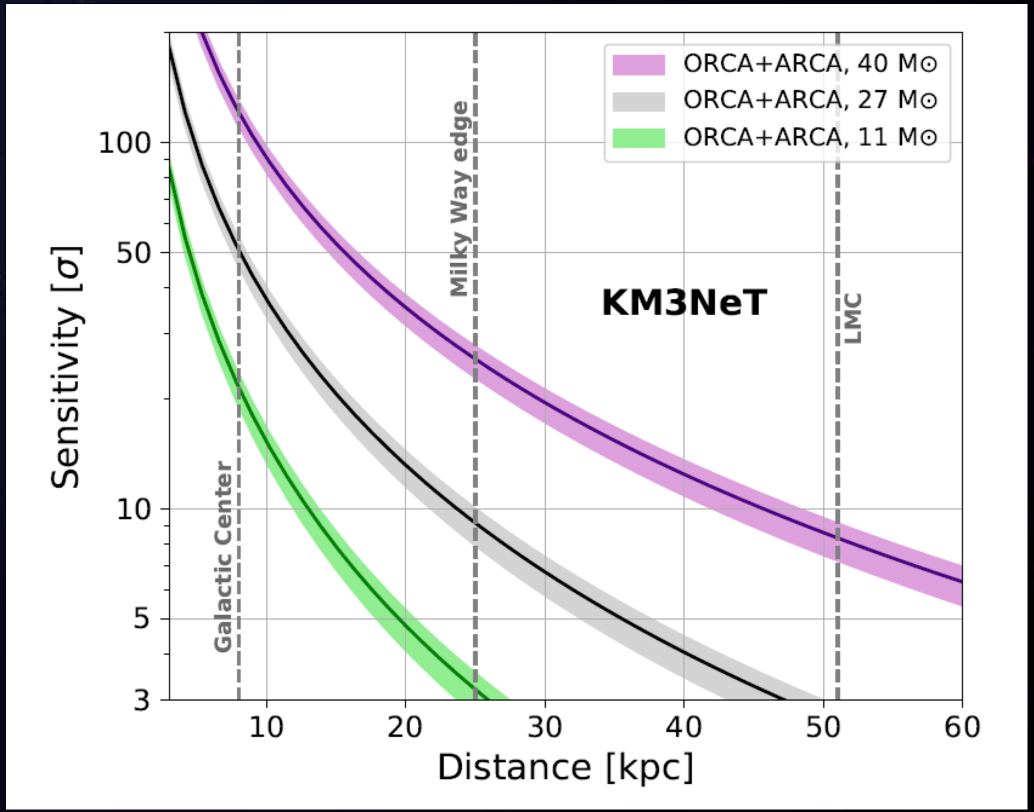

Neutrinos from Supernova – A Global Network

A.Coleiro et al. " Combining neutrino experimental light-curves for pointing to the next galactic core-collapse supernova", Eur. Phys. J. C80 (2020) 856

By exploiting the time delay between the arrival of the signal at different detector sites, it is possible to use a triangulation method to infer the source localisation on the sky

Confidence area computed using triangulation between four detectors: IceCube, KM3NeT/ARCA, Hyper-Kamiokande and JUNO.

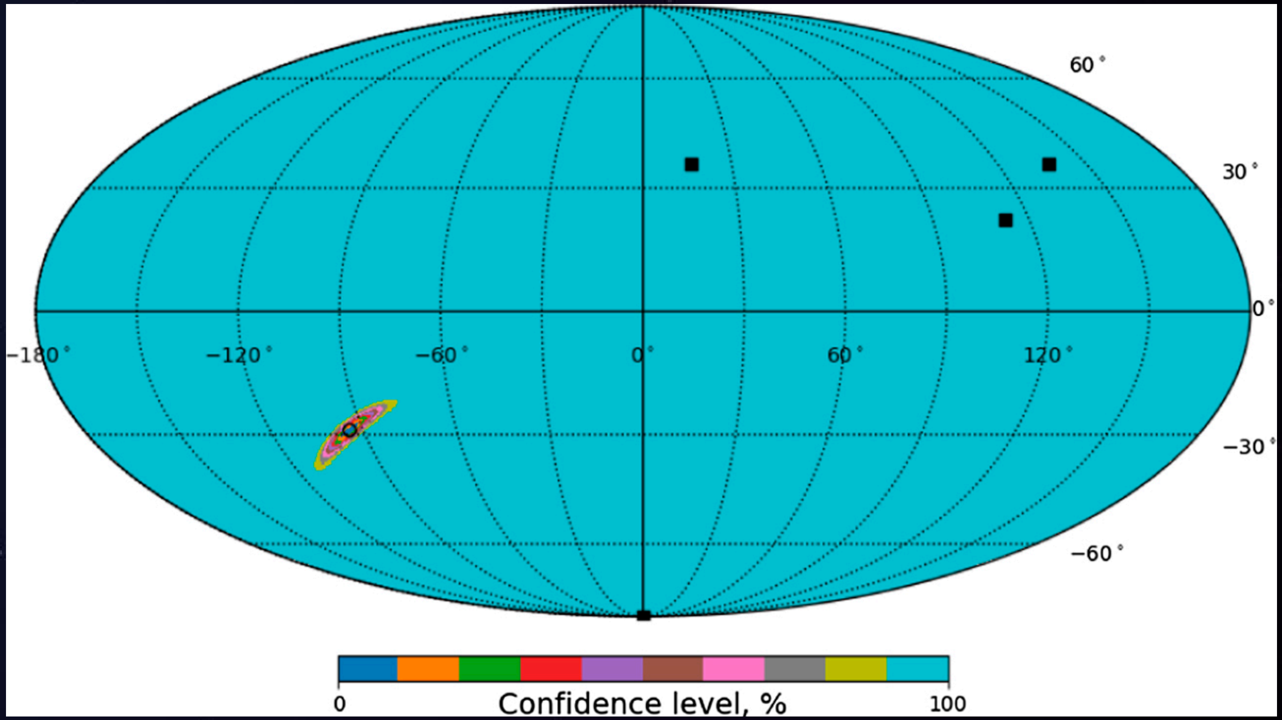

Event Topologies and Detector Response - KM3NeT

ν_μ are the golden channel for neutrino astronomy

Deep sea water properties, i.e. long scattering length allow to achieve very good angular resolution

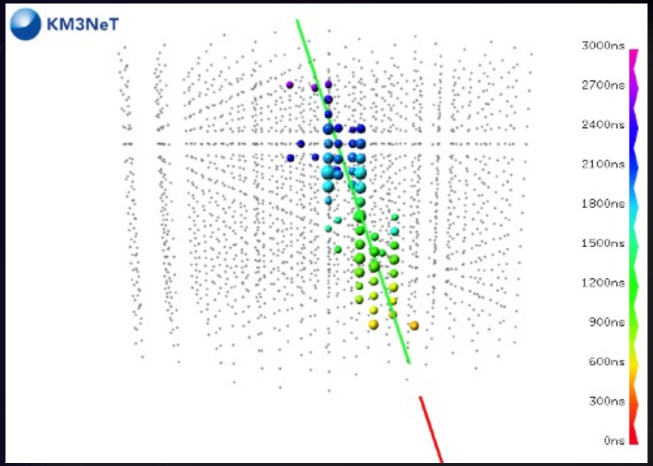

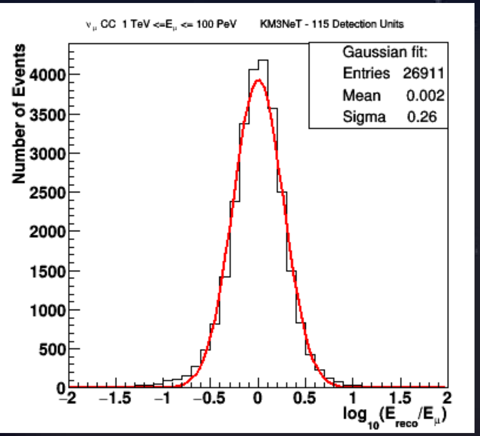

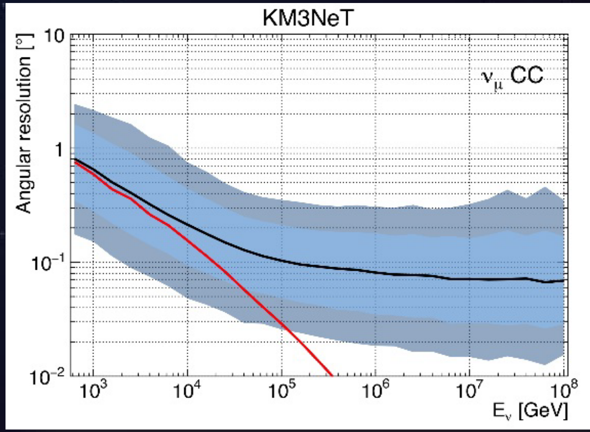

Energy resolution about 0.3 in $\log E_\mu$

Angular resolution about 0.1° (E_ν>10 TeV)

Event Topologies and Detector Response - KM3NeT

Contained shower ν_e

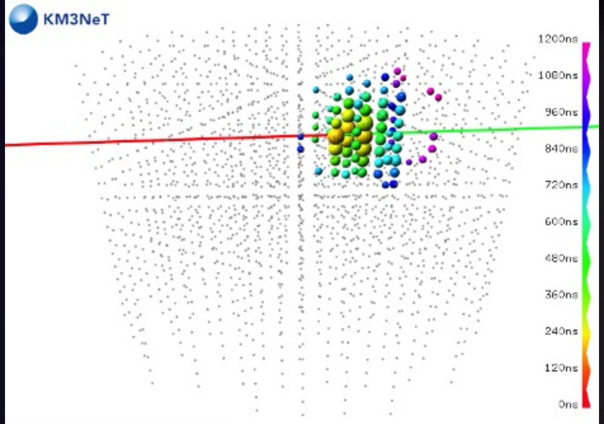

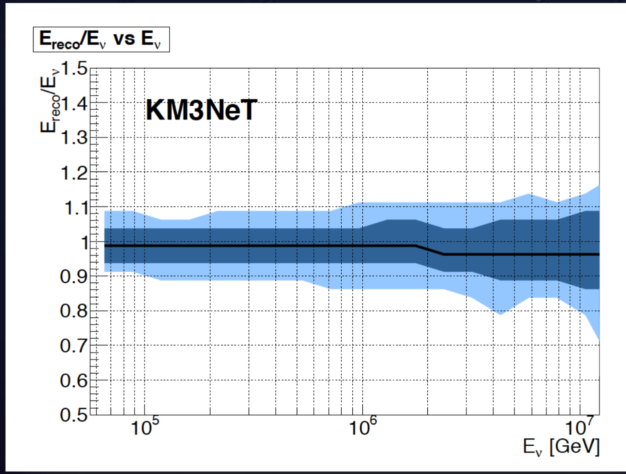

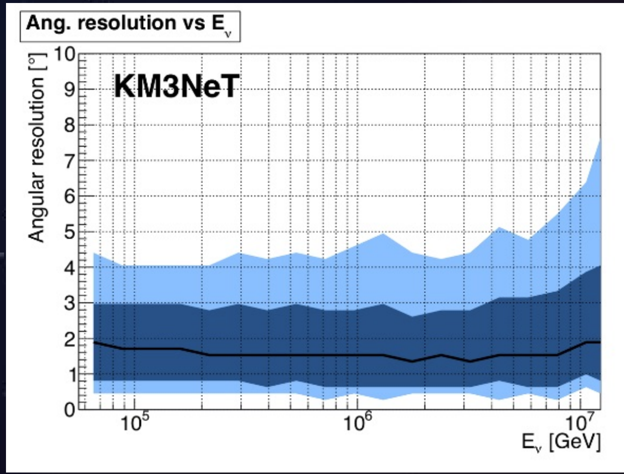

Energy resolution about 10%

Angular resolution about 2° (E_ν>10 TeV)

KM3NeT – Present Status

6 ORCA Detection units deployed and in operation since one year

6 ARCA Detection unit in operation since three months

M.Ageron et al. (KM3NeT Collaboration) "Dependence of atmospheric muon flux on seawater depth measured with the first KM3NeT detection units", Eur. Phys. J. C 80, 99 (2020)

Present results:

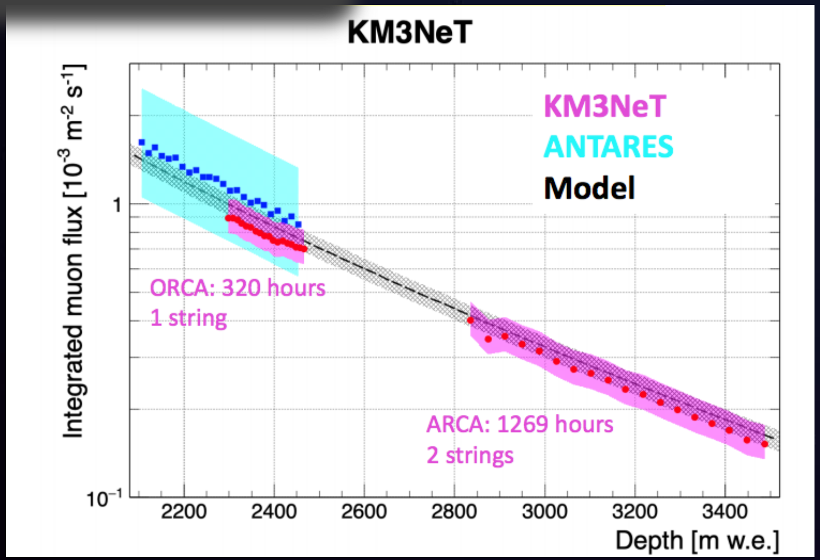

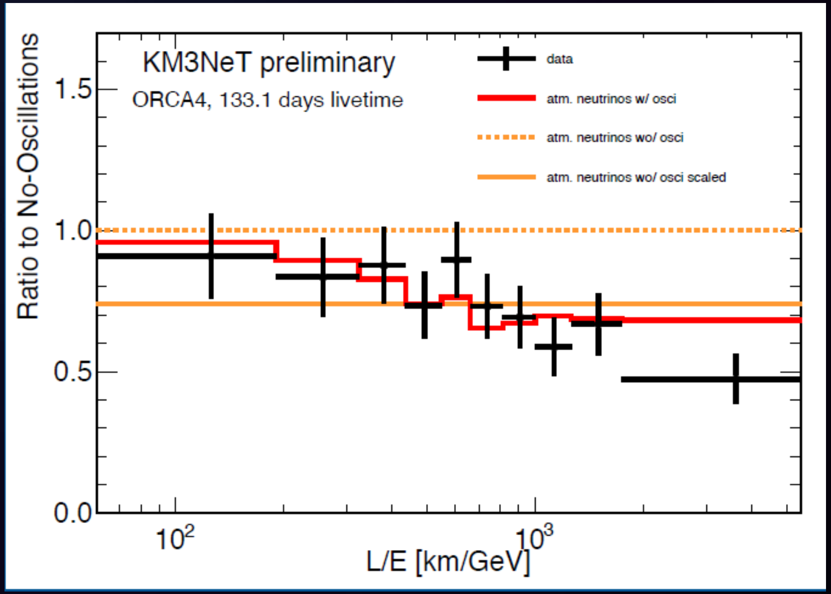

Sensitivity to Point-like Galactic Sources

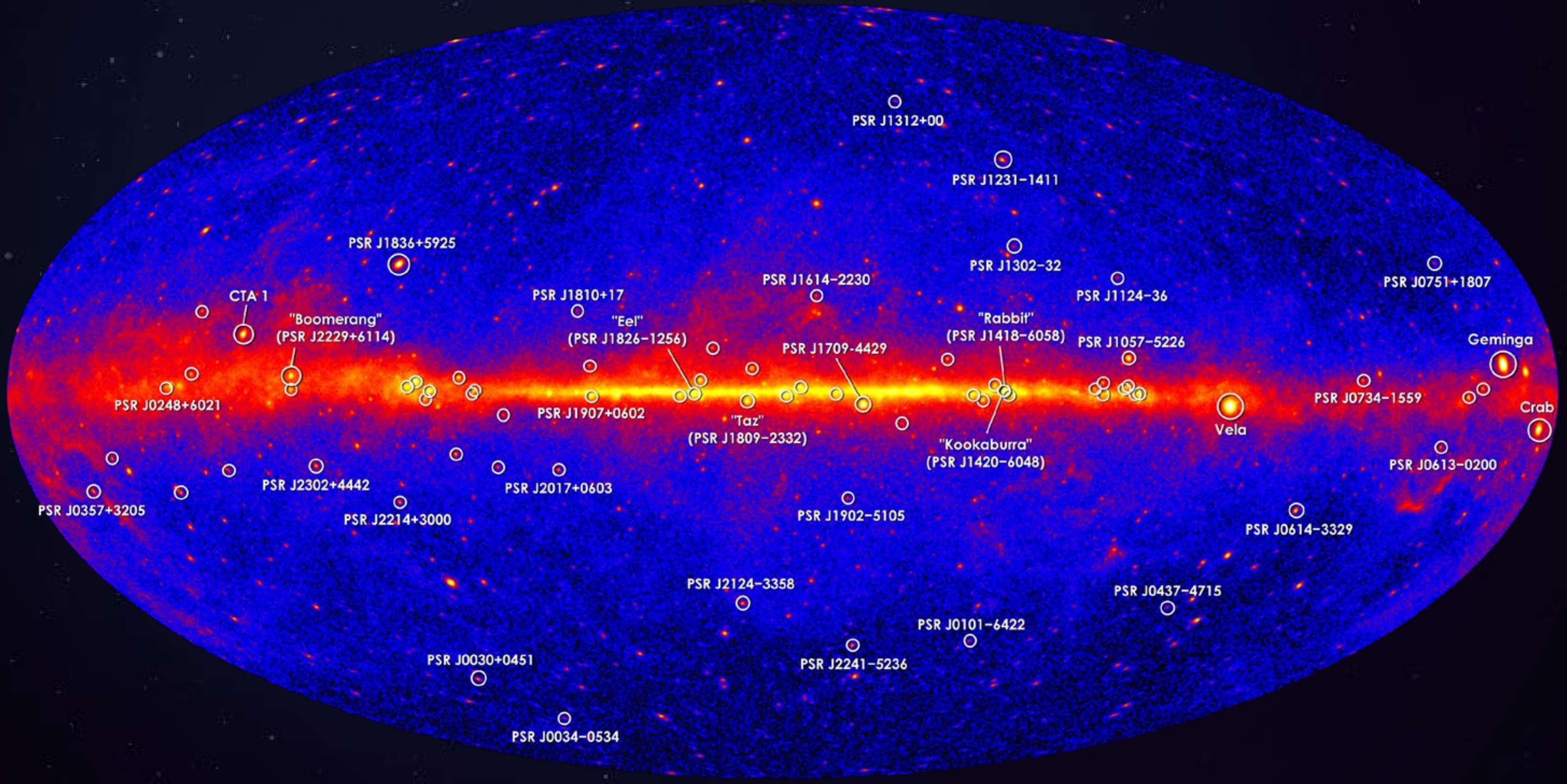

Sensitivity to Point-like Galactic Sources

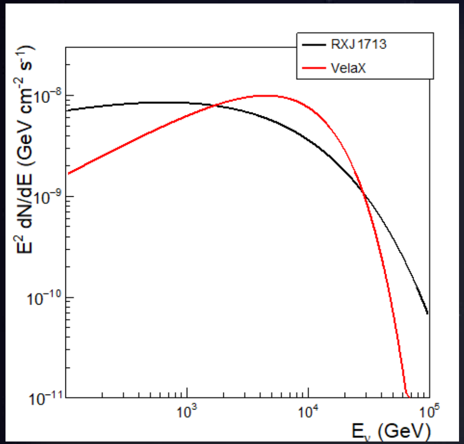

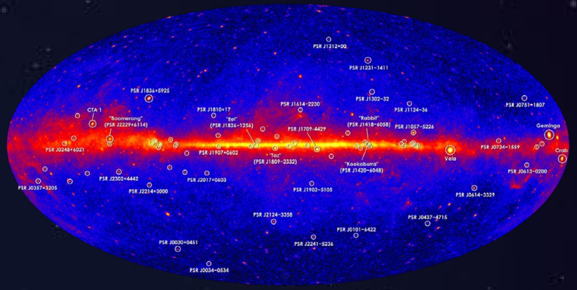

HE gamma emission observed by HESS in SNRs

Neutrino spectra predicted using gamma spectra

- S.R. Kelner, *et al.*, PRD 74 (2006) 034018
- F.L. Villante and F. Vissani, PRD 78 (2008) 103007

Hypotheses: 100% hadronic emission and transparent source

Sensitivity to Point-like Galactic Sources - KM3NeT

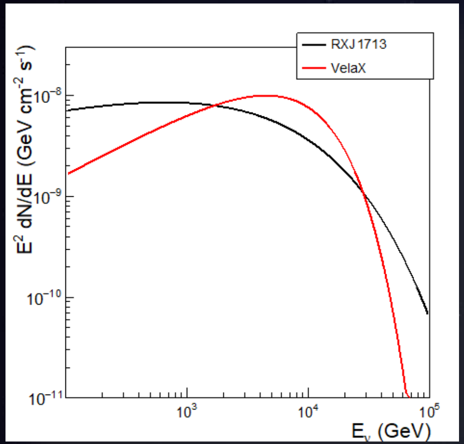

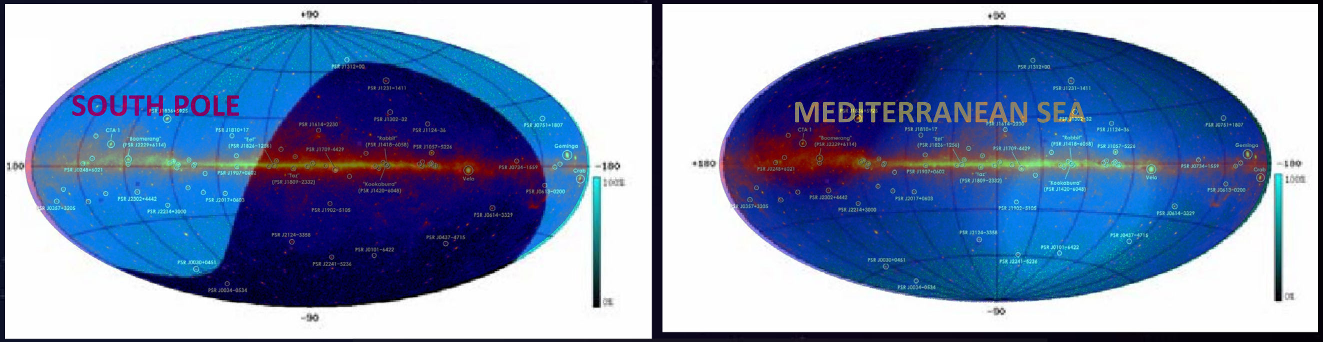

Visibility for up-going neutrinos

HE gamma emission observed by HESS in SNRs

Neutrino spectra predicted using gamma spectra

- ¶ S.R. Kelner, *et al.*, PRD 74 (2006) 034018
- § F.L. Villante and F. Vissani, PRD 78 (2008) 103007

Hypotheses: 100% hadronic emission and transparent source

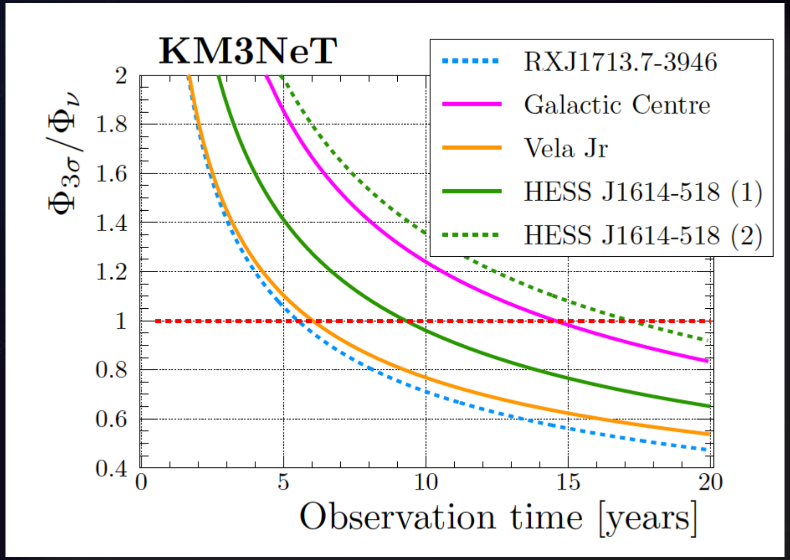

Angular Resolution

6 year HESE data
E > 60 TeV
ϴ<20°
Points : 3FHL, HBL

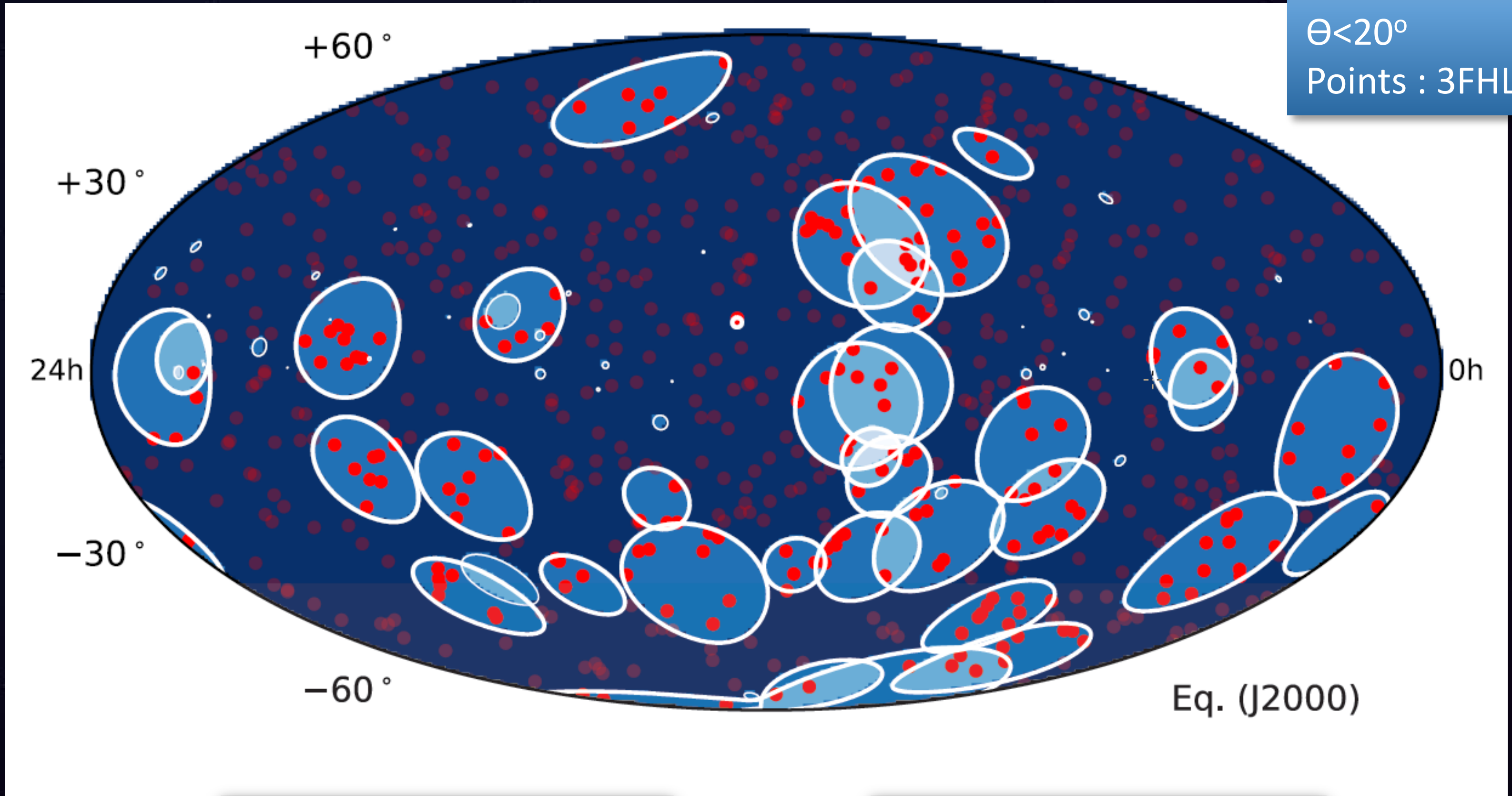

Resolution for ν_e KM3NeT

Resolution for ν_μ KM3NeT

Point-like Neutrino Sources

M. G. Aartsen et al., ” Time-Integrated Neutrino Source Searches with 10 Years of IceCube Data”, Phys. Rev. Lett. 124, 051103 (2020)

5 identified sources

Name	Type	p	Ref.
NGC 1068	AGN	0.008	Aartsen et al. (2020)
TXS 0506+056	blazar	0.001	Aartsen et al. (2018)
PKS 1502+106	blazar	0.01	Taboada & Stein (2019)
PKS 1424-41	blazar	0.05	Kadler et al. (2016)
AT2019dsg	TDE	0.002	Stein et al. (2020)

The IceCube Collaboration et al.,. ” Multimessenger observations of a flaring blazar coincident with high-energy neutrino IceCube-170922A”, Science 361, 146 (2018)

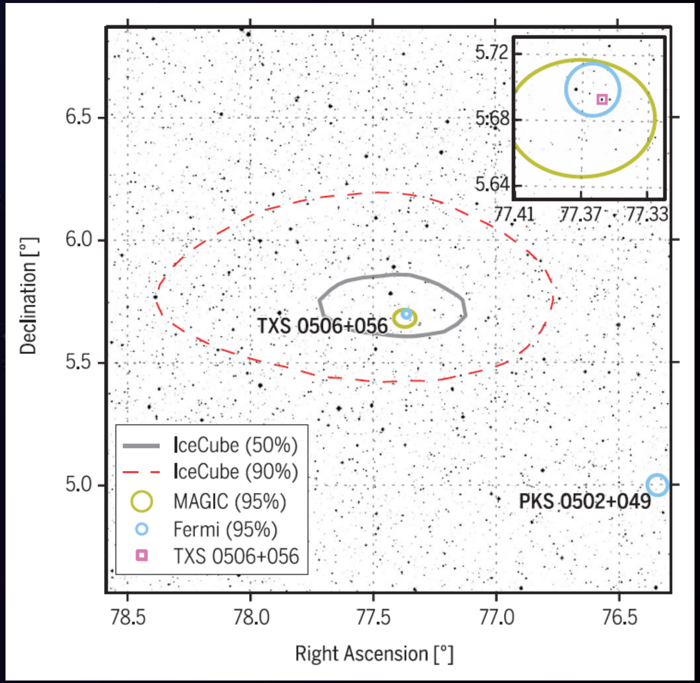

CONCLUSION: The energies of the γ-rays and the neutrino indicate that blazar jetsmay accelerate cosmic rays to at least several PeV. The observed association of a high-energy neutrino with a blazar during a period of enhanced γ-ray emission suggests that blazars may indeed be one of the long sought sources of very-high-energy cosmic rays, and hence responsible for a sizable fraction of the cosmic neutrino flux observed by IceCube.

Point-like Neutrino Sources

5 identified sources

Name	Type	p	Ref.
NGC 1068	AGN	0.008	Aartsen et al. (2020)
TXS 0506+056	blazar	0.001	Aartsen et al. (2018)
PKS 1502+106	blazar	0.01	Taboada & Stein (2019)
PKS 1424-41	blazar	0.05	Kadler et al. (2016)
AT2019dsg	TDE	0.002	Stein et al. (2020)

M. G. Aartsen et al. "Neutrino emission from the direction of the blazar TXS 0506+056 prior to the IceCube-170922A alert", Science 361 (2018) 147-151

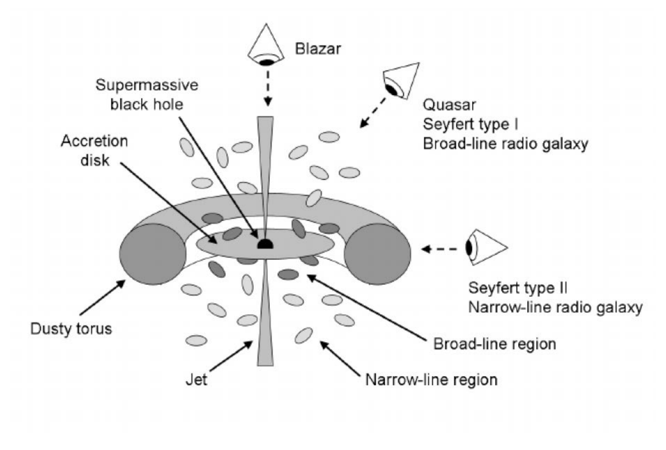

fig. from E. Zackrisson, PhD thesis

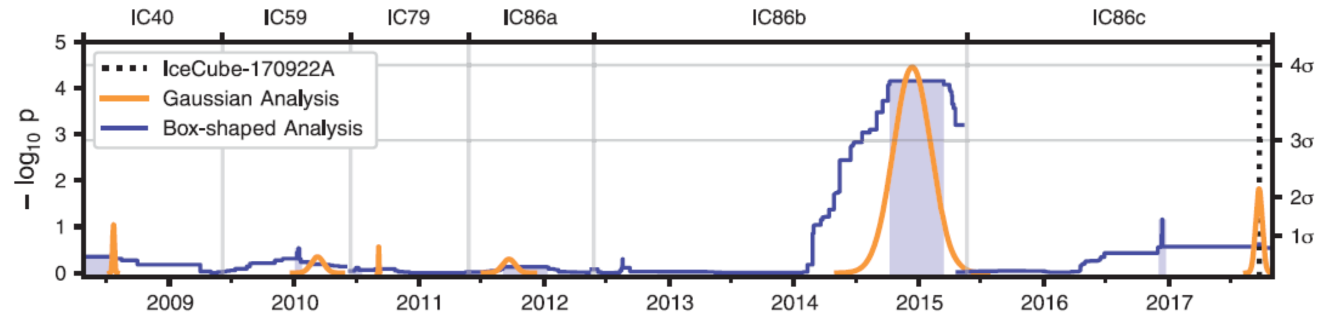

Bibliography

I.J.R.Aitchison & A.J.G.Hey, Gauge Theories In Particle Physics, IoP

C.Giunti & C.W.Kim, Fundamentals of Neutrino Physics and Astrophysics, Oxford University Press

H.Karttunen et al., Fundamental Astronomy, Springer

M.Spurio, Probes of Multimessenger Astrophysics, Springer